Design Criteria and Performance Evaluation of Wire-Wrapped Screens for Steam Assisted Gravity Drainage (SAGD) Wellbores

by

Jesus David Montero Pallares

A thesis submitted in partial fulfillment of the requirements for the degree of

Master of Science

in

Petroleum Engineering

Department of Civil and Environmental Engineering

University of Alberta

©Jesus David Montero Pallares, 2019

ABSTRACT

This thesis presents the experimental results obtained using a large Pre-packed Sand Retention Testing (SRT) facility. Analysis of the results funds the elaboration of novel design criteria for wire-wrapped screens (WWS) in Steam Assisted Gravity Drainage (SAGD) applications. The SRT data improves the understanding of different parameters controlling sand production and flow impairment. The final design criteria combine both sanding and flow performance indicators in a Traffic Light System (TLS) displaying optimum, marginal and adverse slot ranges. Additionally, empirical formulations are introduced to predict and provide the lower and upper boundaries of the optimum aperture window.

The assembly and operational procedures were custom-built to improve existing sand control testing protocols. The facility employs the largest scale-test facility available in the literature allowing better representation of the sand control device (SCD). The operational procedure includes both single-phase and multiphase injection to cover a wide range of production scenarios across the horizontal well. Moreover, a consistent sand preparation method ensures uniform samples in every test with negligible variance among the set of experiments. Flow performance findings are contrasted with fines migration and production analysis. Post-mortem analysis of samples tracks the change in fines percentage after the test and fines production is also evaluated from fluid samples. Remarkably, the data analysis applies relative permeability measurements to estimate the final impact on sand retained permeability. Retained permeability guarantees a normalized indicator of formation impairment that allows the comparison of different formation sands. Previous works employed fixed pressure drop values to evaluate flow performance without considering the effect of permeability.

Test matrix includes a wide range of aperture sizes to cover the existing PSD based criteria (i.e., D10, 2XD50). Furthermore, this research employs three categorized sand classes from McMurray formation with different PSD and fines content. The PSDs represent a fine, medium-coarse and coarse type of sands. Produced sand and plugging measurements for the different PSDs showed that a specific range for slot aperture could provide an effective sand control while keeping the plugging at a minimum. The optimum range of aperture size narrows down with finer PSD and higher fines content, especially at high flow rates and aggressive production scenarios such as steam-influx.

The effect of water cut proves to be stronger in pore plugging than in sand production. A substantial amount of fines are mobilized at high water cuts which can lead to pore plugging and low wellbore productivity. Fines migration and skin buildup are reduced by increasing the aperture width. Beyond a specific aperture size, there is no improvement regarding flow performance and the risk of excessive sand production increases at high flow rates.

Gas injection showed that steam-breakthrough scenarios represent the most adverse conditions when aperture sizes are too wide. The selection of aperture size is drastically dependent on the operating conditions. Existing design criteria provide conservative aperture recommendations that are more suitable for challenging conditions at elevated flow rates.

The study leads to the elaboration of an optimum screen design that accounts for the effect of flow rate, fluid ratio, fines content, and particle size. Notably, the results denote the importance of good production practices to avoid excessive sand production and plugging. Moreover, laboratory testing allowed the elaboration of performance correlations that adequately predict the response of wire-wrapped screens.

DEDICATION

This thesis is dedicated to my dearest parents: Maria Elizabeth Pallares and Ramon Montero Abad. To the memory of my grandfather, Zorobabel Pallares, and my crazy inspiring grandma, Guenola Mangones.

ACKNOWLEDGMENTS

I dedicate the present thesis to my family, without their support and inspiration this work would not have been possible. I owe my deepest gratitude to my mother and father for their unparalleled love and encouragement in pursuing my dreams.

I am forever thankful to my supervisor Dr. Alireza Nouri, for his guidance and contribution throughout this project. The opportunity to work in this research group will always be appreciated.

I would like to thanks all committee members for their valuable suggestions to improve this study.

I want to express my special gratitude to Total E&P Canada Ltd for their scholarship and continuous support to U of A students. I am truly honored to have received their award. My professional goals are moving forward thanks to your generous support.

My sincere gratitude to COLFUTURO (Colombia) for their financial support during this journey and their commitment to the development and progress of our country.

Also, I would like to acknowledge RGL Reservoir Management Inc. for the technical and financial support and Natural Sciences and Engineering Research Council of Canada (NSERC) for funding this research through their collaborative Research and Development (CRD) Grants Program.

TABLE OF CONTENTS

ABSTRACT ii
DEDICATION iv
ACKNOWLEDGMENTS v
TABLE OF CONTENTS vi
LIST OF TABLES ix
LIST OF FIGURES ix
LIST OF SYMBOLS AND ABBREVIATIONS xii
CHAPTER ONE: INTRODUCTION 1
1.1 Background 1
1.2 Problem Statement 3
1.3 Research Objectives 4
1.4 Research Hypothesis 5
1.5 Research steps 5
1.6 Significance of the work 6
CHAPTER TWO: LITERATURE REVIEW 7
2.1 Steam Assisted Gravity Drainage (SAGD) 7
2.2 Sand production 8
2.2.1 Sand control and flow impairment in SAGD operations 10
2.3 Stand-alone screens 12
2.3.1 Slotted Liners (SL) and SAGD performance 13
2.3.2 Wire-Wrapped Screens (WWS) and SAGD performance 16
2.4 Design of Stand-Alone screens 19
2.4.1 Particle size distribution (PSD) 19
2.4.2 Laboratory testing and experimental set-ups 20
2.5 Previous work on SCD design 24
2.5.1 Pre-Packed studies 25
2.5.2 Multiphase Testing 27
2.5.3 Slurry Testing 28
2.5.4 Pre-Packed and Slurry Testing 30
2.6 WWS in SAGD applications 33
2.6.1 Field Performance of WWS 33

2.7 Summary of Wire-Wrapped Screens Design 34
2.8 Failure of Sand-Control Screens 35
CHAPTER THREE: EXPERIMENTAL SET-UP AND TESTING PROCEDURE 36
3.1 Introduction 36
3.2 Experimental set-up 39
3.2.1 Test cell and accessories 42
3.2.2 Fluid Injection System 43
3.2.3 Measuring and Data Acquisition Unit 44
3.2.4 Collection unit and back-pressure column 44
3.2.5 Test Coupons 45
3.3 Experimental procedure 47
3.3.1 Fluids preparation 47
3.3.2 Coupon and cell preparation 48
3.3.3 Sand-pack preparation 48
3.3.4 Sand-Pack saturation and displacement 49
3.3.5 Fluid injection 50
3.3.6 Postmortem analysis 53
3.4 SRT assumptions and limitations 54
3.5 Measurement uncertainties 57
3.6 Testing repeatability 58
CHAPTER FOUR: SAND RETENTION PERFORMANCE OF WWS IN SAGD OPERATIONS 61
4.1 Introduction 61
4.2 Testing program 63
4.3 Results and discussion 64
4.4 Conclusions 72
CHAPTER FIVE: FLOW PERFORMANCE OF WWS AND THE EFFECT OF SLOT WIDTH ON FINES MIGRATION FOR SAGD OPERATIONS 74
5.1 Introduction 74
5.2 Testing program 76
5.3 Results and discussion 78
5.4 Conclusions 85

CHAPTER SIX: NEW CRITERIA FOR WIRE-WRAPPED SCREEN DESIGN FOR SAGD PRODUCTION WELLS AND PERFORMANCE FORMULATIONS 87
6.1 Design criteria for Wire-wrapped Screen 87
6.1.1 Traffic Light design approach 88
6.1.2 Acceptable performance limits 88
6.1.3 SRT testing assumptions and limitations 89
6.2 The new design criteria 90
6.3 Performance formulations 96
6.3.1 An empirical correlation for sand production 96
6.3.2 An empirical correlation for retained permeability 102
6.4 Conclusions 104
CHAPTER SEVEN: CONCLUSIONS AND RECOMMENDATIONS FOR FUTURE WORK 106
7.1 Main results and contribution 106
7.2 Recommendations for future work 107
7.2.1 Effect of PSD curve and a broader spectrum of sand sizes 107
7.2.2 Effect of clay composition 107
7.2.3 Effect of oil-brine-fines emulsions 108
7.2.4 Effect of radial flow 108
BIBLIOGRAPHY 109
Appendix A: Absolute Permeability from all testing 123
A.1 Absolute Permeability for DC-III Testing 123
A.2 Absolute Permeability for DC-II Testing 125
A.3 Absolute Permeability for DC-I Testing 127
Appendix B: Pressure drop readings of the near-screen zone 129
B.1 Pressure drop for DC-III Testing 129
B.2 Pressure drop for DC-II Testing 130
B.3 Pressure drop for DC-I Testing 131

LIST OF TABLES

Table 3-1. Characteristics of synthetic sand classes 38
Table 3-2. Test matrix for the testing program 38
Table 3-3. Review of sand control evaluation tests (After Montero et al. 2018) 41
Table 3-4. Retained permeability for repeated tests 59
Table 5-1. Relative permeability at residual oil conditions 76
Table 6-1. Performance limits and TLS color code 89
Table 6-2. Sand types characteristics 100
Table 6-3. New PSDs and verification tests for retained permeability 104

LIST OF FIGURES

Figure 2-1. Schematic of an idealized SAGD chamber, after IFP Energies Nouvelles (2017) 8
Figure 2-2. Sand production occurrence and governing forces 9
Figure 2-3. Slotted Liner, after RGL Reservoir Management Inc. 14
Figure 2-4. Slot profile for Slotted Liners 15
Figure 2-5. Wire-wrapped Screens, modified after Premium Screens Company 16

Figure 2-6. WWS designs. (a) Direct Wrapped, (b) Slip-on jacket, modified after Ott (2008) 17
Figure 2-7. Slurry test cell, modified after Wu et al. (2006) 22
Figure 2-8. Slurry SRT set-up scheme, modified after Ballard and Beare (2003) 22
Figure 2-9. Pre-Packed SRT set-up scheme, after Montero et al. (2018) 23
Figure 2-10. Selection guide for Stand-alone screens, modified after Gillispie et al. (2000) 29
Figure 2-11. Screen Efficiency Plot (SEM) for WWS, modified after Constien and Skidmore (2006) 31
Figure 2-12. Effect of the coarser tail on sand production, modified after Chanpura et al. (2012b) 32
Figure 2-13. Failure of WWS components, modified after Mahmoudi et al. (2018) 35
Figure 3-1. Particle size distribution of the tested sand packs and corresponding synthetic distribution. (a) DC-III, (b) DC-II, (c) DC-I 37
Figure 3-2. A schematic of the Pre-packed SRT facility 39
Figure 3-3. Picture of the experimental set-up 40
Figure 3-4. Wire profile and support ribs, modified after Guangxing Screens Co., Ltd 45
Figure 3-5. WWS coupon, (a) picture, (b) design specifications 46
Figure 3-6. Fluid injection program 50
Figure 3-7. Cumulative produced sand for repeatability tests. (a) DC-III, (b) DC-II 59
Figure 3-8. PSD verification of three prepared samples (DC-III) 60
Figure 4-1. Cumulative sand production for different flow rate steps for DC-III. Red and yellow lines represent the sanding limits of 0.15 lb/ft2 and 0.12 lb/ft2, respectively 64
Figure 4-2. Cumulative sand production for different flow rate steps for DC-II. Red and yellow lines represent the sanding limits of 0.15 lb/ft2 and 0.12 lb/ft2, respectively 65
Figure 4-3. Cumulative sand production for different flow rate steps for DC-I. Red and yellow lines represent the sanding limits of 0.15 lb/ft2 and 0.12 lb/ft2, respectively. 65
Figure 4-4. Produced sand at the end of liquid stages for different slot widths, (a) Comparison of three sands, (b) DC-III, (c) DC-II, (d) DC-I 69
Figure 4-5. Produced sand at the end of gas-influx stages for different slot widths, (a) Comparison of three sands, (b) DC-III, (c) DC-II, (d) DC-I 72
Figure 5-1. Core sample sections 77
Figure 5-2. Retained permeability at the end of the liquid stages for different aperture sizes. Red and yellow lines represent the retained permeability limits of 50% and 70%, respectively 78
Figure 5-3. Retained permeability and comparison with design criteria. (a) DC-III, (b) DC-II, (c) DC-I 80
Figure 5-4. Change in fines concentration along the sand pack for different slot widths, (a) DC-III, (b) DC-II, (c) DC-I 82
Figure 5-5. The effect of flow rates and fluid ratio on fines production for different aperture sizes: (a) DC-III, (b) DC-II, (c) DC-I 84
Figure 6-1. Linear x-axis representation of the PSD and tested slot sizes, (a) DC-III (b) DC-II (c) DC-I 91

Figure 6-2. Aperture window for DC-III for regular SAGD conditions, (a) sanding performance, (b) flow performance, (c) overall design window 92
Figure 6-3. Aperture window for DC-II for regular SAGD conditions, (a) sanding performance, (b) flow performance, (c) overall design window 92
Figure 6-4. Aperture window for DC-I for regular SAGD conditions, (a) sanding performance, (b) flow performance, (c) overall design window 93
Figure 6-5. Aperture window for DC-III for aggressive SAGD conditions, (a) sanding performance, (b) flow performance, (c) overall design window 94
Figure 6-6. Aperture window for DC-II for aggressive SAGD conditions, (a) sanding performance, (b) flow performance, (c) overall design window 95
Figure 6-7. Aperture window for DC-I for aggressive SAGD conditions, (a) sanding performance, (b) flow performance, (c) overall design window 95
Figure 6-8. Comparison of predicted versus experimental cumulative produce sand..... 99
Figure 6-9. Predicted and experimental results of cumulative produced sand for different sand classes 99
Figure 6-10. New PSDs implemented for verification testing compared to other PSDs ... 100
Figure 6-11. Predicted and experimental results for verification tests 101
Figure 6-12. Comparison predicted versus experimental cumulative produced sand for verification tests 101
Figure 6-13. Comparison of predicted versus experimental retained permeability 103
Figure 6-14. Predicted and experimental results of retained permeability for different sand classes 103
Figure A-1. Absolute permeability for DC-III tests. (a) All readings, (b) top section, (c) medium section, (d) bottom section 124
Figure A-2. Absolute permeability for DC-II tests. (a) All readings, (b) top section, (c) medium section, (d) bottom section 126
Figure A-3. Absolute permeability for DC-I tests. (a) All readings, (b) top section, (c) medium section, (d) bottom section 128
Figure B-1. Near-screen zone pressure drop for DC-III tests..... 129
Figure B-2. Near-screen zone pressure drop for DC-II tests 130
Figure B-3. Near-screen zone pressure drop for DC-I tests 131

LIST OF SYMBOLS AND ABBREVIATIONS

Symbols

A_{ub}	Upper bound for aperture window
A_{lb}	Upper bound for aperture window
C_c	Coefficient of curvature
DC-I	Class I oil sand for Devon Pike I
DC-II	Class II oil sand for Devon Pike I
DC-III	Class III oil sand for Devon Pike I
DC-IV	Class IV oil sand for Devon Pike I
D_{10}	Sieve opening size that retains 10% of the particles in the sample
D_{25}	Sieve opening size that retains 25% of the particles in the sample
D_{30}	Sieve opening size that retains 30% of the particles in the sample
D_{40}	Sieve opening size that retains 40% of the particles in the sample
D_{50}	Sieve opening size that retains 50% of the particles in the sample
D_{70}	Sieve opening size that retains 70% of the particles in the sample
D_{90}	Sieve opening size that retains 90% of the particles in the sample
D_p	Representative particle diameter
DEM	Discrete Element Methods
f_c	Fines content in the sample
K_{abs}	Absolute permeability
$K_{abs,\ i}$	Initial absolute permeability
$K_{abs,\ bottom}$	Final absolute permeability of the bottom section
K_{rel}	Relative permeability

K_{ret}	Retained permeability of the near-screen zone
L_b	Length of the bottom section of the sand pack
m_t	Total mass of sample for fines content analysis
m_f	Mass of fines
P_{sand}	Cumulative produced sand
PSD_c	Particle size distribution parameter
q_w	Water flow rate
μ	Fluid viscosity
μ_w	Water viscosity
SC	Sorting coefficient
SL-SC	Slotted liner with straight cut slots
SL-RT	Slotted liner with rolled-top slots
S_{or}	Residual oil saturation
UC	Coefficient of uniformity
V	Fluid superficial velocity
v_g	Superficial gas velocity
v_w	Superficial brine velocity
v_o	Superficial oil velocity
w	Aperture width or size
W_{cut}	Water cut
w_D	Dimensionless effective formation size
ρ	Density of the fluid
ΔP_b	Pressure drop at the bottom section of the sand pack

δC_f	Absolute uncertainty of fines concentration
δK_{abs}	Absolute uncertainty of absolute permeability
$\delta K_{abs,\ i}$	Absolute uncertainty of the original absolute permeability
$\delta K_{abs,\ bottom}$	Absolute uncertainty of the final absolute permeability (bottom)
δK_{rel}	Absolute uncertainty of relative permeability
δK_{ret}	Absolute uncertainty of retained permeability
δm_f	Absolute uncertainty from the mass of fines measurement
δm_t	Absolute uncertainty from sample mass measurement
δp	Absolute uncertainty from pressure drop reading
δq	Absolute uncertainty from flow rate measurement
δW_s	Absolute uncertainty of produced sand
δW_b	Absolute uncertainty from weighing balance measurement

Abbreviations

CSC	Critical salt concentration
LPSA	Laser particle size analysis
MMS	Metal mesh screen
OFA	Open-to-flow area
PMS	Premium Mesh Screens
PPS	Precise-punched screen
PSD	Particle size distribution
SAGD	Steam Assisted Gravity Drainage
SEM	Scanning electron microscope
SL	Slotted liner

SOR	Steam-oil ratio
SPC	Slot per column (number of slot in one column of a 7” liner)
SRT	Sand retention test
WWS	Wire Wrap Screen

CHAPTER ONE: INTRODUCTION

1.1 Background

The rich petroleum resources encountered in Alberta's oil sands represent a vast energy asset of 166.3 billion barrels of bitumen (AER, 2015). Currently, most of the extraction from heavy oil assets relies on in-situ recovery methods. Steam Assisted Gravity Drainage (SAGD), a thermal technique, has emerged as the primary commercial technology to effectively recover bitumen in western Canada reservoirs (Kisman and Yeung 1995; Edmunds and Chhina 2001; Gates et al. 2007).

SAGD processes employ two horizontal wells and steam injection to reduce the viscosity of bitumen. Steam is injected into the reservoir through the upper well and the heated oil and condensed water flow downwards to the lower wellbore (producer well) due to gravity assistance (Butler, 1992).

Thermal operations are conducted in bitumen-bearing sands that are characterized by their unconsolidated nature. Hence, sand production and fines migration are inherent features during production operations. SAGD completions employ screen or liners to control the influx of particles and keep the integrity of wellbore and surface facilities on acceptable conditions. The main function of any sand control device (SCD) is to provide sand retention at the desirable levels while allowing the inflow of reservoir fluids and the discharge of fine materials to avoid plugging of slots and porous media (Bennion et al. 2009). Additionally, screen pipes provide the support for any flow control device installation, and they must endure the mechanical and thermal loads during the well life.

SCDs vary in manufacturing, open-to-flow area, retention media, and cost. Liner cost usually plays a vital role in the design and selection of the screen due to the high expenditure of SAGD projects. Stand-alone screens such as slotted liners (SL), wire-wrapped screens (WWS) and precise-punched screens (PPS) are extensively used in SAGD wells. Low OFA devices such as SL have historically been selected due to their lower cost. However, the plugging tendencies exhibited by this device have given more attention to devices with higher OFA, such as WWS and PPS (Romanova et al. 2014).

The performance of SCD is evaluated in terms of sanding prevention and flow assurance. The sand retention ability of the SCD is mostly related to the aperture size and its relation to the particle size distribution (PSD) (Coberly 1937; Markestad et al. 1996; Meza et al. 2003; Ballard and Beare 2006; Bennion et al. 2009; Chanpura et al. 2011, 2012a, 2012b). Although it seems reasonable to think that OFA has an impact in sand production, recent results show that their influence is not as strong as the slot aperture (Mahmoudi 2017; Fattahpour et al. 2018). On the other hand, flow performance relates to the OFA and the capability of the slots and neighboring pores to remain unplugged (Kaiser et al. 2002; Furui et al. 2007; Bennion et al. 2009; Romanova et al. 2014; Williamson et al. 2016). The relation between pore size distribution and the fines content plays a significant role in pore clogging, especially when it is linked to inappropriate production procedures under high flow rates (Williamson et al. 2016). Also, in-situ phenomena such as scaling and corrosion damage contribute to formation damage and screen plugging (Romanova and Ma 2013).

Plugging tendencies and maintenance of long-term wellbore performance have been recognized as critical factors in SAGD projects, as plugging can cause a high-pressure difference between the well-pair (Fattahpour et al. 2016a and 2016b; Williamson et al. 2016). This rise in pressure drop reduces oil production, increases the steam-oil ratio (SOR), disturbs the steam trap operation leading to potential steam-breakthrough and jeopardizes the uniform growth of the steam chamber (Bennion et al. 2009; Williamson et al. 2016).

It is believed that the high OFA of WWS (6-12%) delivers a superior response regarding flow performance when compared to other devices (Devere-Bennett 2015; O'Hara 2015; Anderson 2017). Additionally, the profiled wire geometry and stainless steel manufacturing reduce the risk of excessive plugging. The industry is moving towards exploiting more challenging reservoirs, and WWS may be beneficial for low-quality sands with a high amount of fines and reactive clays.

The industry and academy have spent several decades studying sand control and scheming protocols for SCD selection and design. First studies traced back to Coberly (1937), who proposed through simple experiments an upper limit of $2xD_{10}$ for slot width. Similarly, many authors have provided recommendations of slot size based on one or more points of the PSD (Rogers 1971; Gillispie et al. 2000; Ballard and Beare 2012). However, SCD design and

selection should consider factors other than PSD. Previous approaches neglect factors such as flow rates, fluid properties, flow ratios, formation-fluids interaction, and stresses.

Additionally, experimental assessments require closer emulation of specific field conditions. Notably, in SAGD wells there is a need for establishing a reliable protocol based on field data or physical model testing in the lab for SCD design specifications (Montero et al. 2018). Design criteria should not limit to provide an aperture size that controls sanding but also discretizes the performance under different production scenarios.

1.2 Problem Statement

The selection of optimum aperture sizes for WWS has been extensively examined over the years for conventional petroleum operations (Rogers 1975; Gillispie et al. 2000; Ballard and Beare 2012). SAGD operators have relied on laboratory testing to evaluate the sanding and flow performance of WWS and field experience to suggest an aperture selection. Moreover, existing design criteria provide aperture ranges or even fixed values based on one or two points of the PSD (e.g., <2XD50, D30). This approach neglects the influence of operational conditions, flow rates, fluid chemistry, stress, mineralogy and assumes that slot size and the sand face condition remains constant. In fact, design criteria of WWS for thermal operations often follow the empirical rule of thumbs based on other devices such as SL (0.004in less than equivalent SL selection) (Fattahpour et al. 2018). Relating the performance of one device to another is not appropriate since the particles retention mechanisms of each device are different and operationally dependent. Furthermore, previous experimental assessments employ small SCD samples that might not be representative of the actual OFA and poor sample preparation procedures (Montero et al. 2018; Ktob 2019). Therefore, previous work requires verification and validation.

Despite the several years spent on sand control evaluation for SAGD projects, there is still uncertainty regarding the selection of the SAS completion. The central debate is related to the dominant factors of SCD performance, slot aperture or OFA. SAGD wells typically yield low production rates that questions if high OFA devices are worth employing considering the increase in the cost of other devices. For instance, comparative studies show that differences in OFA not necessarily translate in significant improvements of flow performance and that slot aperture is the stronger factor in SCD design (Mahmoudi 2017; Fattahpour et al. 2018).

However, additional OFA provides the benefit of countering the impact of severe and progressive plugging (Romanova et al. 2014). In brief, the application of WWS must be justified, and further experimental work and field indicators help to improve the selection criteria.

This thesis employs a large pre-packed testing facility to assess the performance of WWS. Testing operation procedures are modified to better capture typical field flow rates, fluid ratios, fluid properties, and production scenarios. Also, consistent sand preparation and packing methods are employed in every experiment to ensure the representativeness and uniformity of the sample. The impact of previous characteristics in sand production and plugging are also discussed. Additionally, both single-phase (brine flow) and multiphase scenarios (oil, water, and gas) are evaluated to provide a broader insight into WWS's performance under SAGD environments. This approach will allow the evaluation of the impact of flow rate, water cut, gas rates, and fines content. Finally, experimental results fund the elaboration of WWS design criteria for representative PSD of the McMurray formation.

1.3 Research Objectives

The primary objective of this research is to improve the selection of WWS apertures by implementing the results of laboratory testing on different sands with representative PSDs of the McMurray formation. The novel WWS design criteria are based on the sand production weight as the sand control indicator and retained permeability as the flow insurance indicators. By employing three PSD's with different fines content and sizes, the final design criteria and empirical formulations will represent a relevant industrial tool.

This study intends to analyze the movement of fines through the sand pack, its repercussion on flow impairment, as well as the flow rate and water cut dependence. It seeks to evaluate the assumption of less flow convergence effect on solids detachment and to appraise the apparent great control of WWS in retaining different PSDs with a single and equal slot size. The research also assesses the effect of water cut and steam-breakthrough scenarios on sand production and plugging evolution.

1.4 Research Hypothesis

Logic states that particles production increases when the slot aperture increases; hence this is expected to happen in WWS completions. The critical aspect of the design is to find the perfect balance between produced sand and flow performance.

The high OFA seems to attribute WWS superior flow performance, usually reported as low-pressure drop outcomes. Besides the OFA, the increase in sand production observed in previous tests (O'Hara 2015; Devere-Bennett 2015) would in turn also enhance the retained permeability of the screen and near screen zone. The lower pressure drop infers the effect of larger OFA and apertures on fines migration and plugging. However, existing studies do not provide any analysis for the fines movement after laboratory testing. The close distance between the slots generates fewer convergence effects, and the high OFA reduces the velocity. Consequently, the drag forces acting on particles depends both on the flow rate (velocity) and also on the screen geometry. By measuring the fines accumulation in the zone close to the coupon, it is possible to correlate fines content with plugging. It is expected that WWS allows substantially more fines to be washed out of the sample.

There is apparent optimum retention provided by a single aperture of a WWS over a different range of particle size distributions. The probabilities for sand particles of varying sizes to bridge increase as the area also does, sand grains would eventually achieve stability (Anderson 2017). However, the previous observation may be related to the implementation of narrow apertures that logically will promote bridging for a wider range of sands. WWS may be compared to an SL of extreme slot density; it is believed that the proximity between slots helps to control different grain distributions. However, in the event of bridge disruption during challenging flow conditions, the close distance increases the chances of drastic particle production.

1.5 Research steps

This research is performed in the following steps:

1. A critical review of the current design for SCD's and laboratory approaches implemented by previous studies.

2. Identification of the limitations and opportunities for improvement of current laboratory testing. Design of a new experimental operating procedure.
3. Perform single-phase and multiphase testing. Analyze the effect of slot apertures, flow rates and production scenarios on WWS's performance.
4. Generate design criteria for WWS accounting for both sand production and plugging.

1.6 Significance of the work

This research provides comprehensive knowledge to further enhance the completion strategies in SAGD projects, primordial to ensure the effective extraction of oil sand assets. Sand production impacts the integrity of the wellbore operation; from down-hole equipment to surface facilities may suffer erosion and collapse due to the abrasiveness of the sand particles. Moreover, sand can accumulate in the long horizontal well sections or damage the pumps, blocking the free flow of fluids. The amount of sand reaching surface have to follow special treatment, increasing the costs of the operation. Therefore, sanding jeopardizes the safety and economic viability of thermal projects. Accordingly, there is an imminent necessity to improve the selection and design of SCDs to avoid the issues mentioned above. The liner or screen should retain the sand and allow the production of fluids while providing reliability for a long-term, reducing the workover and remediation activities.

SLs and WWSs represent the typical means to control the production of sand. This research will yield an applicable industry output, consisting of objective design criteria for WWS based on a better replication of SAGD operating conditions in laboratory testing. Evaluation of the performance of the screen samples with various representative sands of McMurray formation broadens the understanding concerning the influence of slot apertures, flow rates, and fluid characteristics on the sand retention and plugging tendency (fines migration) of WWS. Moreover, the study would decrease the uncertainty when it comes to the selection and design of SCD.

CHAPTER TWO: LITERATURE REVIEW

2.1 Steam Assisted Gravity Drainage (SAGD)

The extensive heavy oil resources encountered in Alberta oil sands place Canada at the third place in the list of global proved reserves accounting for the 10.3% of world oil reserves (CAPP 2016). According to Alberta Energy Regulator (AER), the cumulative oil reserves of Canada to the end of 2017 were 170 billion barrels, tar sands from the province of Alberta account for almost 97% of those reserves (165.6 billion barrels). This kind of resources commonly called bitumen resources play a significant role in Canada's economy, hence the importance of efficient extraction.

Current development of oil sands is mostly carried out through thermal in-situ operations such as Steam Assisted Gravity Drainage (SAGD) and Cyclic Steam Stimulation (CSS) (Gates et al. 2007; Zhang et al. 2007). Due to the extremely high viscosities that characterize the bitumen, heat is provided to the unconsolidated formations to enhance the mobility of the oil and facilitate the production towards surface facilities.

SAGD operations combine two technologies: the injection of large volumes of steam and horizontal wells (**Figure 2-1**). The success of this procedure relies on two horizontal wells intended to be parallel with a separation distance of 4 to 6 meters. The upper well serves as a steam injector and the lower one as the production well. The continuous injection of steam creates a vapor chamber that rises through the formation allowing the progressive contact of cold bitumen and steam. The bitumen is heated, and its viscosity decreases to low levels, 8-20 cp (Devere-Bennett 2015). This allows the assisted gravity flow of oil and condensed stem around the heating chamber towards the producing well.

The temperatures reached during the SAGD process typically surpass the 200°C, and the length of the horizontal section ranges between 500m and 1000m in sand layers from 150m to 450m of depth. At these depths, the sand layer is too deep to be extracted through conventional surface mining, and approximately 80% of Alberta's oil sands cannot be developed using excavation (Alberta Government, 2015).

For SAGD projects the lifespan of the wells is critical, it is pertinent to consider the interaction of sand control methods with the reservoir during the life cycle of the field

(Fattahpour et al. 2016a). Screen installation, production parameters, and thermal conditions should be taken into account to prevent a change of equipment and remedial procedures.

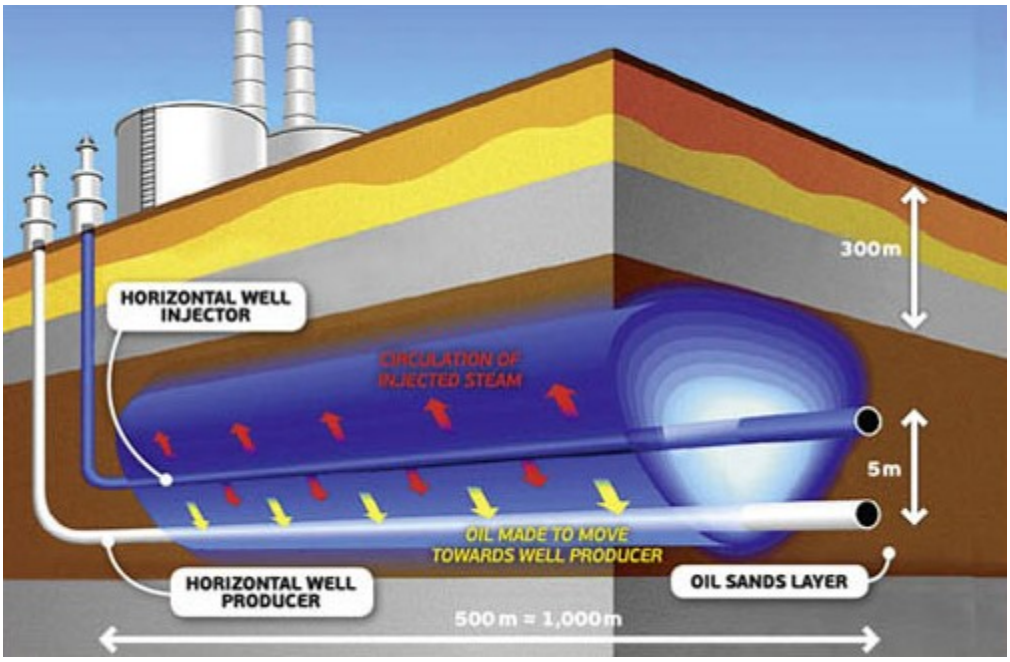

Figure 2-1. Schematic of an idealized SAGD chamber, after IFP Energies Nouvelles (2017)

2.2 Sand production

The production of formation sand is a serious problem encountered in many areas during oil and gas extraction. Excessive production of sand particles raises the risks for integrity failures. An inadequate approach could lead to productivity loss, mechanical failure of surface and down-hole equipment's, cost increase due to sand produced disposal and treatment, formation collapse, tubular collapse, and skin damage.

Sanding phenomena are not new in the petroleum industry; it has been present since the early beginnings of hydrocarbon production (Matanovic et al. 2012). Oil sands, which are geologically young formations, are characterized by negligible compressive strength resulting from their unconsolidated nature. This kind of reservoirs favors the production of solids where the flow itself is enough to overcome the forces that hold the grains together (Penberthy and Shaughnessy 1992).

Reservoir formations release sand or fines particles if the forces caused by fluid flow, pressure differentials, and drag force, exceed the opposing contact forces (Islam and George

1989) (**Figure 2-2**). Rock strength, given by the degree of cementing material, capillary pressure and friction between the grains act as the natural barriers to solids detachment or mobilization (Suman et al. 1985; Penberthy and Shaughnessy 1992; Ott and Woods 2003; Oyeneyin 2015). Whereas for fine particles and clay, electrostatic forces represent an essential resistance factor.

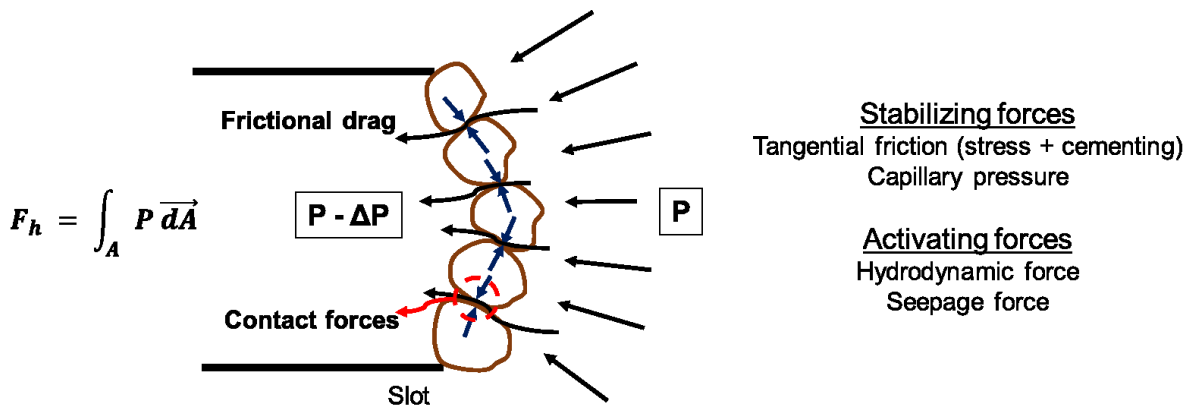

Figure 2-2. Sand production occurrence and governing forces

The intensity and severity of sand production vary with the degree of cementation of the grains of the producing sand and with the way the wells are completed. The forces caused by the flow of fluids fall into two types of factors affecting sand production (Bratli and Risnes, 1981). An operational factor that takes into account the pressure drop and flow rate, and the driving factor that groups the local interstitial velocities, saturation distributions and drag forces due to the viscosity-velocity ratio. In non-cohesive sands like those found in western Canada, the flow of solids along with bitumen is practically unavoidable.

According to Islam and George (1989), the overburden pressure acting on horizontal wells increases the stability of sand bridges as the gravitational forces are collinear with inertial forces. However, this phenomenon was said to occur when production is only from the top part of the horizontal well.

Tippie and Kohlhass (1973) studied the stability of sand arches around perforations. The results showed that gradual increases in flow rate allow lower sand production than a sudden increase in a full rate. Moreover, small arches have shown better stability, and the shape of the arch seems to depend on the state of stresses (Clearly et al. 1979).

Islam and George (1989) evaluated the sand retention performance on horizontal wells using an experimental setup on WWS. Interestingly, the authors concluded that higher flow rates could enhance sand bridge stability in horizontal wells, the opposite of vertical wells. However, the impact of flow rates was not evaluated concerning the slot size, and the conclusion may be limited to the specific range of apertures and sand sizes.

2.2.1 Sand control and flow impairment in SAGD operations

Sand control methods such as gravel packs and plastic consolidation are not affordable in SAGD projects due to the high cost and operational difficulties for deployment in high temperature and long horizontal wells. On the other side, pre-packed and expandable screens have not selected due to their higher cost when compared to other SCD.

SAGD operators have adopted Stand-alone screens (SAS) as a cost-efficient and straightforward solution for sand control. Presently, SL, WWS, and Precise-Punched screens (PPS) are the primarily employed devices. However, the selection and design of the SCD must be customized to the characteristics of the rock material, the estimated flow behavior (Chanpura et al. 2011) and the expected lifetime of the well to avoid premature failures (Fattahpour et al. 2016a). Sand control techniques are not definitive preventive measures (Penberthy and Shaughnessy 1992; Gillespi et al. 2000; Chanpura et al. 2011), particularly in thermal methods like SAGD, where operations are subjected to certain restrictions and changes in the operating conditions during the development of the field.

For instance, factors such as the reservoir thermal expansion, poroelastic sand expansion, and shear dilation generate an increase in the effective stress around SAGD wells. Regarding mechanical integrity of the liner or screen, this may cause failure or collapse due to load contact points and constraint of thermal expansion of the pipe (Xie et al. 2008; J. Van Vliet and Hughes 2015; Ma Guobin et al. 2015). On the other side, sand retention performance improves over time as the compaction provides additional strength to the collapsed sand (Hodge et al. 2002; Ballard and Beare 2003; Fattahpour et al. 2016b). However, this enhancement in sand retention is achieved at the cost of a significant reduction of the near-screen zone permeability (Guo et al. 2018).

Moreover, during the life cycle of a well, different fluids break into production at various stages. Water and gas flow complicate solids control. An increase in sand production is observed when water flows along with oil because of the preference of particles to be water-wet and consequent reduction in capillary forces (Wu & Tan 2001; Vaziri et al. 2002; Han and Dusseault 2002; Ballard and Beare 2006; Bennion et al. 2009). The dispersive action of brine, especially over small particles (fines), generates detachment and mobilization of these solids (Ballard and Beare 2006). Furthermore, when water comes into production, companies tend to increase rates (to maintain oil production) which generate more drag forces (Penberthy and Shaughnessy 1992). In SAGD operations, the production of bitumen is always accompanied by water (Mahmoudi 2017), as a result of the steam condensation, circulation phase, and connate water. On the other hand, gas-influx events generate instability of the sand bridges that can lead to erosion and damage problems due to the high flow velocities (Bennion et al. 2009; Romanova et al. 2014). Excessive sand production can be obtained under these conditions when gas is accompanied by liquid flow (Fattahpour et al. 2018).

Furthermore, temperature changes, although not entirely clear, influence the production of sand. High temperatures can damage the cementing and granular bonding (Penberthy and Shaughnessy 1992). An increase in temperature is also known to induce changes in rock wettability and relative permeabilities (Bennion et al. 2007), hence promoting different flow patterns and drag forces. Romanova et al. (2015 & 2017) and Williamson et al. (2016), reported the development of smectite particles coating grains after elevated temperatures were achieved due to steam injection in SAGD wells. However, the formation sands evaluated in the study had mineralogy rich in feldspar, chert, and traces of chlorite which differs from the clean and mainly composed quartz sands found in the McMurray formation.

Salinity and pH of water in SAGD wells is continuously evolving. Mixing and production of the steam condensate and formation water result in different levels throughout the wellbore operation. The salinity of the water decreases with time while pH increases (Mahmoudi et al. 2016b). The production of oil and the mixture of water and condensate generates a reduction in brine salinity. Whereas ion exchange occurs between the adsorbed cations and hydrogen (H+) in solution, produce minor increments on levels pH (Mohan et al. 1993).

Bennion et al. (2009), briefly reported experimental results on the effect of brine pH on plugging tendencies of slots by examining pressure drop readings. The authors pointed out that clays encountered in McMurray formation, kaolinite and illite, exhibit de-flocculation at high values of pH as a result of new electrical charges distribution. Significant reduction in pressure drop was observed after treating the fluid with HCL (Low pH).

Mahmoudi et al. (2016b) carried out extensive tests in order to evaluate the effect of brine salinity and pH on the near-screen zone using a pre-packed experimental setup. From the results, it was concluded that higher pH values trigger the release of fines and that its effect increases proportionally with flow velocity. The increase in pH rendered lower retained permeability. Further, an inverse relation between salinity and permeability impairment was also reported. One crucial aspect of the previous research is that only fines production showed dependence on pH and salinity, sand production was not affected. Low salinity levels and high pH values alter the electrical charges of clay materials and the close-distance repulsive forces between fines and grains (Khilar et al. 1984).

The aspects above demonstrate how sand control screen selection and design must consider a variety of constraints and changes throughout the well-life. Sand production and formation damage are not static phenomena.

2.3 Stand-alone screens

Stand-alone screens such as SL, WWS, and PPS provide the cheapest and more suitable option for thermal projects. SCD selection incorporates elements such as expected reliability, initial cost, productivity impairment, sand quality (PSD), reservoir heterogeneity and characterization, fines content, the possible cost of reparation and workover, production estimates and company policies (Suman et al. 1985).

The filtration ability of SCDs relies on what is called, mechanical retention (Penberthy and Shaughnessy 1992; Suman et al. 1985). The SCD serves as a filter to restrain the entry of solid particles into the tubing system and surface facilities. The conception is that certain grains of sand will be retained and those grains will provide additional retention to the remaining sand grains.

Some authors have stated that mechanical retention using stand-alone completion lack of effectivity when the formation sand is poorly sorted, and the uniformity coefficient (Uc = D40/D90) is high (Schwartz, D. H. 1969; Tiffin et al. 1998; Gillespie et al. 2000; Oyeneyin 2015). According to Gillespie et al. (2000), plugging tendencies would increase with these characteristics, and the sensitivity to these variables grows with smaller particle sizes. Although there seems to be agreement that sorting and uniformity have an impact on screens performance, there is no robust criterion that supports the influence of broad grain size distribution, neither a particular percentile of the PSD.

Ballard and Beare (2006) did not find a clear relationship between the uniformity coefficient (UC) and plugging through experimental tests on Dutch twill screens. Two points of the particle size distribution (D_{40} and D_{90}) only provide an idea of the sorting and do not adequately represent the whole distribution. Constien and Skidmore (2006) found a better correlation between PSD and screen performance when implementing the ratio d50/Uc against sanding and pressure drop results. On the other side, Chanpura et al. (2011) stated that the most governing characteristic of sand retention is found in the variation of the grain sizes coarser than the slot size.

2.3.1 Slotted Liners (SL) and SAGD performance

Slotted liners consist of a pipe manufactured with small slots machined by a rotating saw (**Figure 2-3**). Solid-state laser technology sometimes is implemented, although this implies higher costs of manufacturing. The tubular used are commonly carbon steel on standard grades. SL prevent the production of sand based on the width of the slots, creating a filter that allows bridging of formation material at the entrance of the liner slots and fluids production.

Figure 2-3. Slotted Liner, after RGL Reservoir Management Inc.

Typically, the industry employs the "gauge" terminology when referring to slot sizes (Suman et al. 1985). Slot "gauge" represents the width of the opening in thousands of an inch. For instance, a 20-gauge screen has slot openings of 0.020 inches. Commercial slot widths range from 0.010 inches to 0.090 inches (0.3mm to 2.286mm) (Petrowiki, 2017). A particular historical drawback of SL manufacturing was the difficulty to reach very narrow slot sizes (Xie et al. 2008).

SLs are easier to install and generally used in wells of low productivity where it is not economically feasible to cover the costs of premium sieves or other screens. Since SAGD horizontal wells are associated with low flow rates, SL provides the most straightforward and cheapest method for sand retention. Besides the previous characteristics, SL offers higher mechanical strength regarding tension, compression, and bending compared to other SCD (Xie et al. 2008; Van Vliet and Hughes 2015). A staggered pattern is usually employed because it preserves most of the original strength of the pipe (Ott et al. 2003). The typical longitudinal separation between slot rows is 6 inches.

SL delivers the lowest OFA among stand-alone screens which depends on the slot density and the slot width. Standard slots specifications would result in OFA between 1 to 3%. OFA

corresponds to the area of slots divided by the total surface area (Matanovic et al. 2012). The lower the OFA the fastest the device can achieve severe plugging.

Three slotted liner configurations are available based on the profile of the slots (**Figure 2-4**). Standard straight-cut slots provide the same width along the slot, and a single plunge blade is used for manufacturing. The keystone shaped slots present an inner width larger than the outer width, providing a mechanism that reduces plugging tendencies by facilitating the passage of produced sand grains and fines through the wider section of the slot (Bennion et al. 2009; Fermaniuk 2013). Two separate blades plunging at different angles create the keystone shape at the desired aspect ratios (outer width/inner width). Rolled/seamed top slots are a variation of keystone slots. The application of longitudinal stresses on the surface of the slot increases the aspect ratio by plastically deforming the aperture around 1mm inwards.

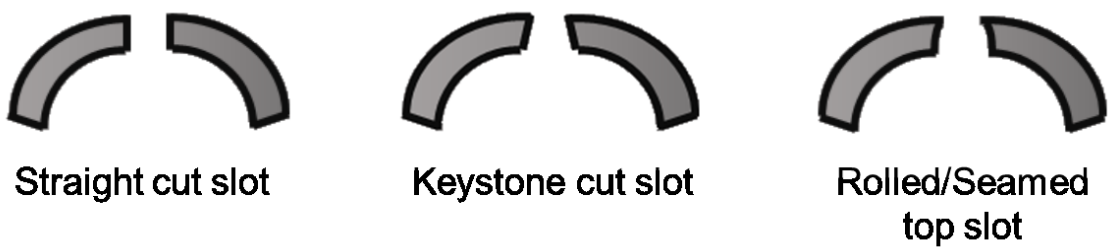

Figure 2-4. Slot profile for Slotted Liners

Any SCD induce alteration of the flow streamlines in the porous media close to the screen (Kaiser et al. 2002; Chanpura et al. 2011). This flow disturbance is commonly referred as convergence, and play a crucial role in the screen performance since the pressure drop caused may boost fines displacement, reducing the retained permeability (Mahmoudi et al. 2017). Some authors have related the pressure drop through screens to an additional skin factor (Markesad et al. 1996).

Kaiser et al. (2002) stated in their work that the pressure loss through an open slot is negligible compared with the pressure drop induced by the flow convergence related to slot distribution or spacing. Slot density has a considerable effect on the distance at which the flow start to converge from the formation sand. If the pressure drop performance of a slot with a certain width is compared to two slots of half-width maintaining the same inflow area, the convergence streamlines initiate deeper into the formation sand for the wider single slot

(Ott et al. 2003). Therefore, pressure loss for the wider slot is expected to be higher than the two slots; narrower slots grant low pressure-drop for the case of constant flow area is kept constant. Again, this highlights that the design of SLs should aim to provide not only the correct aperture sizing but also slot spacing. On the other side, close spacing of slots may reduce the "range of bridging," where the bridging stability of a slot affects the performance of surrounding slots (Coberly 1937); this is called slot to slot interaction.

2.3.2 Wire-Wrapped Screens (WWS) and SAGD performance

Wire-wrapped screens consist of a continuous triangular or trapezoidal wire wrapped onto a base pipe, ribs or rods usually support the wires. The final result is a single helical slot that functions as the sand control medium with a large OFA, adequate integrity and plugging-resistant due to the wedge-shaped wire. The OFA of WWS ranges from 6% to 12% (Romanova et al. 2014) and depends on the slot size, wire thickness and the screen percentage per joint. The components of a WWS can be observed in **Figure 2-5**.

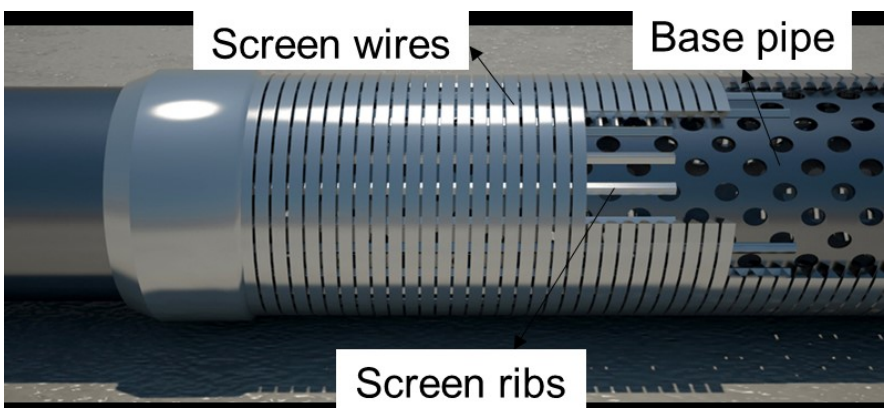

Figure 2-5. Wire-wrapped Screens, modified after Premium Screens Company

The wire jackets are fabricated in stainless steel. AISI 304L or 316L steel wires are generally used in order to provide a corrosion resistant feature (Romanova et al. 2014; Van Vliet and Hughes 2015). There are two common commercial designs available (**Figure 2-6**). For Direct Wire-wrapped Screens, resistance welding is applied to set the wires over a rod based system that is directly in contact with the base pipe. On the contrary, for slip-on jacket designs, there is an annular clearance between the screen ribs and the base pipe outer diameter. This clearance is the result of separate manufacturing of the screen over a mandrel larger than the base pipe (Van Vliet and Hughes 2015). This procedure allows for base pipe manufacturing

tolerances. Direct-wire-wrapped screens are more robust regarding mechanical integrity than the jacketed option. The base pipe supports applied loads, and the screen is more reliable during installation.

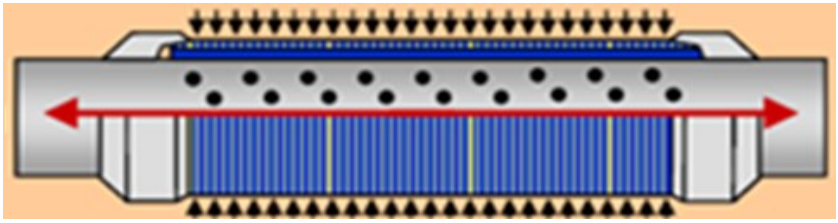

(a)

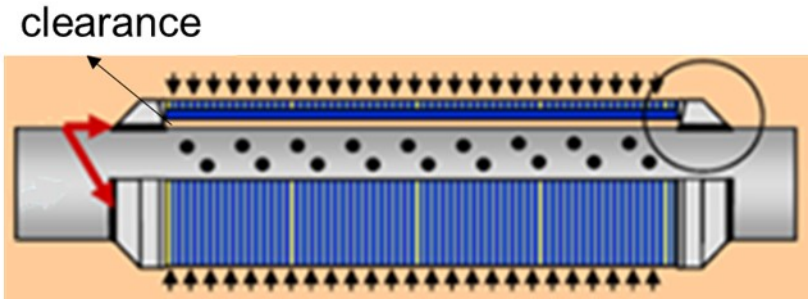

(b)

Figure 2-6. WWS designs. (a) Direct Wrapped, (b) Slip-on jacket, modified after Ott (2008)

Base pipes employed in the industry are usually perforated, although, slotted pipes are also available. The base pipe provides structural support with higher OFA than the wire screen so that the flow losses and pressure drop through the base pipe are less than the flow losses through the wire mesh (Xie et al. 2008). These perforations range from 0.375 inches to 1.0 inch in diameter and usually arranged in a diamond pattern to provide robust mechanical strength (Van Vliet and Hughes 2015). Manufacturing techniques of WWS allow reaching a broad range of sizes, including narrow slots of 0.005 inches.

WWSs are more expensive compared to SL due to the material and the design employed. Cost is one of the main reasons why SL are usually selected over WWS in SAGD operations (Romanova et al. 2014; Fattahpour et al. 2018). The main advantage of WWSs is their large OFA that translates into lower pressure drops and productivity impairment resistance. Additionally, the close distance between wire slots may decrease the effect of flow convergence, enhancing the near wellbore permeability (Kaiser et al. 2002; Mahmoudi

2017). However, the additional OFA of WWS does not necessarily translate into better performance than SL (Fattahpour et al. 2016; Fattahpour et al. 2018). Recent studies show that pressure drop trends do not always follow the differences in OFA (Mahmoudi et al. 2018).

Darcy's linear equation does not capture the additional pressure drop generated by convergence streamlines (Markesad et al. 1996; Chanpura et al. 2011). Interpretation of pressure data from laboratory testing must consider this effect (Chanpura et al. 2011). When the fluid approximates the openings, velocity increases and so does the drag force. Fines movement may be intensified in the zone close to the screen. Fluid velocity through the wire apertures will rise by a factor of 10 to 20 controlled by aperture size and width of the wires (Markesad et al. 1996). The converging flow results in a differential pressure that is higher than expected from the Darcy equation, where it appears as the possible skin factor. In this way, the inflow properties of the screen are very dependent on the permeability of the adjacent thin layer of sand. Romanova et al. (2014) suggested that WWS also provide better plugging performance due to the micro-smoothness of the surface of the wire. This feature is the result of the cold extruded procedure used in manufacturing and reduces the clay adhesion tendency. However, no additional data was provided to support this statement.

Knowing the conditions of the well and the estimated productivity is essential when it comes to WWS selection. If estimations and design are not correct the use of WWS may not provide any other benefit regarding sand control and productivity than SL (Fermaniuk 2013; Fattahpour et al. 2016a and 2018). Considering the mechanical constraints of WWS, adequate deployment of the screen is crucial to successful control and to avoid premature failures. The industry had experienced some difficulties for which it was not primarily applied in SAGD operations despite their benefits. Screen erosion, installation problems, and the production of solids take part in these challenges (Romanova et al. 2014).

Interestingly, WWSs were used for early SAGD pilots because of the associated better productivity and the difficulties for SL manufacturers to produce the required narrow slots (Xie et al. 2008). More recently, WWS and other high OFA devices have gained attention, and its implementation has been proposed due to laboratory testing (O'Hara 2015; Anderson 2017) and field indicators such as low well-pair pressure differences (Romanova et al. 2014;

Williamson et al. 2016). Especially for low-quality reservoirs, the application of WWS is a recommended completion strategy (Romanova et al. 2015; Williamson et al. 2016).

The mechanical and structural strength of WWSs is one of the main concerns in SAGD projects. Thermal stresses plus the installation and operation loads can deform the screen that is subjected to thermal-induced cyclic loads. Xie et al. (2008) examined the stability of WWS during installation. Authors such as Ma et al. (2015) and Van Vliet and Hughes (2015) have addressed this topic for the different components of the WWS (base pipe, screen, welded points, rods) considering the cyclic thermal conditions created by operational shutdowns and workovers procedures using finite-element modeling. One of the main risks is the closure or expansion of the spacing of the slots due to the deformation of the pipe components. The constraint of thermal expansion generates compression loads (Xie et al. 2008), and it is sufficient to yield the entire liner in compression (Van Vliet and Hughes 2015).

WWSs offer higher torque allowance than SL, but they are weaker in tension, compression, and bending. As a quality control, an aperture change by less than +0.001/-0.002 inch or 25.4 microns during thermal service is considered as a threshold (Xie et al. 2008). Studies by Xie et al. (2008) and Van Vliet and Hughes (2015) showed that WWS delivers excellent stability when it is adequately designed and perfectly withstand the different loads encountered in SAGD wells.

2.4 Design of Stand-Alone screens

The design of SCD should involve several factors such as grain size, specific operating conditions, flow rates and fluid properties (Fattahpour et al. 2016a; Mahmoudi et al. 2016a). Formation sand characterization is the first step, and particle size distribution (PSD) is the main input to any sand control design.

2.4.1 Particle size distribution (PSD)

Laser-particle size analysis (LPSA) and sieve analysis have been widely utilized for determining grain size distribution. As reported by Ballard and Beare (2003) and Chanpura et al. (2011) each method presents advantages and disadvantages. Clay content determination in sieve analysis is influenced by the adhesion of fine particles to bigger grains (Ballard and Beare 2006). While LPSA allows accurate measurement of clays. The overall results of the

LPSA technique are affected by the fluid in which the sample is dispersed, and the repeatability of the test is a common inconvenient (Chanpura et al. 2012b). Moreover, selecting a small representative sample from the sand is critical for accurate PSD measurement through LPSA (Zhang et al. 2015).

Comparison of the measurements on the same samples can display remarkable deviation between the two methods (Ballard and Beare 2003). However, for clean specimens, the difference between the two techniques reduces significantly. Certain synthetic sands can render a bimodal distribution that implies the absence of specific grain sizes within the distribution. The nature of the diffraction measurements in LPSA results in particles shape being the principal cause of the deviation between sieve analysis and LPSA measurements (Zhang et al. 2015). Sticking of clay particles showed not to be the reason for PSD variances according to laboratory testing.

Moreover, uncertainties in LPSA measurements such as obscuration levels, solvent type, and pumping rates generate doubts about the reliability of LPSA. The fact that LPSA provides a non-physical dimension for a non-spherical particle question the applicability of LPSA for sand retention studies (Zhang et al. 2015). The mechanical sieving approach consists of size exclusion screening which is similar to the retention mechanism in slurry tests. In such tests, it is recommended that formation sand PSD is obtained through sieve analysis and that synthetic samples are measured and obtained with mechanical sieving as well. For pre-pack tests, size exclusion and particle bridging contribute to the sand retention ability (Chanpura et al. 2012b; Zhang et al. 2015). Both mechanisms are influenced by the shape and volume of the particles due to the limited space for particle orientation in the near-screen region (Zhang et al. 2015).

2.4.2 Laboratory testing and experimental set-ups

Experimental set-ups have been employed in the industry to assess the performance of SCD through sand retention tests (SRT). The objective of laboratory testing is to evaluate the sand retention ability of a screen and the associated production impairment. Production impairment is usually evaluated in terms of pressure drops or retained permeability. The

retained permeability is the ratio of final to initial permeability at the region close to the SCD (Markesad et al. 1996; Mahmoudi et al. 2016a).

Slurry and Pre-Packed tests are the regular scaled tests implemented in sand control studies. Each test simulates different conditions of the sand-face. Presently, there is no standard set-up or operational procedure for any of the sand control testing types. Hence, differences are encountered in the published literature on aspects such as height, diameter, sand preparation, fluid and flow characteristics, phase ratios and measurements (Montero et al. 2018).

2.4.2.1 Slurry tests

In slurry tests, a sand slurry sample dispersed in a viscous fluid (water with polymer) is mixed with brine (clean carrier fluid) through narrow tubes or static mixers to dilute the slurry entering a test cell (**Figure 2-7**). The final slurry flows towards a coupon located at the bottom of a cell, sand production below the coupon is collected, and pressure drop is recorded throughout the testing (Ballard et al. 1999). The flow rates selected for the injection units will determine the final sand particles concentration which is usually below 0.1% in volume (Wu et al. 2016; Ballard et al. 1999). Slurry tests resemble the scenario of an annular space between the screen and the wellbore with low-concentration particle flow (Ballard and Beare 2003 and 2006; Chanpura et al. 2011). Also, slurry conditions are referred to as progressive borehole collapse, and there is no application found in thermal studies. It is reasonable to assume that the unconsolidated formation collapses onto the SCD closing the annular space, perhaps during preheating stages (Fattahpour et al. 2016b). A schematic of a conventional slurry sand retention assembly is presented in **Figure 2-8**.

Clearly, slurry tests seem not to apply to SAGD operations. However, scab liners installation is a common procedure to remediate the damage of failed SCD by placing a new SCD inside the damaged zone. In such a scenario, particles dispersed in the production fluids reach the secondary SCD, and slurry testing may be relevant to study the sand control performance. Distinctive aspects such as particles concentration, flow rates, and fluid ratios must be appropriately captured in laboratory testing to obtain accurate results under the specific SAGD conditions.

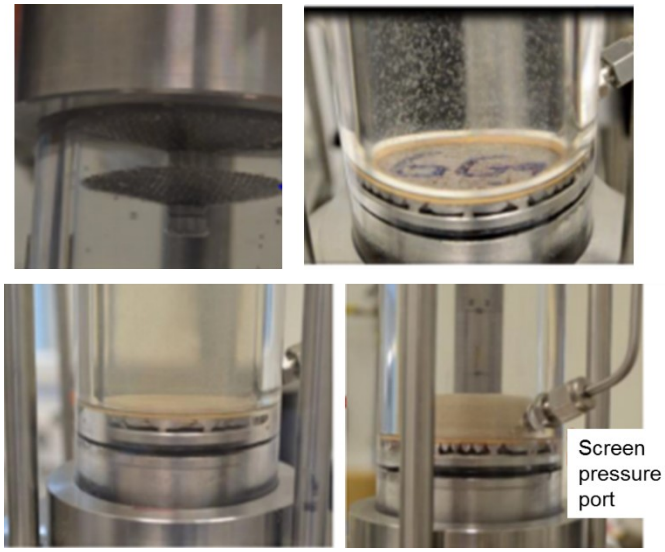

Figure 2-7. Slurry test cell, modified after Wu et al. (2006)

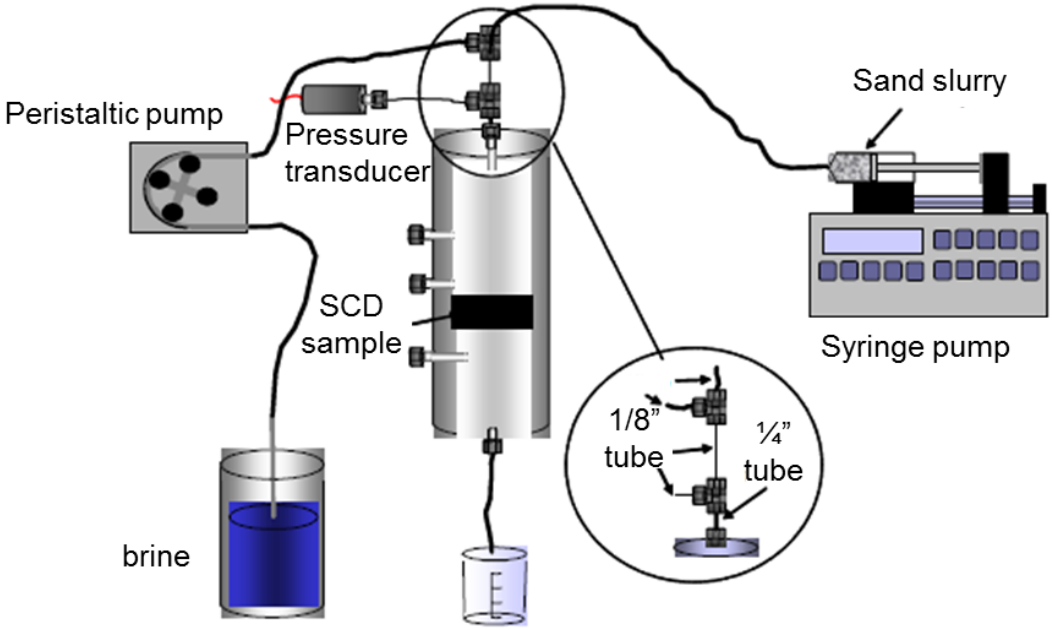

Figure 2-8. Slurry SRT set-up scheme, modified after Ballard and Beare (2003)

2.4.2.2 Pre-packed test

For Pre-packed testing, the sand sample is deposited and packed directly on top of a coupon inside a test cell. The fluids flow through the sand pack and towards the coupon. This test represents the case where there is a rapid collapse of formation sand over the SCD, filling the gap between the formation and the screen (Chanpura et al. 2011). The annular space is filled

with loose sand creating a high porosity zone. In other words, initially, the liner is in contact with a high-permeability porous medium (Guo 2018). In unconsolidated sands, the start of flow is enough to fail the rock surrounding the screen (Ballard and Beare 2003 and 2006; Chanpura et al. 2011). Heavy oil bearing sands are prone to quicky collapse due to factors such as rock/fluid thermal expansion, drag forces and bitumen melting around the SAGD wells (Fattahpour et al. 2016b). **Figure 2-9** presents a typical pre-packed assembly.

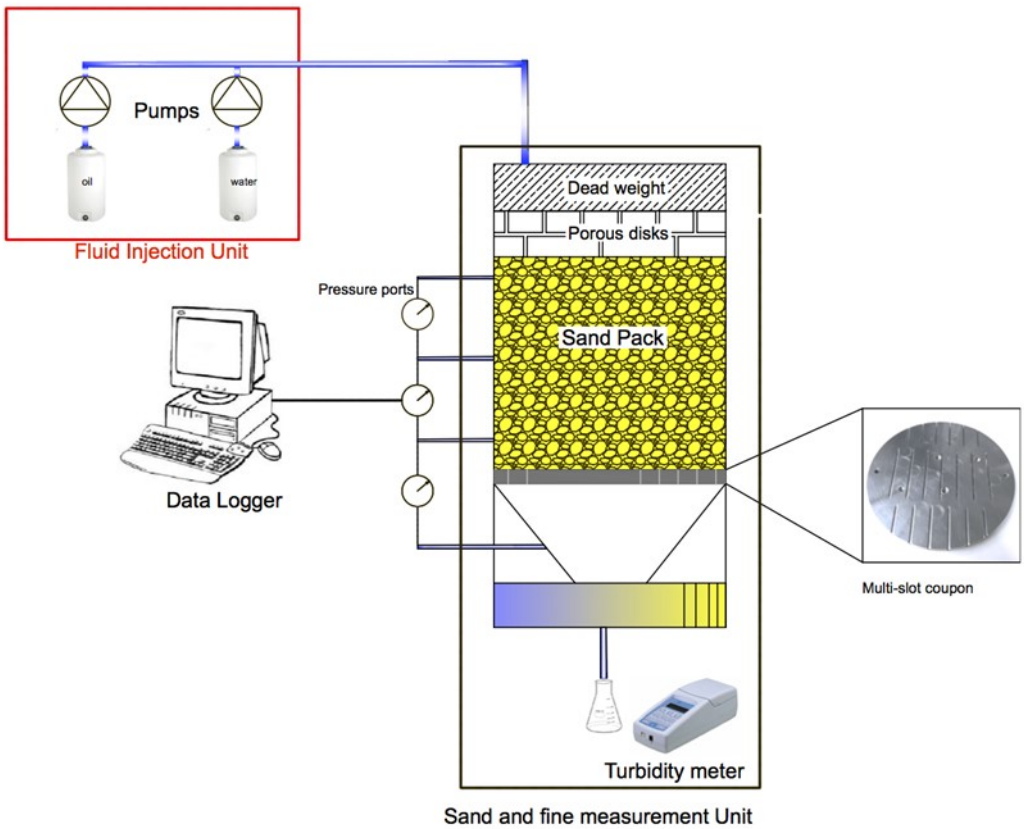

Figure 2-9. Pre-Packed SRT set-up scheme, after Montero et al. (2018)

Some companies have reportedly retrieved long sections of the liner after several months of production (Romanova and Ma 2013). Although this may suggest that sand collapse over the liner is not that significant, retrieval operations are rare in long horizontal wells. In such cases, it is believed that sand pack conditions dominate over slurry settings and time will result in a fully collapsed scenario.

2.4.2.3 Slurry tests vs. Pre-packed tests

Ballard and Beare (2003) performed slurry and pre-packed tests for different PSDs in premium screens (Dutch Twill weaves). In their observations, there was no substantial difference regarding sand production for the two methods. However, there is a perception that slurry settings are more challenging than pre-packed tests (Chanpura et al. 2012b). Chanpura et al. (2012b) carried out laboratory testing and numerical simulation of WWS and concluded that slurry tests do not always produce more sand than pre-packed tests. The fact that one of the approaches may produce more than the other depends on the acting sand retention mechanism; size exclusion or bridging. Size exclusion occurs when the aperture size is smaller than a specific particle while bridging is the result of the simultaneous flow of different particle diameters towards a restriction (Vitthal and Sharma, 1992).

Generally, in slurry conditions where particle concentrations are typically low, the opportunities for particles bridging are low and requires extended time. For concentrations below 1% by volume, particle retention is by size exclusion only (Valdes and Santamarina 2006). Whereas, the distribution of particles directly over a screen results in the dominance of particle bridging in pre-packed settings (Chanpura et al. 2011).

The relation between the particle size distribution and SCD apertures can also change the retention mechanism. Chanpura et al. (2012b) noted that pre-packed tests produced more sand when using PSDs without bridging particles because the dominant mechanism is size exclusion. Some bigger particles of the sand may be “wasted” sitting over the wires of the WWS. On the other hand, during the slurry test, all particles larger than the aperture are covering the opening. When the grain sizes decrease in general, and there are more bridging grains, slurry tests tend to produce more sand since there are fewer particles that can be excluded by size. The dominant mechanism changes towards particle bridging.

2.5 Previous work on SCD design

Most of the work developed on SCD design has followed an experimental approach. Numerical studies require the inclusion of the several physical phenomena involved in sand production and are computationally demanding (Fattahpour et al. 2016a). The primary

objective of laboratory testing has been the selection of the aperture width. Notably, Mahmoudi et al. (2016a) included the impact of slot density (hence OFA) in their research.

Coberly (1937) carried out the first attempt at determining the correct aperture width for unconsolidated formation sands. Using a simple set-up concluded that stable bridges are formed over a slot whose size is up to twice the 10th particle diameter ($2xD_{10}$). Therefore, the criterion is based on just a single point of the PSD. The 10th percentile of the PSD represents the sieve size which retains 10% of the material mass.

Despite the fact Coberly's work was based on simple testing procedures, the industry adopted with certain validity this approach for many years. Suman et al. (1985) stated that when the formation sand has a wide grain size distribution, the design criteria proposed by Coberly (1937) is reasonable, whereas slots apertures between a 10th to the 15th percentile are the best approach for uniform sands. These recommendations have great limitations since they neglect the overall shape of the PSD and the operating conditions.

2.5.1 Pre-Packed studies

Markestad et al. (1996) firstly introduced a set-up similar to pre-packed testing in which a sand pack was fluidized by injection of a fluid. They argued that design criteria for WWS should take into account the overall size distribution and not just a single point. Additionally, it was suggested that the use of PSD to evaluate sand control and plugging is not suitable due to the importance of fines particles. PSD is based on cumulative weight, and the distribution curve focuses on big particles which have more mass. Regardless of the number of fine particles, the PSD does not accurately portray the impact of smaller grains. In order to create a different approach, the authors employed a fractal model for developing a distribution based on the number of particles. Then, a dimensionless analysis allowed to determine two critical factors on both plugging and sand retention: grain size and initial fines content.

Four critical slot widths were identified in the analysis to account for the variability of PSDs encountered in a reservoir. The smallest slot size for continuous sand production (d++), the largest slot size where severe plugging was observed (d--). Similarly, the largest slot size where sand production did not occur (d+) and the smallest slot size that resulted in no

plugging (d-). The objective is to select a slot width between d+ and d- to have control over both sand production and plugging.

The experimental setup consisted of a pre-pack assembly in a radial flow cell in which the screen coupon was located either at a top or lower position. The top position resembles an open annulus while the lower placement represents the collapse of the formation. Plugging occurred with top placements, especially when the injection was suddenly started at a relatively high rate.

It was one of the first studies that highlight evaluation of screen performance not only concerning sand retention but also permeability impairment. Measurement of the pressure drop along the sand pack and the area combining screen and adjacent sand were recorded separately. Analysis of the observed results and prediction stated that the risk of screen plugging increase for fine sands and coarse sands with a significant fraction of fine material. However, the risk of plugging is reduced for finer sands with a high fines content because the initial permeability of these sands are so low that it is in the same range as the permeability of the filter cake (Markesad et al. 1996).

Tiffin et al. (1998) also highlighted the impact of fines content on screens performance and delivered criteria for selection between stand-alone screens (SAS) and gravel packs. Fines particles with the right size, in large quantities or present in poorly sorted formations, would generate a significant reduction in near wellbore permeability due to the plugging potential associated with bridging and fines displacement through pore throats. Hence, the completion strategy would depend on formation sorting. Authors proposed selection criteria based on sorting and uniformity coefficients. Based on experimental data, D40/D90 values of 5 or above are more likely to allow fines to plug the screen and porous media. Laboratory set-up involved core plugs subjected to stress and flow. Results analysis denoted that formation sands with D10/D95<10, D40/D90<3, sub 325 mesh<2% can apply stand-alone screen completions. For sands of D10/D95<10, D40/D90<5 and sub 325 mesh<5% screens may also be suitable, but woven mesh screens provide better control of fines. For D10/95 and D40/D90 values higher than the above, a gravel pack is recommended.

Pre-packed settings have also been studied through numerical analysis using Discrete Element Methods (DEM). Mondal et al. (2010) introduced a dimensionless mass parameter

(M_D) to predict screens sand retention performance using an entire representation of the PSD curve. As a result, the authors generated a correlation that predicts the number of produced particles of a specific grain diameter. The proposed correlation seemed to be in fair agreement with experimental results where the number of produced particles depends both on the grain size/slot size ratio and on the number of particles of that size present in the original sand.

Finally, Mahmoudi (2017) conducted several testing using a novel pre-packed assembly. The testing involved coupons with different slot densities in accounting for the effect of different convergence scenarios. This study is a significant contribution since previous work employed single-slot coupons, neglecting the slots interaction. New criteria were introduced that takes into account both slot width and density for slotted liners, based on acceptable sand production ranges (0.12 – 0.15 lb/ft^2) and retained permeability limits (>50%).

2.5.2 Multiphase Testing

Bennion et al. (2009) presented detailed information about plugging and retention features of different SL geometries for SAGD operations. Results using a customized pre-packed test with the multiphase flow (oil, water, and gas N_2) showed the advantage of rolled top slots in preventing plugging and sand production. A significant observation from this study was the role that clay particles play on plugging tendencies. Microfilms of clay forms on the surface of the slot and propagate up to the slot entrance to plug spaces around the sand grains.

A good comparison of SL and WWS performance on SAGD operations was presented by Romanova et al. (2014). The pre-packed assembly follows the protocol introduced by Bennion et al. (2009). A particular aspect was that the productivity impairment assessment used a rigid maximum pressure drop across the screen (5 psi). The previous threshold was not supported and seemed to be defined arbitrarily. Whereas, sand production should not exceed 0.1 grams at any flow stage with particles of less than 50 microns in size. This sanding limit is more conservative than those proposed by Hodge et al. (2002) and Mahmoudi et al. (2016a). In general, results exposed a superior performance of WWS over SL regarding pressure buildup and plugging, while WWS produced slightly more sand.

Devere-Bennet (2015) also employed multiphase flow pre-packed testing in order to find a range of apertures for SL and WWS for the McMurray formation. Analysis of the results

showed that the mass of produced sand itself could be misleading and proposed the use of the percentage of solids produced accounting for the cumulative volume of fluid injected. The guideline used for sand control was a maximum of 0.1% and 5psi for pressure differential. The final purpose of the study was to narrow down the screen aperture design, for the laboratory testings the author employed SL samples between the 10th percentile and two times this size. However, due to the higher open flow area (OFA) of WWS, a range between 0.6 to 1.5 times the 10th percentile was utilized. The large area of WWS would suppose an increase in solids production.

Similarly, O'Hara (2015) evaluated the performance of PPS, SL, and WWS using sand samples from the Jackfish and Pike 1 SAGD project areas (McMurray formation). An interesting feature of the study was the employment of pre-packed testing with constant rate and also constant pressure techniques. Both testings resulted in the superior performance of WWS. However, the results followed normalization by OFA which can be biased towards high OFA devices.

A large-scale sand control test in SAGD operations was conducted by Anderson (2017) to validate previous scaled tests. Their work introduced a novel large-scale apparatus that accommodates full-scale SCDs with a 7" outer diameter (OD). Sand was packed over a horizontally installed SCD sample, and fluid injection followed a radial geometry. The results showed general agreement with those of scaled tests, being WWS the best performing device.

2.5.3 Slurry Testing

Ballard et al. (1999) firstly introduced the slurry sand retention assembly which consisted of the flow of dispersed sand particles in a carrier fluid towards a coupon fitted in a cell. The authors pointed out the possible impact of artifacts on the results, and several trials were necessary to obtain representative and consistent results.

Gillespie et al. (2000) presented criteria for screen selection and considered that the standard guidelines used for WWS and SL do not fit woven screens or other premium completions. Authors performed several experiments using a slurry sand retention assembly and suggested the employment of screen efficiency plots (SEP) for performance evaluation. The plot consisted of the percentage of sand through the coupon against the rate of pressure drop.

From the sand retention figures in WWS, it was concluded that aperture ratios of two or more cause a slow development of an unstable filter cake whose outcome would be unacceptable sand production. As a conclusion, slot width for WWS should be less than two times the fiftieth percentile (50th) provided that the formation sand is uniform (D_{50} does not show significant variation). In the case of premium screens, openings not larger than 2.5 times the D_{50} sand size would result in good retention performance if the uniformity coefficient (D_{40}/D_{90}) is less than 6 (**Figure 2-10**).

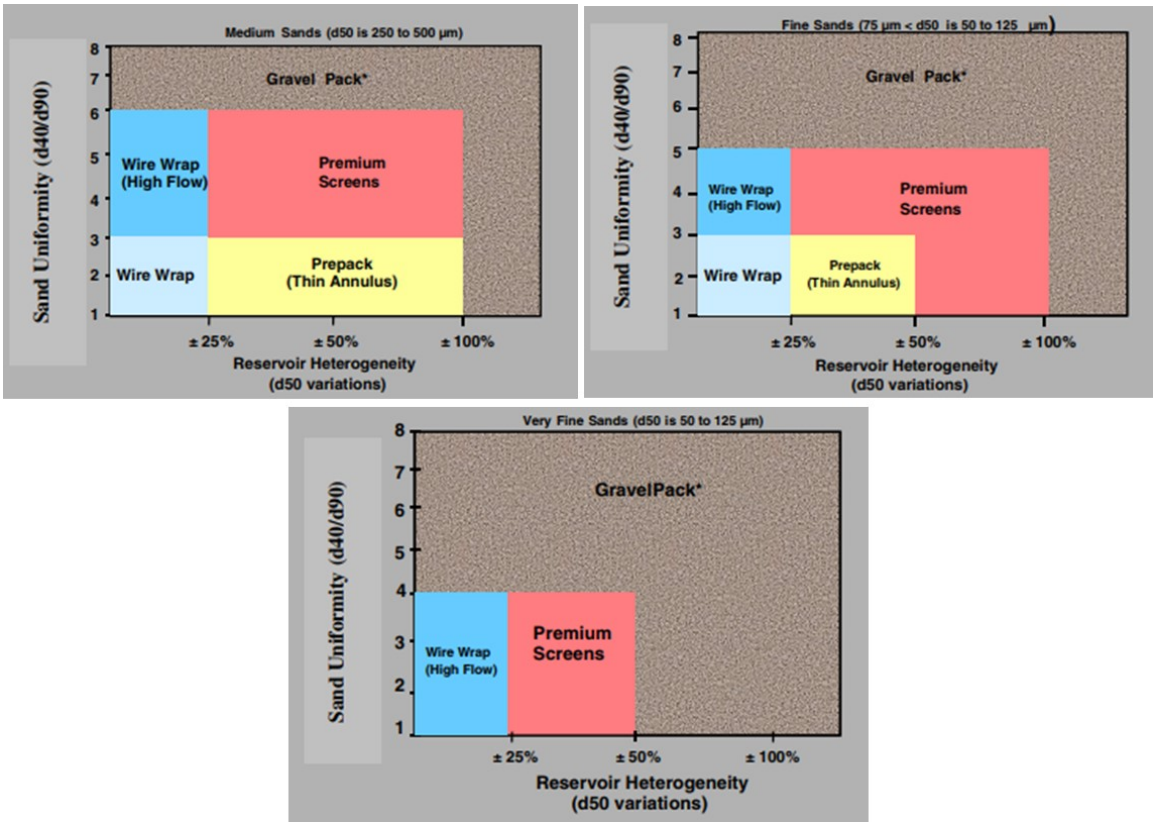

Figure 2-10. Selection guide for Stand-alone screens, modified after Gillispie et al. (2000)

Sand retention test results are affected by fluid properties, flow rates and artifacts such as channeling. Ballard and Beare (2006) shortly described the possible impact of these aspects on pre-packed tests. Authors executed slurry sand retention tests to evaluate the performance of premium screens and WWS, with the premise that the selection of premium screens over WWS is based on the uniformity of the sand. In this case, retention results showed that there is not a strong correlation between the biggest particles (D_{10}) and produced sand. These results are in contrast with previous design criteria that focused on the largest particles.

On the other side, Mondal et al. (2011) simulated a slurry test using analytical and numerical methods where size exclusion was assumed as the unique acting retention mechanism. From the results, concluded that around 90% of the cumulative sand production occurred during the formation of the first layer of sand and that the shape of the coarser part of the PSD has a significant impact on sand retention. The two previous studies did not provide any insights concerning the flow performance of the system.

Also, slurry experiments were employed in a comparative study of the performance of metal mesh screens (MMS) and WWS by Ballard and Beare (2012). The authors examined the effect of reduced flow rates and the employment of denser brine to compare previous results. It was observed that deposition patterns are significantly affected by the fluid properties; dense and viscous brine caused particles to be entrained in the flow and directed towards the slots. Moreover, pressure gradients were used to evaluate plugging and found a moderate correlation with fines content. Although they recognized pressure might not be a good indicator, there was a considerable difference between WWS and MMS pressure drops when fines content is above 5%, and this aspect ruled the selection of MMS over WWS. Results on WWS suggested that D_{10} sizing criteria not necessarily render satisfactory retention and proposed that the use of 30th percentile (D_{30}) for more reliable results.

2.5.4 Pre-Packed and Slurry Testing

Hodge et al. (2002) conducted several experiments to emulate two different scenarios, gradual formation failure (Low concentration slurry test) and rapid formation failure (Sand-Pack fluidization). A distinct difference from previous authors was the implementation of constant pressure drop tests with uniaxial stress application. The vast majority of previous studies employed a constant flow rate approach. Remarkably, this study defined limits for sand production and retained permeability criteria. Comparison of laboratory results with successful sand-control field applications in the North Sea, United States, and Indonesia demarcated 0.12 lb/ft^2 of produced sand (pounds per square foot of screen inflow area) as a reasonable threshold for sand production. On the other side, analytical models showed 20% as the minimum acceptable value for annular retained permeability and screen permeability. The permeability of any SCD is much greater than that of a typical reservoir formation resulting in high values of plugging to result in loss of productivity. In order to account for

additional damage sources in the formation sand, authors proposed 50% as an acceptable fail/pass criteria.

In one of the first studies on premium screens, Ballard and Beare (2003) determined that the biggest particles still are an essential factor in sand retention (D_5, D_{10}). The study attempted to assess plugging using pressure gradient measurements. However, the authors mentioned that gradient pressure gradients simply might be associated with the size and sorting of the sand.

Constien and Skidmore (2006) introduced master-curves to interpret data from laboratory testing on SCD. Testing combined both slurry and pre-packed approaches. Produced sand and formation permeability are plotted against a ratio of effective formation size divided by the size of the screen opening (**Figure 2-11**). The effective particle size function may be the ratio of the 10th percentile over slot size as it was found to be the case for WWS. However, the authors pointed out that this is not always the case since the samples used in the study had similar uniformity coefficients. For most cases, uniformity should be considered, and d50/Uc was used successfully for premium screens. Accordingly, this representation of the data would be more useful in determining ratios of formation particle sizes and screen opening sizes that will produce satisfactory solids control for a specific range of PSDs.

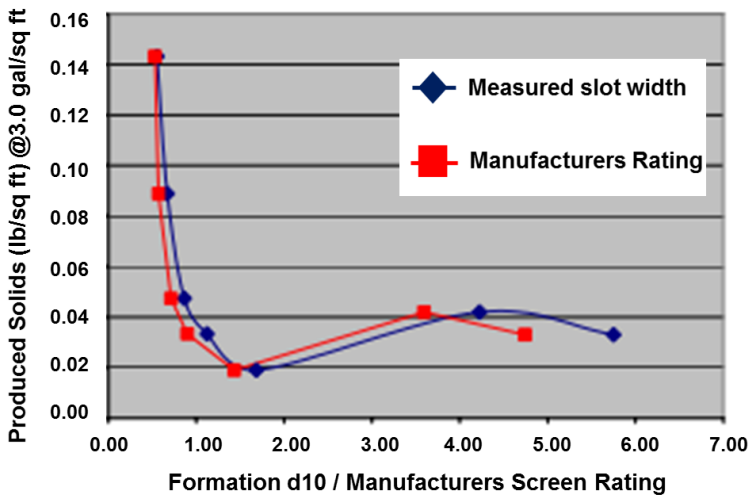

Figure 2-11. Screen Efficiency Plot (SEM) for WWS, modified after Constien and Skidmore (2006)

Furthermore, Chanpura et al. (2011) stated the precautions to consider when analyzing data from current sand retention tests, in particular, pressure readings from slurry tests. The

pressure response during slurry tests is masked by the permeability and geometry of the forming sand-pack. Using a rigid pressure drop value to evaluate the flow performance is not valid. Instead, the authors proposed the identification of the point at which the sand-pack itself starts dominating the pressure response as the test finalization point.

It was suggested that production shutdowns might induce sorting of the fines fraction at the screen interface increasing the risk of plugging once production is resumed. According to pre-packed results, although there is not a definitive correlation between the 10th of the distribution and sand retention, sizing WWS with screen opening/D_{10} <1 appears always to render acceptable levels of produced sand.

In order to review previous studies, Chanpura et al. (2012a & 2012b) summarized common misassumptions in the oil industry about screen performances and laboratory testing (Slurry versus Pre-Packed), especially on WWS. By inspecting numerical and DEM modeling of pre-packed testings, it was concluded that the coarser portion of the PSD plays a major role in sand retention. Coarser tails would have a fewer number of particles larger than the aperture which results in higher production of particles until those big grains manage to cover the apertures (**Figure 2-12**). Accordingly, for WWS, flow convergence would increase the probabilities of bridging in comparison with PMS due to a higher ratio of large particles to open flow area. On the contrary, grains finer than the aperture seemed not to had an impact on the mass of produced sand.

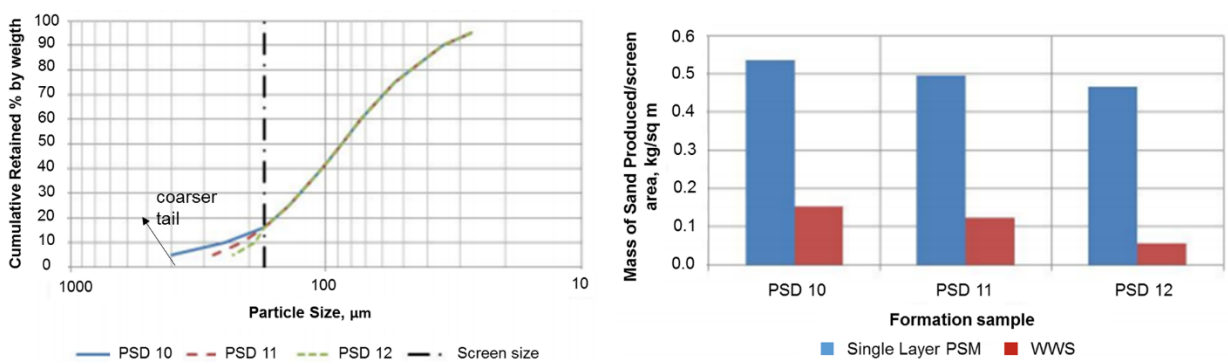

Figure 2-12. Effect of the coarser tail on sand production, modified after Chanpura et al. (2012b)

Conducted experiments showed that WWS permit slightly more sand production than SL, and this is associated with the larger open flow area which causes longer times for bridge formation. Also, analysis of produced sand PSD exhibit that particles are larger for WWS,

possibly related to the higher aspect ratio. As expected, lower pressure drops were encountered for WWS. However, the authors mention that both sand control methods can meet acceptable requirements.

2.6 WWS in SAGD applications

Devere-Bennet (2015) performed 26 pre-packed tests for determining a safe range of sizes for the Long Lake project with five representative sand batches of the McMurray formation. The author recommended slot widths between 0.008” and 0.010” as the optimum sizes for WWS and 0.016” – 0.020” rolled top slots for SL. Despite having smaller apertures, all WWS tested delivered better pressure differential performances. Furthermore, O’Hara (2015) also conducted tests on typical sands from Pike 1 project that demonstrated the convenience of WWS when OFA normalizes results. Additionally, the authors pointed out the importance of size apertures since they noticed remarkable differences in changing sizes and proposed gauge variation of 0.002 inches.

Consequently, Anderson (2017) aimed to confirm the results of O’Hara (2015) studies by introducing a large-scale sand pack set-up that accommodated 50kg of sample above a full-scale liner or screen of 7 inches. The performance of WWS was verified, and the range of safe aperture sizes was similar, indicating that a universal undersized WWS may produce excellent reliability in well-sorted sands. Completions in the JACOS Hangingstone SAGD trials implemented WWS of 0.005 inches with no problems observed at the time of publication. From the assessment using the new set-up, 0.008 inches for apertures in WWS was recommended for the future wells in Pike 1 and Jackfish fields.

2.6.1 Field Performance of WWS

Data from SAGD projects allowed to draw some conclusion on the performance of WWS and SL at field conditions (Romanova et al. 2014). Regarding pressure drawdown, both devices showed similar values during the first two years. After this period, measurements displayed an increase in pressure drawdown in wells completed with SL while WWS remained relatively constant. Although it was too early to bring a definitive conclusion, the additional pressure drop for SL did not seem to affect the production at the time. Additionally, one aperture of WWS managed a wider range of size distributions when compared to SL.

Williamson et al. (2016) presented a review of the operations developed in the Lower Grand Rapids Formation SAGD project. As described by the authors, the formation has good areal distribution, homogeneity and low fines content (2.2-3.4%) with characteristic D_{10} between 225 – 239 microns. The completion system of the wells included rolled-top SL and WWS. 0.014 inches of aperture size for WWS was employed taking into account that the mineralogy quality was not good (initially 0.010 inches was considered). Feldspar and chert were present in the sand, posing an additional threat of plugging due to thermal formation damage.

Field data suggested that plugging of the SL in the producer well was the main cause of high-pressure differentials which eventually translate into a high steam-oil ratio and lower production rates. Using WWS proved to be the choice for producer wells as lower differential pressures and higher production rates were observed. Moreover, the authors highlighted the importance of good operating practices. An excessive ramp-up of the pumps after an operation shut-down seemed to generate the plugging observed in SL wells.

Operators carried out a comparison of sand samples before and after steam injection, using the sand of the well that displayed plugging. Remarkable results of SEM images concluded that smectite and calcite/aragonite were created due to thermodynamic diagenesis.

2.7 Summary of Wire-Wrapped Screens Design

The main criteria proposed for aperture sizing can be summarized as:

- Coberly (1937): two times the 10th percentile ($2xD_{10}$).
- Suman (1985): the 10th percentile of formation sand.
- F.G Driscoll (1986): the 40th percentile (For groundwater wells).
- Gillespie et al. (2000): less than two times the 50th percentile if the sand is uniform ($2xD_{50}$).
- Ballard and Beare (2012): the 30th percentile of formation sand (D_{30}).
- Weatherford Screen Selection Guideline: the 25th percentile of formation sand (D_{25}).
- Industrial rule of thumb (Fattahpour et al. 2018): 0.004” less than the equivalent SL selection.

2.8 Failure of Sand-Control Screens

SCD encounter different risks that may lead to potential failures and loss of the intended purpose of the screen design. The primary failure sources are plugging, corrosion, erosion, and collapse.

Erosion is a major issue when an annular exists between the screen and the borehole; inflow velocities can wear the screen wires or slots damaging the original aperture. Plugging of the slots worsen the effects of erosion (Hamid and Ali 1997; Gillespie et al. 2009). Since the borehole is considered to collapse at the onset of production, the risk of erosion has a positive control except for the scenarios of steam-breakthrough.

Slot plugging in SAGD operations due to sand grains is not likely to occur (Bennion et al. 2009; Chanpura et al. 2012b; Romanova and Ma 2013). The main plugging materials are corrosion by-products, scales and clay particles (Romanova and Ma 2013). Bennion et al. (2009) showed the evolution of clay films inside the slots over time. This highlights the importance of allowing the fines to be discharged from the SCD and formation. Wires on WWS are fabricated from stainless steel which provides corrosion prevention, and the smooth surface plus tapered shape prevents clay adhesion. Conversely, the carbon-steel base pipe can suffer severe corrosion damage as reported by Mahmoudi et al. (2018). Significant erosion-corrosion was found at the inner wall of the pipe (**Figure 2-13**), whose extent depends on the flow rates (Schmitt and Rothman 1977) and brine properties (Addis 2014). Integrity losses in the base pipe may also cause deformation in the wires, affecting the sand control ability of the screen (Mahmoudi et al. 2018). Another plugging source is the installation of SCDs in unconditioned mud systems; small particles might plug slots during deployment or by mixing of mud particles with sand grains (Chanpura et al. 2012b).

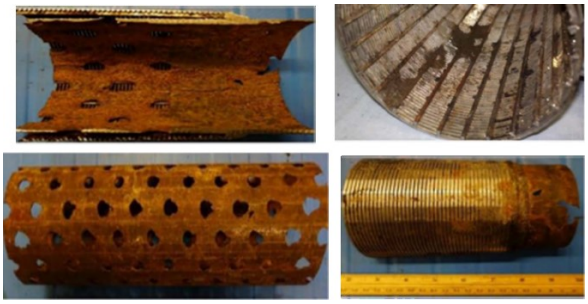

Figure 2-13. Failure of WWS components, modified after Mahmoudi et al. (2018)

CHAPTER THREE: EXPERIMENTAL SET-UP AND TESTING PROCEDURE

3.1 Introduction

This study employs a large Pre-Packed Sand Retention Test (SRT). The experimental set-up is a modification of the assembly introduced by Mahmoudi et al. (2016a & 2017). The main objective parameters of the laboratory testing are the produced sand and the retained permeability of the WWS coupon and the adjacent sand. A set of different tests were performed using three representative sand classes from the McMurray formation. Abram and Cain (2014) categorized McMurray formation into four major groups. **Figure 3-1** shows the cumulative size distribution of these sands and the corresponding synthetic sand-pack mixtures. PSD replication is achieved by mixing several commercial sands and fines. Commercial mixtures showed to have similar strength properties and shape factors as the formation sands (Mahmoudi et al. 2016c).

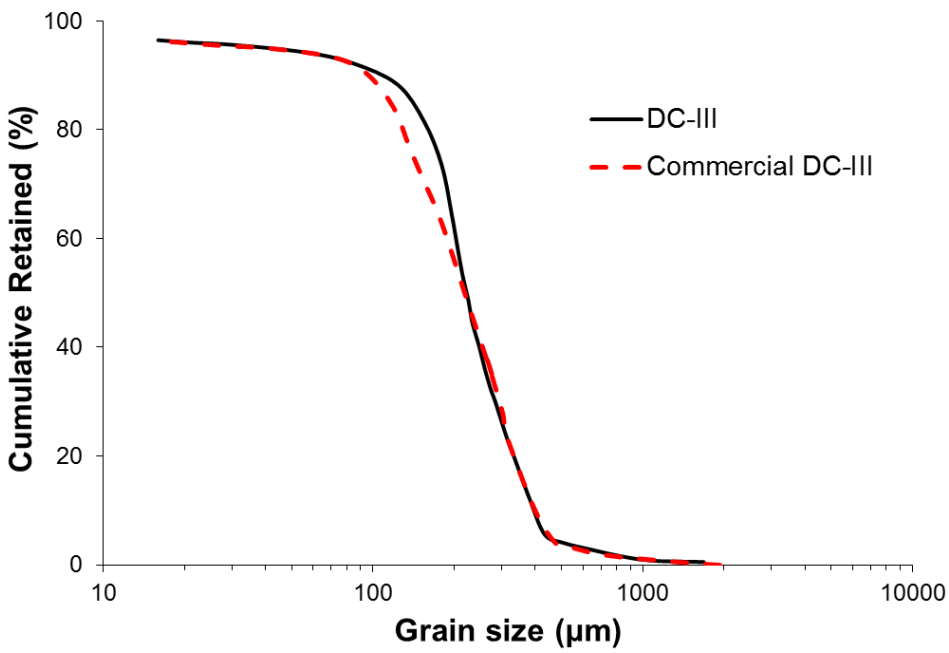

(a)

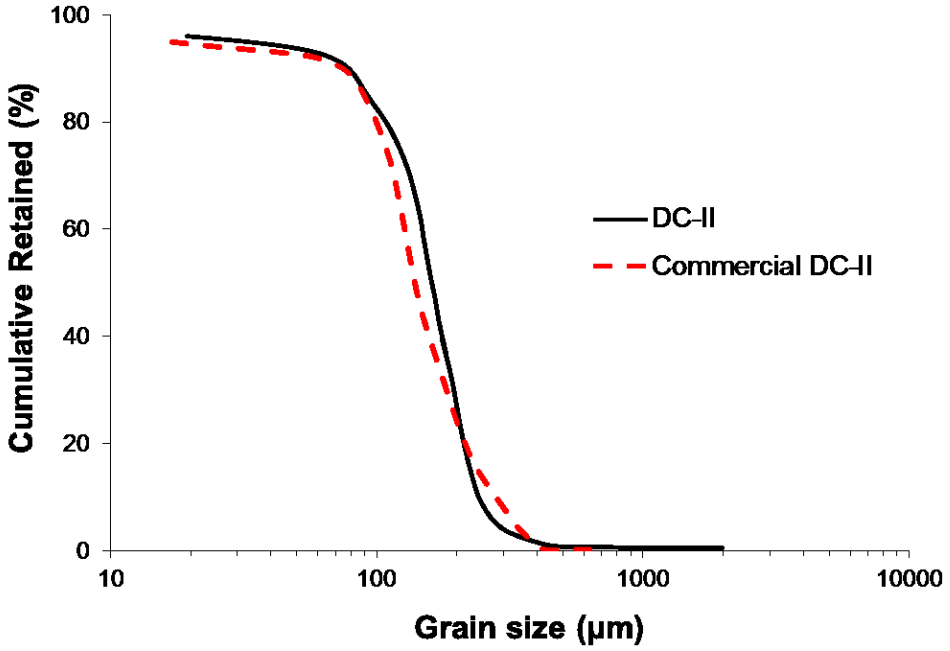

(b)

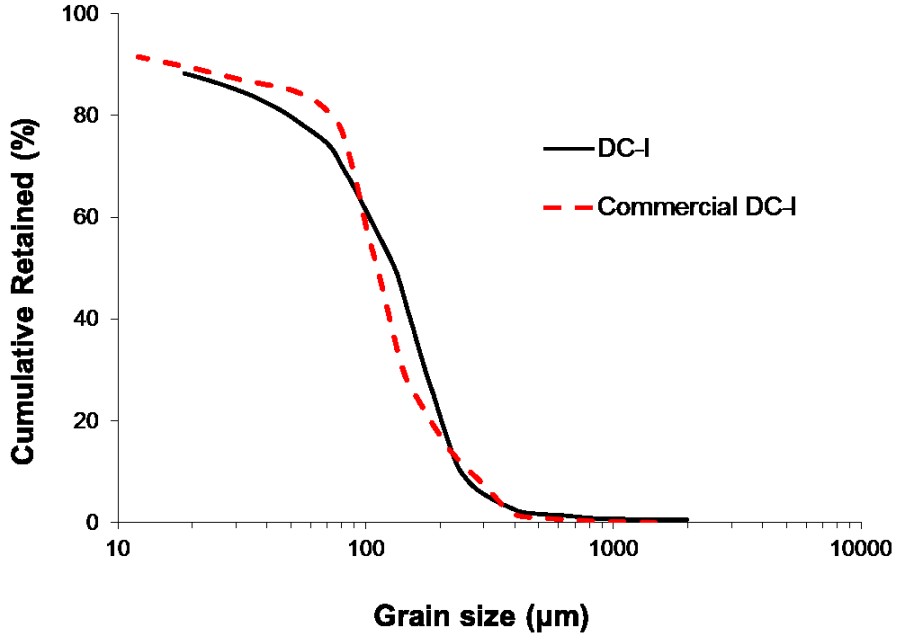

(c)

Figure 3-1. Particle size distribution of the tested sand packs and corresponding synthetic distribution. (a) DC-III, (b) DC-II, (c) DC-I.

DC-I is regarded as fine-to-very fine sand, while DC-II and DC-III are considered as fine and medium-coarse sand respectively. In general, synthetic samples provide a good replication of the actual sands. Synthetic DC-III deviates 25 microns from the actual sand, while synthetic DC-II and DC-I show a maximum deviation of ±50 and ±55 microns, respectively.

Table 3-1 presents some characteristic points of the synthetic sand classes. Previous laboratory testing showed that WWS has a great capacity to produce fines and maintaining formation damage above the acceptable limits (Montero Pallares et al. 2018). Therefore, DC-I provides an excellent opportunity to evaluate the response of WWS with fine sands with high contents of fines and clay (Low-quality sand). On the other hand, DC-III represents sand of good quality, allowing the assessing of WWS performance under different conditions.

The test matrix was designed to cover a wide range of aperture sizes including empirical design criteria presented in the previous chapter (**Table 3-2**).

Table 3-1. Characteristics of synthetic sand classes

Type of sand	D90	D70	D50	D10	% fines	Uniformity Coefficient	Sorting Coefficient
DC-I	25	80	135	232	14.5	5.9	9.3
DC-II	76	118	175	260	7.4	2.7	3.4
DC-III	110	187	215	341	5.4	2.4	3.1

Uniformity Coefficient (UC=D40/D90), Sorting Coefficient (SC=D10/D90)

Table 3-2. Test matrix for the testing program

Aperture Size	PSD		
0.006"	DC-I	DC-II	DC-III
0.010"	DC-I	DC-II	DC-III
0.014"	DC-I	DC-II	DC-III
0.018"	DC-I	DC-II	DC-III
0.022"			DC-III

As mentioned in the previous chapter, this test emulates the rapid borehole collapse over the SCD. An increasing flow rate test with several scenarios and fluid ratios allows evaluating the influence of flow velocity and water cut on the WWS performance. Besides the standard measurements of the mass of produced solids and sand-pack pressure drops, postmortem analysis includes the assessment of fines migration and production.

3.2 Experimental set-up

Figure 3-2 presents a schematic of the pre-packed SRT. The facility consists of four distinct and interconnected units: (1) Cell and accessories; (2) Fluids injection unit; (3) Measuring and data acquisition unit; (4) Collection and back-Pressure units and (5) Load frame. **Figure 3-3** shows an image of the experimental arrangement.

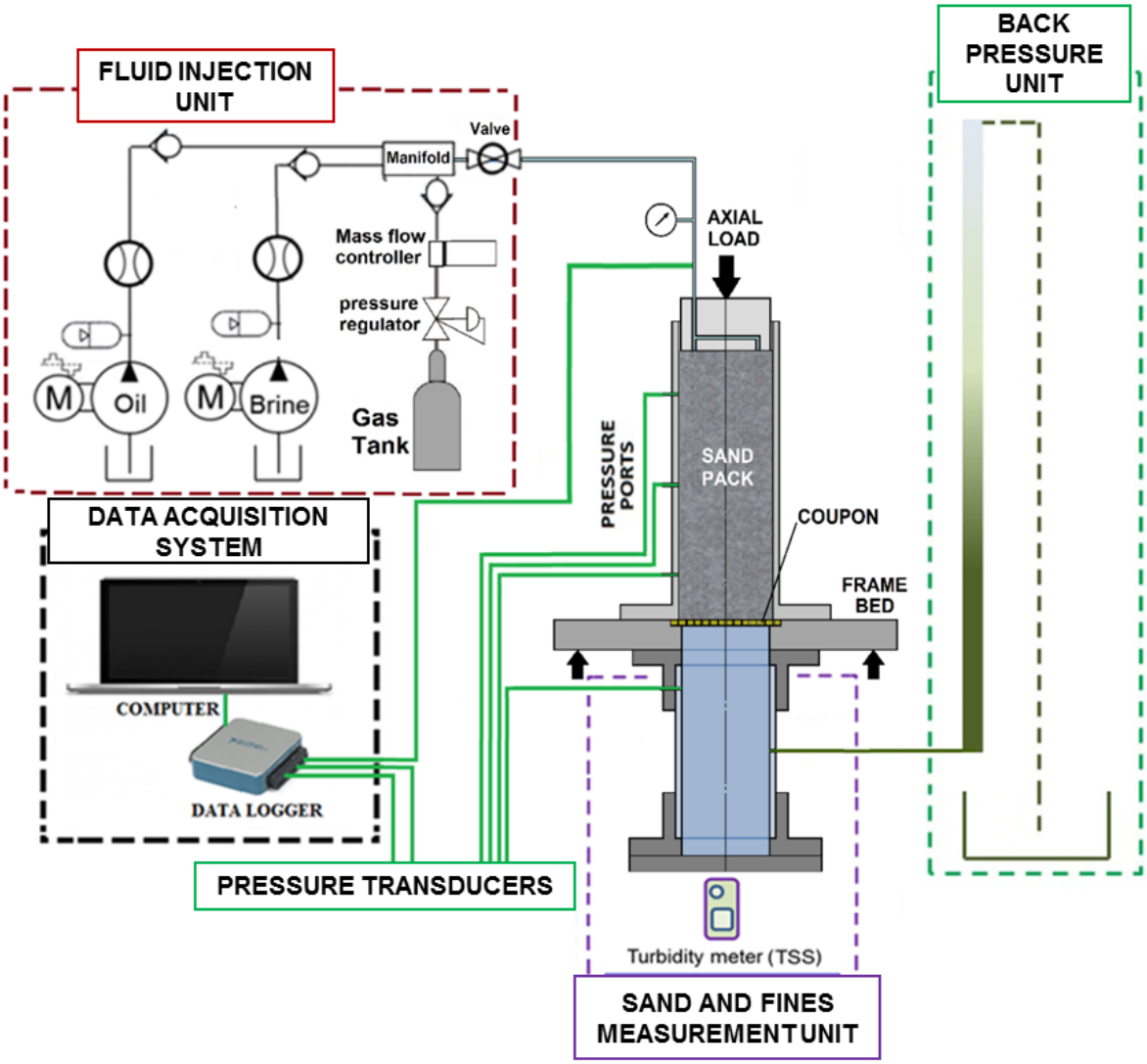

Figure 3-2. A schematic of the Pre-packed SRT facility

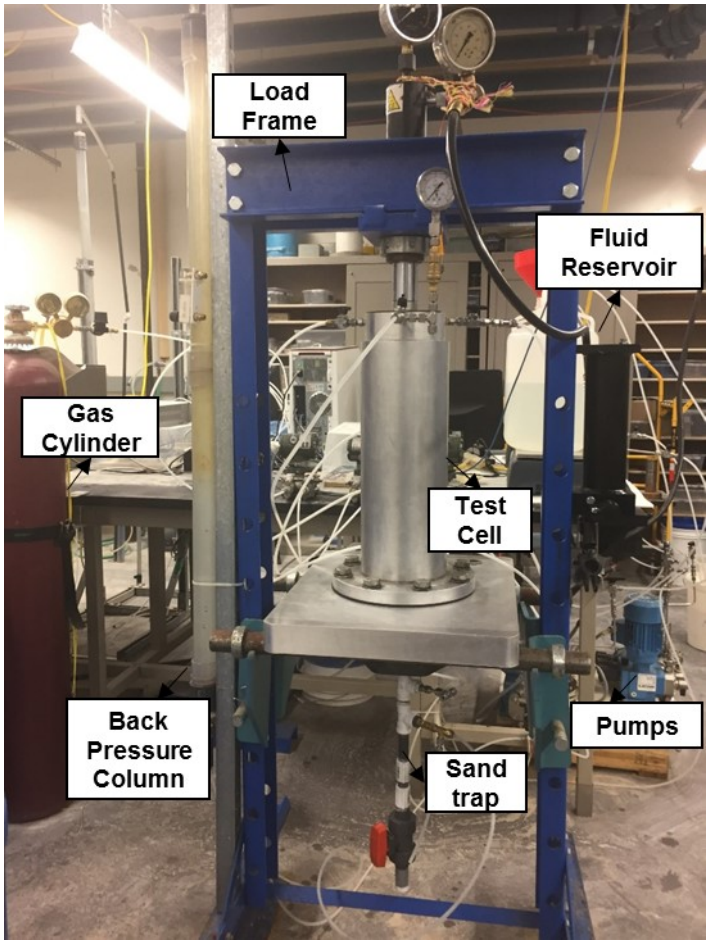

Figure 3-3. Picture of the experimental set-up

Published literature presents different assemblies and procedures for pre-packed experiments. There are similarities and differences regarding dimensions of the assembly, sand pack preparation, flow rates, measurements, testing procedure, and other features. **Table 3-3** presents a summary of the different design and operational characteristics from previous authors. The laboratory set-up employed here intends to honor as close as possible the conditions of SAGD wells by employing reasonable flow rates, fluid ratios, and production scenarios. Additionally, improved post-mortem analysis and consistent sand preparation methods guarantee reliable results.

Furthermore, this assembly allows the use of different coupons types and geometries (WWS, SL, PPS) and it is equipped to handle single-phase and multi-phase testing (oil, water, and

gas). Modification of testing features such as fluid characteristics and rates allows developing sensitivity analysis and parametric studies.

Table 3-3. Review of sand control evaluation tests (After Montero et al. 2018)

Author	Year	Experiment Design						Sand Used	Fluids and rates		
		SCD type	Core Diameter cm	Core Length, cm	Number of phases	Constant Drawdown or rate	Stress applied, psi	Testing sand source	pH	Salinity, ppm	Equivalent SAGD flow rate, bbl/d
Markestad et al.	1996	WWS	19.05	57.15	One: Brine	Constant rate	None	Formation	N/M	Seawater: 35,000-40,000	N/M
Tiffin	1998	GP	2.54-3.81	5.08	One: Brine	Applied pressure surges at 50 psi increments reaching 1000 psi	Axial: N/M Confining: N/M	Formation	N/M	N/M	First phase: 36-832 N/A
Hodge	2002	GP	1.5748	1.27	One: Oil	Constant drawdown 200 psi	Confining increases in 200 psi increments	Formation	N/A	N/A	N/M
Ballard and Beare	2003	PS	N/M	N/M	One: Methanol	Constant rate	Axial 10	Formation	N/A	N/A	88,000
Williams et al.	2006	GP PS ES	N/M	N/M	One: Brine	Constant rate	None	Formation	N/M	2,000	100cc/hr
Constien and Skidmore	2006	WWS PS	Variable	Variable	One: Oil	Constant drawdown 200 psi	None	Formation	N/A	N/A	Variable
Bennion et al.	2007	SL-SC SL-RT	5	20	Three: Brine, Oil, Nitrogen	Constant rate	Axial: 500	Formation	N/M	N/M	Oil: 1141-4565 Water: 2282-9130
Bennion et al.	2009	SL-SC SL-RT	7	20	Three: Brine, Oil, Nitrogen	Constant rate	Up to 5,000 psi	Formation	Varied	N/M	$team:944-2,831 Water: 1,510-6,038 Oil: 755-3,019
Chanpura et al.	2011	WWS PS	3.81	N/M	One: Oil	Constant drawdown 200 psi	None	Formation	N/A	N/A	Variable
Agunloye, and Utunedi	2014	WWS	N/M	N/M	One: Brine	Constant drawdown	Cyclic Brine test: 700 Constant Drawdown: Variable	Formation & Commercial	N/M	N/M	N/A
Romanova et al.	2014	WWS SL-SC SL-RT	6.36	N/M	Three: Brine, Oil, Nitrogen	Constant rate	N/M	Formation	N/M	1,000	Steam:944-2,831 Water: 1,510-6,038 Oil: 755-3,019

Author	Year	Experiment Design						Sand Used	Fluids and rates		
		SCD type	Core Diameter cm	Core Length, cm	Number of phases	Constant Drawdown or rate	Stress applied, psi	Testing sand source	pH	Salinity, ppm	Equivalent SAGD flow rate, bbl/d
Devere-Bennett	2015	WWS SL-RT SL-SC	5	20	3	Constant rate	Axial 500	Formation	Used formation water	Used formation water Salinity: N/M	WWS_Water: 515-6,871 WWS_Oil: 172-3,436 SL_Oil: 288-4,565 SL_Water: 685-9,130
O Hara	2015	PPS WWS SL PS	4.42	1.3	One: oil	Constant drawdown 200 psi	None	Formation	N/M	N/A	Oil: 540
O Hara	2015	SL-RT WWS PS	6.35	20	Three: Brine, Oil, Nitrogen	Constant rate	Axial: 500	Formation	N/M	1,000	WWS_Water: 1718-6871 WWS_Oil: 859-3436 SL_Oil: 1141-4565 SL_Water: 2283-9130
Mahmoudi et al.	2016	SL-Seamed	17	34.29	One: Brine	Constant rate	Axial: 2	Commercial	6.8,7.9,8.8	0-7,000-14,000	800-40,000
Anderson	2017	WWS SL-RT PPS	30	100	Two: Oil & Brine	Constant rate	Axial: 35 psi	Formation	6-8	1,000	Oil: 1,490-11,921 Water: 4,470-13,411

3.2.1 Test cell and accessories

The test cell and main body are supported by a structure consisting of a load frame and a thick metal work-table. A hole located in the middle of the table provides the sitting for the coupon. Threaded holes around the coupon allow the installation of the cell and the sand trap unit below it. The cell consists of an aluminum cylinder that holds the sand pack and a top platen. The total height of the cell is 18.5 inches (47 cm), and the top of the sand pack reaches approximately 15 inches (38 cm). The inner diameter of the cell is 6.031 inches (15.2 cm). The platen located at the top of the cell transmits the axial load provided by the piston to the sand pack. Additionally, the platen provides the necessary seals to avoid leakage and several connections for the inflow lines.

Along the cell, three connection points specially tapered at the wall of the cell allow the connection of pressure transducers tubings. Pressure differential readings are recorded throughout the test to capture the evolution of flow impairment. The most significant measurement point is located 2 inches above the test coupon, and its function is to evaluate the flow performance of the near-screen zone. Factors such as flow convergence, sand re-sorting over the screen, fines migration and the associated plugging of porous media contribute to the pressure drop in this area. The other pressure reading points are 7 and 12 inches above the coupon to provide measurements at the middle and top zones of the sand-pack.

Naturally, cell dimensions are limited to the amount of available sand, cost, and operational complexity. However, some authors argue that bigger assemblies offer an improved emulation of the reservoir conditions because of the larger coupon area and larger volumes of injected fluids (O'Hara 2015). Moreover, the significance of plugging on SAGD performance requires the implementation of a representative volume of sand to study fines migration and the interaction of slots-porous media. The set-up employed in this study represents one of the biggest scaled test assemblies. As shown in **Table 1** Bennion et al. (2009), Romanova et al. (2014), O'Hara (2015), and Devere-Bennett (2015) employed a typical core length of 20 cm, while the coupon diameter usually ranged from 5 cm (Devere-Bennett 2015) to 7 cm (Bennion et al. 2009; Romanova et al. 2014; O'Hara 2015). The 15 cm cell diameter of this study provides a larger coupon area, a remarkable feature, due to the better representation of the OFA of an SCD. The set-up in this study provides a sample volume ten times bigger than that of previous studies. In the case of SL, it allows multi-slots samples and not the single slots coupons employed in previous studies (Mahmoudi 2017).

3.2.2 Fluid Injection System

The injection unit includes two hydraulically-actuated diaphragm metering pumps (LEWA ecodos® ESC 0006-13) for brine and oil injection, each with a maximum output rate of 6 lt/hr at 50 psi. For gas flow, nitrogen (N_2) is controlled by a gas flowmeter (OMEGA, ±3% accuracy) at the outlet of a reservoir cylinder. The fluid injection inlets are independent, and

mixing does not occur before entering the test cell. The frequency and length of the strokes determine the discharge liquid flow rate.

Injection pumps are connected to reservoir tanks with a capacity of 40 liters. For the procedure presented here, the outlet flow from the cell does not follow any treatment for the fines content. Additionally, each liquid reservoir lays on top of weight balances (ULINE Deluxe Counting Scale H-5822, ±1g accuracy) to record the liquid mass input, injection flow rates and perform mass balance calculations based on the collected output of each flow stage. Graduated cylinders (± 2mL accuracy) are also used to verify flow rates and measure volumes.

3.2.3 Measuring and Data Acquisition Unit

Measuring devices include three differential pressure transducers (Yokogawa DPharp EJX110A, ± 0.006 psi of accuracy) for the pressure drop evolution at the different points of the sand pack. Instantaneous visualization of pressure recordings is possible through NI-DAQmx Express software, that integrates data in a computer device. A rotameter or graded tubes quantify the flow rate during the flow test. Additionally, absolute pressure gauges (Hy-Lok Elite, ±1psi accuracy) are installed at the inlet and outlet of the cell to monitor the overall pressure drop in the system. Previous tests showed that pressure drop across the slots is negligible due to their high permeability (Mahmoudi 2017), plugging in laboratory settings is rarely observed.

Additional measuring devices include weight balances, turbidimeter, graduated cylinders and sieves that are mainly incorporated in the postmortem analysis. Below the coupon, close to the collection unit, a metering valve fitted to a small tube of 1/4 inches captures some of the outlet fluid for post-mortem analysis. Fluid samples are collected in small recipients to analyze the content of fines particles using a turbidimeter (HACH 2100P, ±2% accuracy).

3.2.4 Collection unit and back-pressure column

Accurate recording of sand production is indispensable to perform a proper analysis and comparison between different designs. Any produced sand trapped in flow lines and corners

or wedges could produce a “false” acceptable performance, when the SCD may not have fulfilled the selected pass/failure criteria (Montero et al. 2018).

In this set-up, a sand trap captures and accumulates the produced sand coming from the outflow. This section consists of a cone with two compartments below separated by a ball valve. The lower compartment can be detached from the assembly after closing the valve, allowing the measurement of the produced sand accumulated at the bottom during a particular flow stage. Sand production at different flow stages is measured using a weigh scale (American Weigh ZEO-50, ± 0.001g) and then reported in pounds per square feet of the screen area (lb/ft^2). Interestingly, the amount of produced sand obtained from conventional sand retention tests is usually small. A review of the literature shows that cumulative sanding measurements, often reach values below one gram (Devere-Bennett 2015; O’Hara 2015; Mahmoudi et al. 2016a). A thorough cleaning procedure is carried out after each experiment to ensure that sand particles correspond to the actual test.

Moreover, a back-pressure column attached to the outlet of the cell provides a counterforce to avoid any flow surge or turbulence. Additionally, the hydrostatic pressure from the column provides three psi of pore pressure inside the sand-pack.

3.2.5 Test Coupons

The coupons are disk-shaped samples of 6.75 inches in diameter, specially designed and manufactured to represent a portion of an actual WWS. The wires consist of stainless steel material and triangular wedge-shaped geometry with supporting rods beneath (**Figure 3-4**). **Figure 3-5** shows the picture and a schematic of a test coupon with design specifications. Maximum aperture tolerances are around ± 0.001 inches.

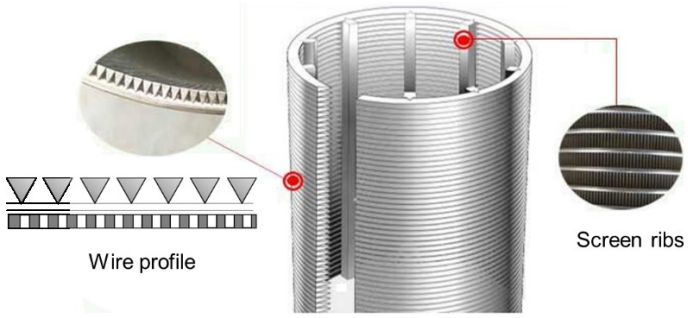

Figure 3-4. Wire profile and support ribs, modified after Guangxing Screens Co., Ltd

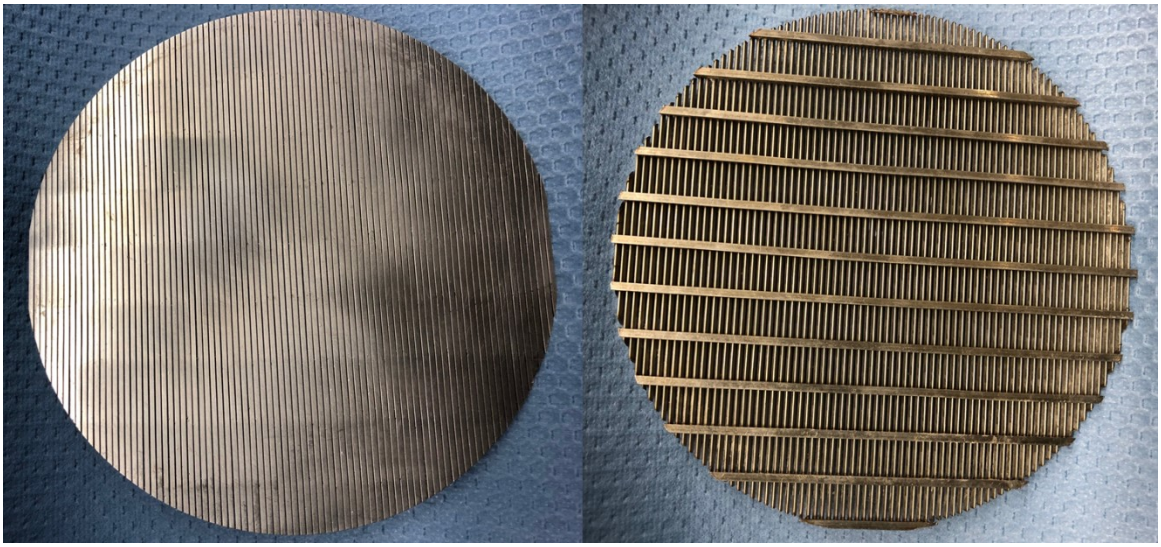

(a)

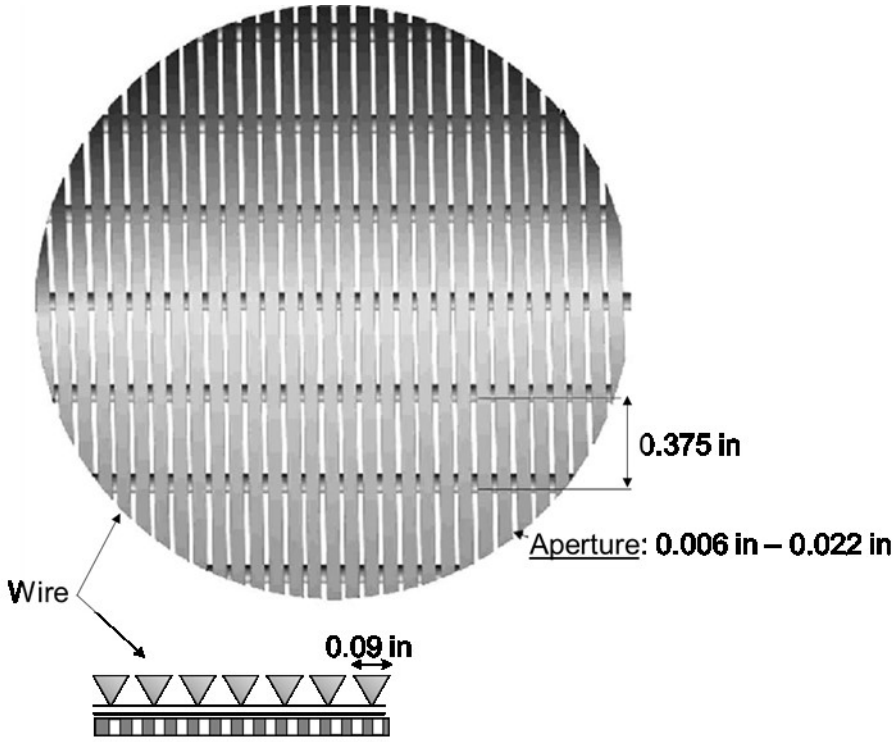

(b)

Figure 3-5. WWS coupon, (a) picture, (b) design specifications

3.3 Experimental procedure

Commercial sands were found to be able to match the PSD of distinctive McMurray formation sands. Mahmoudi et al. (2016c) presented a detailed work on unconsolidated sand replication, which showed that synthetic samples besides matching formation sands PSD also provide similar mechanical properties, as well as comparable shape factors. Several commercial sands and silts mixtures are necessary to duplicate the typical sand-prints or classes of the McMurray formation.

The fluid injection follows a constant-flow rate approach with pressure drop measurements along the sand-pack. Hodge et al. (2002) proposed the use of constant pressure differentials while recording the fluctuations in flow rate. This procedure has also been employed by Constien and Skidmore (2006) for conventional sand control analysis and by O'Hara (2015) in a SAGD application study. Pressure drops reported in the literature are higher than typical SAGD operational constraints, varying between 100 psi and 200 psi (Hodge et al. 2002; Constien and Skidmore 2006; O'Hara 2015). Adequate selection of experimental pressure drops is a difficult task due to the limited size of the samples, whereas flow rates can be scaled through comparison of coupon and SCD tubular areas (Montero et al. 2018). Furthermore, constant flow rate tests are easier to control compared to constant pressure drops, limiting experimental artifacts.

3.3.1 Fluids preparation

Clays content present in McMurray formation sands shows pH and salinity sensitivity to the flowing water (Bennion et al. 2009; Mahmoudi et al. 2016b). A change in the properties of brine can induce electrical changes on clay's surface, possibly leading to fine particles detachment from the grains and the initiation of fine particles migration through the porous media (Khilar et al. 1990).

The pH and salinity of produced water in SAGD projects changes during the life cycle of the well because of the progressive extraction of fluids and mixture between the condensed steam and formation water takes place. Therefore, the pH would depend on the caustic nature of the injected steam and steam condensate and the presence of carbon dioxide (CO_2) and hydrogen sulfide (H_2S) in the reservoir (Bennion et al. 2009). Mahmoudi et al. (2016b) summarized

the reported pH values of SAGD production water from several projects. The pH range from 7.3 to 8.8, being 7.9 an average value. In this study, 7.9 is selected as the pH value for all tests. Before the test, the pH is adjusted by adding pH chemical boosters such as sodium bicarbonate (Na_2CO_3 – increaser) or sodium bisulfate (NaHSO4 – reducer). Usually, small amounts render the desired pH and coated paper strips determine the pH of the fluid.

On the other hand, the test brine has a salinity of 400 ppm. This value represents the lowest value for NaCl in the literature for representative of SAGD projects. The use of monovalent cations such as NaCl appears to be the worst-case scenario for fines mobilization (Khilar and Fogler 1984). Besides, Na+ and Cl- (sodium and chlorides) are the governing ions in the produced water from SAGD wells (Cowie 2013). Mixing of deionized water with salt (NaCl) produced the desired salinity level.

The experimental procedure does not incorporate high-temperature due to operational complexity. A 10 cp mineral oil is employed in order to match the bitumen condition at high formation temperatures in SAGD wells (Devere-Bennett 2015).

3.3.2 Coupon and cell preparation

Thin wire mesh prevents any sand from plugging the tubings connected to the pressure transducers. Once the coupon is ready, the test cell sits over a gasket placed around the coupon, and it is carefully tightened for the following procedures.

3.3.3 Sand-pack preparation

First, a container receives all the different commercial sands and clays in the precise weights and proportions dictated by the recipe of each sand class. The sand is mixed with 10% by weight of water, and a sand mixer machine distributes all the different type of grains uniformly. The success of the SRT test is subject to an appropriate sand-pack preparation; the sand should be homogeneous and uniform regarding porosity and permeability. If the fines content changes dramatically over the length of the pack, plugging analysis lack of accuracy, especially for the porous media close to the coupon (Montero et al. 2018). As mentioned before, a critical operational factor in SAGD projects is to maintain a low-pressure differential between the well pair. Fines migration can influence the pressure drop between

the injector and the producer, resulting in plugging of the slots and porous media around the production well due to excessive ramp-ups (Williamson et al. 2016). The synthetic samples obtained after the mixing were verified to determine the PSD and consistency of the preparation.

As the size of the sample increases, the need for adequate packing becomes more relevant due to the higher risk for heterogeneous distribution along the sand-pack (Montero et al. 2018). However, there is not much discussion about this issue in the published literature. Chenault (1938) reported trials with various methods of tamping and recommended mixing one-unit weight oil in 20-unit weight of sand. Sand layers are poured in a container attached to a jolt ramming machine that vibrates the sand layers in four 15-seconds intervals. Although this method may be useful, the procedure is laborious and requires additional equipment. In this study, the moist tamping method proposed by Ladd (1978) is employed to create the sand pack. This technique renders acceptable uniform samples with a maximum density variation of 1.5% according to Bradshaw and Baxter (2007). The procedure consists of a layer-by-layer packing till the top of the cell is reached. The weight of the final sand pack is around 11 kg with 10% water content.

3.3.4 Sand-Pack saturation and displacement

Brine flow in an upward direction ensures the full saturation of the sample and avoids premature plugging. An axial load of 60 psi is applied on top of the sand pack by the load piston acting over the top platen. The application of stress prevents the fluidization of the sand pack due to the unconsolidated nature of the samples and low effective stresses. Furthermore, sand packing produces samples with partial saturation of 70-75%, depending on the sand class. This allows the employment of low flow rates (450 cc/hr) to saturate the high permeability sand pack thoroughly. When brine starts flowing from the top of the cell at a constant rate, the saturation process is considered to be finalized. The adequacy of the packing and saturation process can be determined by checking the permeability of the sand pack at different points. If the variance of permeability is high (>5%), the sand preparation is regarded as a failure.

After achieving brine full-saturation, the oil injection initiates towards the coupon at 1250 cc/hr in order to displace the brine and reach an irreducible water saturation state. Displacement lasts for approximately two hours. This scheme was suggested by Bennion et al. (2009), and it emulates the initial saturation condition of the reservoir. Similarly, a low flow rate is employed to prevent damage to the sample. Flowing oil from top to bottom translates into a better displacement due to the gravity assistance on water flow (Peters 2012). Once oil production is observed at a constant rate with no water production and stable pressure readings, the sample is considered to be at irreducible water saturation condition.

3.3.5 Fluid injection

The injection scheme employs different flow conditions including single-phase flow, two-phase flow, and three-phase flow with varying flow rate levels and fluid ratios (**Figure 3-6**). Three liquid rate levels were employed during the tests and time for achieving pressure-stability depended on the flow rates and flowing phases. Each flow stage lasts for sufficient time after stabilization; the duration of a stage varies from 0.5 to 1.5 hours. Including displacement, liquid stabilization before the gas flow and the flow injection program, the duration of one test is approximately 13 hours.

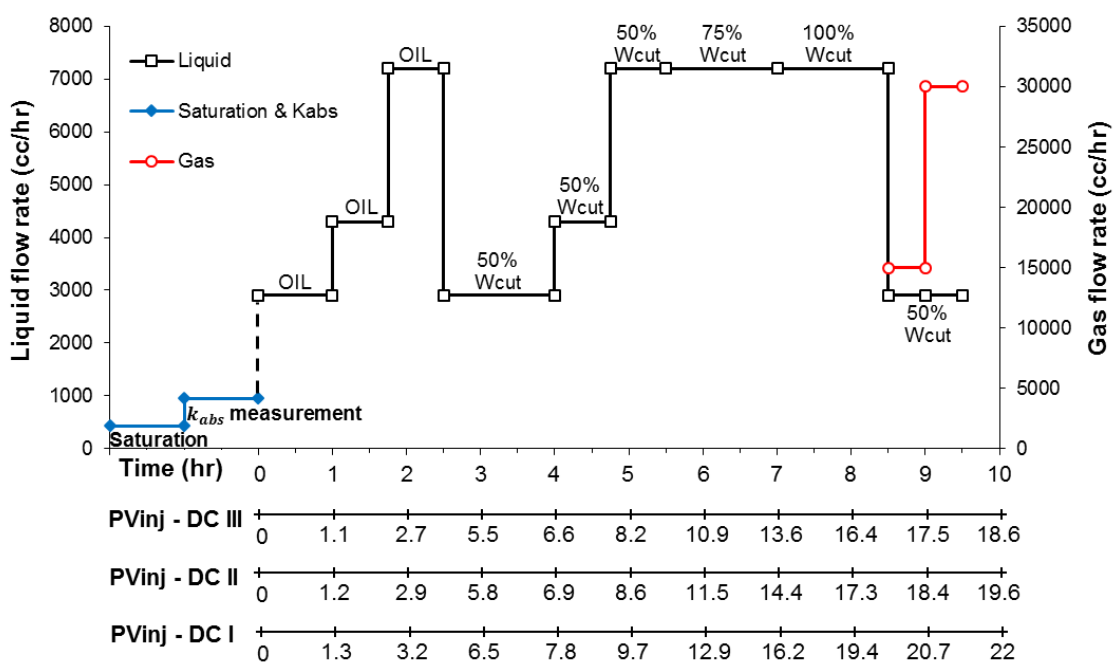

Figure 3-6. Fluid injection program

Reynold numbers (Re) during the tests ensure laminar flow during liquid and gas stages. Chilton and Colburn (1931) evaluated non-Darcy flow for packed particles and redefined Reynold numbers (**Equation 3.1**) to identify turbulent flow.

$$\mathrm{Re} = \frac{\rho * D_p * v}{\mu} \tag{3.1}$$

Where ρ is the density of the fluid, D_p is a representative particle diameter, v is the superficial velocity and, μ is the fluid viscosity. Turbulent flow or non-Darcy flow are usually observed for Re > 10. The maximum Re during the tests is approximately 2.

The test initiates with single-phase oil flow to emulate early stages of SAGD production. Then, two-phase oil and water are injected in three stages at the same liquid rates as the oil flow steps. After reaching the maximum flow rate, the water cut is increased in two steps to reach 100% water injection. This progression is designed to emulate changing wellbore conditions over time, where the water-cut levels show an increasing trend during field operations (Stahl et al. 2014). Although single-phase brine injection has been criticized by some authors (Romanova et al. 2017) due to the questionable representativeness to bitumen production, water cuts as high as 90% have been reported in the field (AER 2017). Single-phase brine injection would represent a worst-case scenario for both sand production and fines migration (Gabriel and Inamdar 1983; Wu and Tan 2001; Mahmoudi 2017). Also, some parts of the wells at the late stages of production may produce only water. Therefore, brine injection broadens the spectrum of challenging conditions for WWS, where the advantage of high OFA can be evidenced. The method presented here allows assessing the impact of flow velocity and water cut independently.

Next, two stages of co-injection gas (N_2), brine and oil resemble the event of steam-breakthrough in some sections of the well. Although the precise influx conditions during such episodes are not known, several authors have implemented simultaneous injection of oil, water, and gas to simulate steam breakthrough (Bennion et al. 2009; Romanova et al. 2014; Devere-Beneet 2015; O'Hara 2015). However, in previous studies, the injection of gas is accompanied by high liquid injection rates, that already account for low effective-flow percentages. It is possible that the high steam mobility may restrict liquid inflow (Montero

et al. 2018). Therefore, during gas-liquid stages, oil and brine rates are reduced to the initial level.

SAGD wells production typically range from 800 bbl/day to 7000 bbl/day of liquid (AER, 2017), 400 bbl/day to 1000 bbl/day is an industry average bitumen production per well pair (Handfield et al. 2008; Medina 2010). Moreover, the horizontal sections of SAGD wells go from 600 meters to 1000 meters, which translates into 0.13 bbl/day to 1.81 bbl/day per square feet area of the liner or screen provided that flow is uniform along the well. Coupons tested have an area of 0.27 ft^2, the downscale flow rate would be 0.03 bbl/day (200 cc/hr) to 0.27 bbl/day (1790 cc/hr) for the typical range mentioned above.

However, fluid influx along such length is rarely uniform, and previous studies have usually employed much higher flow rates when compared to the equivalent uniform field rates (**Table-1**). For instance, Mahmoudi (2017) used a maximum equivalent flow rate higher than 40,000 bbl/d in their single-phase study. The previous rate was implemented to take into account excessive plugging and the non-uniform production profile along the well.

In-situ processes generate conditions that can lead to slot plugging due to corrosion, scale precipitation, and clay adhesion inside the slots (Romanova and Ma 2013). Plugging reduces the OFA in some parts of the SCD, hence increasing the influx velocity. Factors such as reservoir heterogeneity, wellbore trajectory excursions, and completion factors may also induce a non-uniform flow along the length of the screen. For instance, non-uniform flow distribution has been analyzed by authors such as Beshry et al. (2006) and Stone & Bailey (2014). Some sections of the well can double (50-60%) the calculated uniform influx rate.

Additionally, due to the gravity-assisted flow and the temperature difference observed between the top and bottom of the well (Beshry et al. 2006), it is expected that most of the flow occurs along the upper portion of the well. Rapid ramp-ups associated with increasing pressure drops (Williamson et al. 2016) are often experienced after workover procedure or shut-ins. The previous aspects justify the application of effective flow factors to account for diverse scenarios of production when downscaling flow rates to laboratory conditions.

Effective flow percentages were applied assuming different non-uniform production and plugging scenarios to an average equivalent field rate of 4000 bbl/day (340 m^3/d), assuming

an 800-meter wellbore length. The first flow rate accounts for high influx uniformity and 50% restricted area for flow (top of the well). The first stage also represents a well producing 6000 bbl/d of liquid at 100% effective flow (no plugging, uniform flow). Next, the second stage incorporates 30% effective flow to account for non-uniform flow, and the third liquid flow rate applies 15% of effective flow considering a plugging case. Examination of exhumated liners by Romanova and Ma (2003) showed that over 90% of the slots in an SL presented severe plugging. While there is no evidence of excessive plugging in WWS in SAGD operations, it is crucial to evaluate extreme conditions, especially when considering low-quality sands.

Likewise, high flow rates have been used in previous works. Romanova et al. (2014) employed equivalent oil rates close to 3000 bbl/d and water rates of 6000 bbl/d. Devere-Bennett (2015) used oil rates up to 4500 bbl/d and a maximum water rate of 9000 bbl/d. As expected, the flow rate has a significant impact on sand production, fines mobilization and plugging (Bennion 2002; Tronvoll et al. 2004; Bennion et al. 2009). Accordingly, Devere-Bennett (2015) carried out some tests at reduced flow rates. It was observed that the influence of flow rates is related to the degree of appropriateness of the slot size for specific sands. The impact of sanding and plugging for an adequately designed SCD is less than the same for an exceedingly small or large slot width.

3.3.6 Postmortem analysis

During the flow test, fluid samples are collected from the discharge in the production outlet, immediately after the coupon. The postmortem measurements include the determination of the concentration of fines in the produced fluid during each step rate using a turbidimeter (HACH 2100P, ±2% accuracy). On the other hand, the cumulatively produced sand is reported in pounds per square feet of coupon area and is monitored at every flow stage.

An improvised core barrel consisting of an aluminum tube extracts core samples from the sand-pack that follow a splitting process into three sections. Samples are then dried in a fume hood to remove oil and water. Subsequently, samples from the near-screen zone, middle, and top of the sand-pack undergo a wet sieving technique using a mesh #325 or 44μm (ASTM Specification E-11, ±3 μm permissible variation) to remove the fines particles of each

sampling point. The grains retained by the mesh go into an oven for 24 hours and the mass difference measured allows the determination of fines content. Therefore, the difference between initial and final fines content inspects the mobilization of fines through the porous media from top to bottom.

3.4 SRT assumptions and limitations

Ideally, a large pre-packed SRT incorporating a radial flow cell at high temperatures and varying stress levels would more closely resemble the conditions of the borehole. However, this type of assembly is limited by cost and operational complexity (Montero et al. 2018). Temperatures of the steam chamber reach values higher than 200 degrees Celsius and facilities including this operational aspect may be laborious and dangerous to manipulate.

Besides the effect of temperature on the bitumen viscosity, rock properties such as wettability and permeability are affected by high temperatures (Bennion et al. 2007; Romanova et al. 2015; Romanova et al. 2017). For instance, high water-wet conditions are achieved due to the dissolution of asphaltic components (Bennion et al. 2007). Mineral alterations can result in thermal formation damage reducing the sand permeability as diagenesized material coat sand grains (Williamson et al. 2016; Romanova et al. 2017). Also, grain expansion and silica re-precipitation can plug the pore space (Bennion et al. 2007). Regarding the SCD, there is a potential for slot plugging due to the corrosive materials generated by in-situ gases such as CO_2 and H_2S (Romanova and Ma 2013). Continuous aquathermolysis reactions take place at reservoir conditions that generate these corrosive gases due to the high temperatures and water content. Nonetheless, technical limits such as the time scale to capture any of the possible effects of high temperature in the porous media would result in a costly experiment, hard to replicate regularly.

The tamping and dead weights during the packing of the sand do not suppose any significant level of stress. Low axial stress is applied (60 psi), and the constraint boundaries of the cell generate radial stress. For a complete analysis of the effect of stresses, the facility should be able to control both radial and axial stresses (Guo et al. 2018). The SRT employed in this investigation relates to that scenario were the collapse zone around the liner just formed, and no significant stress build up is acting.

Moreover, conventional SRT devices employ linear flow injection instead of the radial flow expected in the proximity of the well at reservoir conditions. Radial flow geometry causes zones of varying flow velocity which influences near-wellbore phenomena such as seepage drag forces, fines migration, wellbore plugging, and pressure drops (Montero et al. 2018). Valdes and Santamarina (2006) performed experiments that showed progressively thicker radial bridges forming under radial flow due to fine particles retardation. Retardation occurs due to the collision of fine particles on pore walls as the flow streamlines converge towards the outlet. Eventually, these radial bridges will achieve stability preventing further solids production (Valdes and Santamarina 2006), but perhaps increasing the flow impairment.

In the experiments, sodium chloride (NaCl) was used to adjust the salinity of the brine. Although Na^+ and Cl^- are the dominant ions in produced water for SAGD projects, various ions and minerals are also present. Magnesium (Mg), Calcium (Ca), Barium (Ba), carbonate (CO_3), bicarbonate (HCO_3) and sulfate (SO_3) are commonly found in produced water at different concentrations (Cowie 2003). Since the release and mobilization of fines and clays increase for brine containing monovalent cations (Khilar and Fogler 1984), NaCl is implemented as a worst-case scenario.

Sand specimens for SRT testing were reproduced using commercial sands and silts. The final mixtures replicate the main features of the actual PSD while having similar shape factors and mechanical properties as the formation sand (Mahmoudi et al. 2016c). Each test consumes around 12 kg of sand mixture which makes impractical the implementation of real formation sand. The availability of formation sand is usually limited. Additionally, the employment of formation sands complicate the repeatability of the tests since they are heterogeneous and duplicating the same PSD would require additional work.

Formation sands must follow cleaning and preparation procedures that could alter the characteristics of sand particles. Most heavy oil reservoirs are water-wet sands in which the heavy asphaltic components of the bitumen provides certain oil wettability to some grains. However, high temperatures during SAGD operations results in higher water-wet conditions (Bennion et al. 2007). Commercial sands display strong wettability towards water, and it is assumed that the drag forces arising under these conditions are similar to the ones presented in the reservoir. Moreover, the preparation of sand mixtures and clay with water (moist

tamping) intends to replicate the equilibrium status of clay particles with formation water (Bennion et al. 2002).

During the tests, immiscible fluids flow as separate phases at different pore scale distributions depending on the level of saturation of each phase. Nevertheless, apart from free phase flow, in-situ emulsions occur in SAGD process due to the transfer of steam-condensate microbubbles into the oil phase (Ezeuko et al. 2013). This type of emulsion is known as a water-in-oil emulsion, and it is stabilized at reservoir conditions by asphaltene components in the bitumen. Asphaltenes act as surface-acting agents that are absorbed in the water-bitumen interface (Zhao et al. 2009; Kar et al. 2014). Emulsions exhibit different viscosities than that of constituents components. Water-in-oil emulsion display viscosities typically higher than the oil at the same temperature conditions (Sasaki et al. 2011). Also, emulsion flow changes the relative fluid conductivity by reducing the amount of water distributed at narrow pores and coating grains as a separate phase (Ezeuko et al. 2013). This phenomenon results in less multiphase flow and increasing effective permeability of the oil. PSD and wettability are the dominant aspects of the relative permeability displayed from sands. Since synthetic samples match the PSD of formation sands and higher water-wet conditions are expected with time, it is assumed that the relative permeability of the synthetic sand-pack results in a similar condition as in the reservoir. Moreover, ensuring consistent and stable emulsions at laboratory conditions is complicated to achieve and requires the addition of emulsifiers and continuous quality control.

Fines particles and solids are also capable of stabilizing emulsion (Sztukowski et al. 2005). Fines locate at the interface between the droplets and the continuous phase (Menon et al. 1988). Therefore, the presence of stabilizing fines may affect fines migration, and the interaction of microbubbles with fines are not captured in this study.

In summary, the perceived limitations of scaled SRTs do not translate into non-valuable results. When representative flow rates, fluid properties, and sand types are implemented, the scale SRT tests allow the analysis of physical phenomena, offering an insight of the impact of different aspects controlling sand production and pore clogging.

3.5 Measurement uncertainties

The produced sand is measured by a weight balance in grams and then converted to lb/ft^2 by multiplying recorded mass by a constant (c) based on the coupon area and unit conversion. The accuracy of the balance (δW_b) is of ±0.001g, and the absolute uncertainty of cumulative produced sand (δW_s) is expressed by **Equation 3.2** as:

$$\delta W_s = c * \delta W_b \tag{3.2}$$

Permeability calculations are a function of flow rate and corresponding pressure drop. The uncertainty of retained permeability is a combination of the two absolute permeability measurements. **Equation 3.3** calculates the absolute uncertainty for permeability (δK_{abs}). δp and δq are the absolute uncertainties of pressure drop (ΔP_b) and water flow rate (q_w), respectively. Accuracy from pressure transducers and weight scales determine the uncertainties for pressure drop and flow rate measurements.

$$\delta K_{abs} = |k_{abs}| * \sqrt{\left(\frac{\delta q}{q_w}\right)^2 + \left(\frac{\delta p}{\Delta P_b}\right)^2} \tag{3.3}$$

Therefore the error from absolute permeability measurements is propagated to retained permeability (δK_{ret}) as:

$$\delta K_{ret} = |k_{ret}| * \sqrt{\left(\frac{\delta K_{abs,i}}{K_{abs,i}}\right)^2 + \left(\frac{\delta K_{abs,bottom}}{K_{abs,bottom}}\right)^2} \tag{3.4}$$

$\delta K_{abs,\,i}$ and $\delta K_{abs,\,bottom}$ are the absolute uncertainties of original absolute permeability ($K_{abs,i}$) and absolute permeability of the bottom section ($K_{abs,bottom}$), respectively. $\delta K_{abs,bottom}$ also accounts for the uncertaintes obtaining relative permeability at residual oil conditions. An additional quadratic term $\left(\frac{\delta K_{rel}}{K_{rel}}\right)^2$ is added to **Equation 3.3.**

Finally, the uncertainties of fines concentration measurements (δC_f) involve the weigh accuracies of the total mass of sample (δm_t) and measurement of the mass of fines (δm_f) from the sample as shown in **Equation 3.4**. Where m_f is the mass of measured fines and m_t is the mass of both sand and fines.

$$\delta C_f = \left|\frac{m_f}{m_t}\right| * \sqrt{\left(\frac{\delta m_t}{m_t}\right)^2 + \left(\frac{\delta m_f}{m_f}\right)^2} \tag{3.4}$$

3.6 Testing repeatability

The repeatability of the experimental results was examined for sand production and final retained permeability. Additional tests were performed for coupons with slot widths of 0.018" and 0.014" for DC-II and DC-III, respectively.

Figure 3-7 shows an excellent agreement in sand production between two sets of test for both sands. DC-III presented a maximum difference of only 3% in cumulative sanding while DC-II display similar results with 5.2% of difference. Moreover, produced sand throughout the tests showed consistent trends and sanding modes. **Table 4** shows the finals retained permeability results for the repeated tests. As shown, the values of retained permeability are almost the same (±1%).

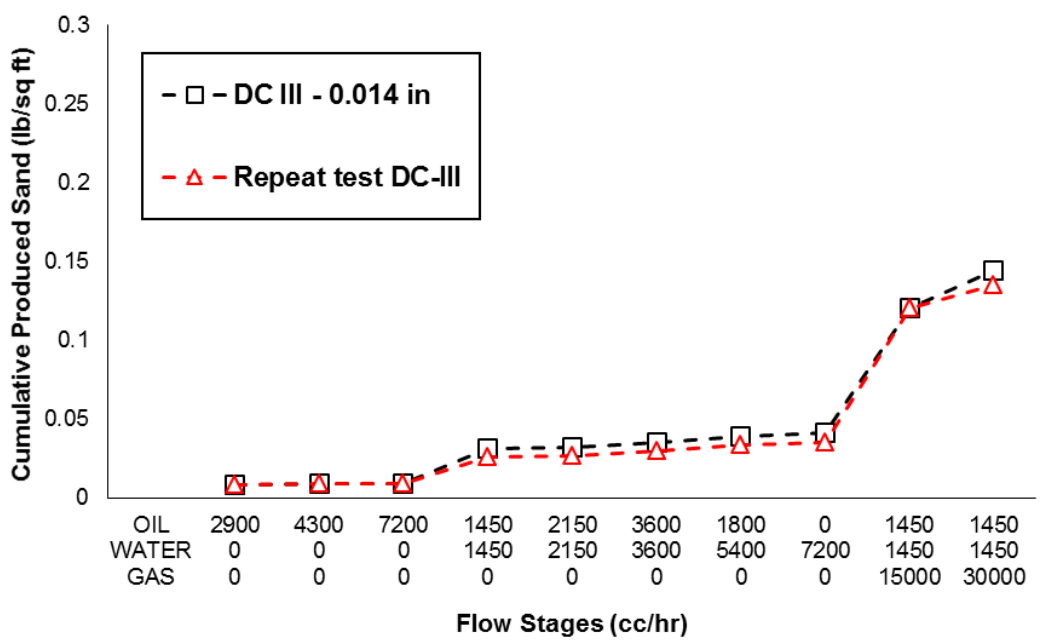

(a)

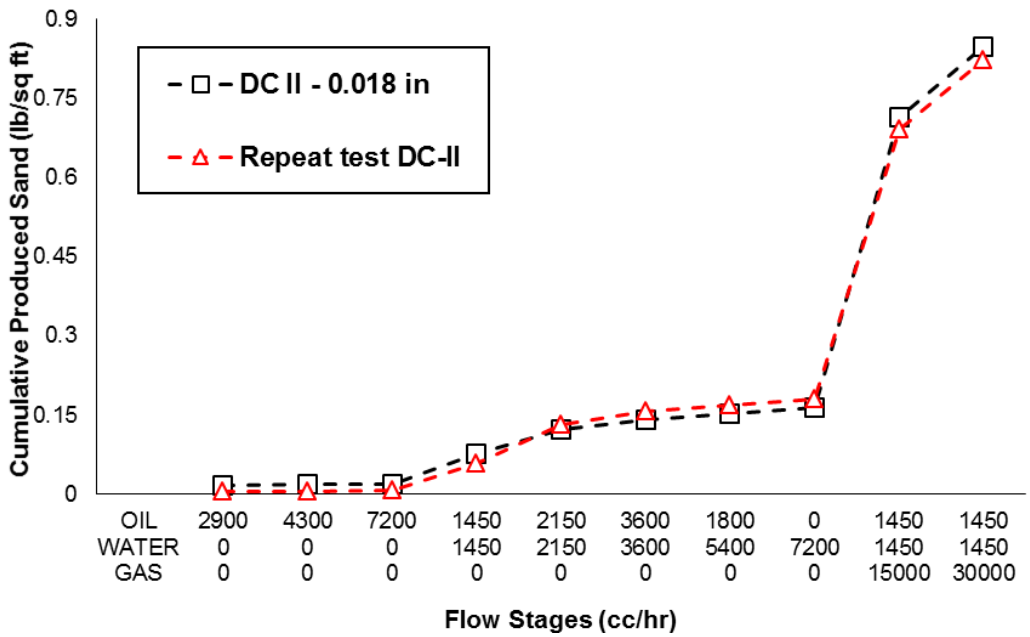

(b)

Figure 3-7. Cumulative produced sand for repeatability tests. (a) DC-III, (b) DC-II

Table 3-4. Retained permeability for repeated tests

DC-III		DC-II	
K_{ret} (%)		K_{ret} (%)	
0.014"	**0.014" - repeat**	**0.018"**	**0.018" - repeat**
85%	86%	94%	94%

The PSD of commercial sands is regularly checked to maintain consistent sample preparation. **Figure 3-8** shows the PSD of three DC-III samples in which the maximum deviation is less than 1%.

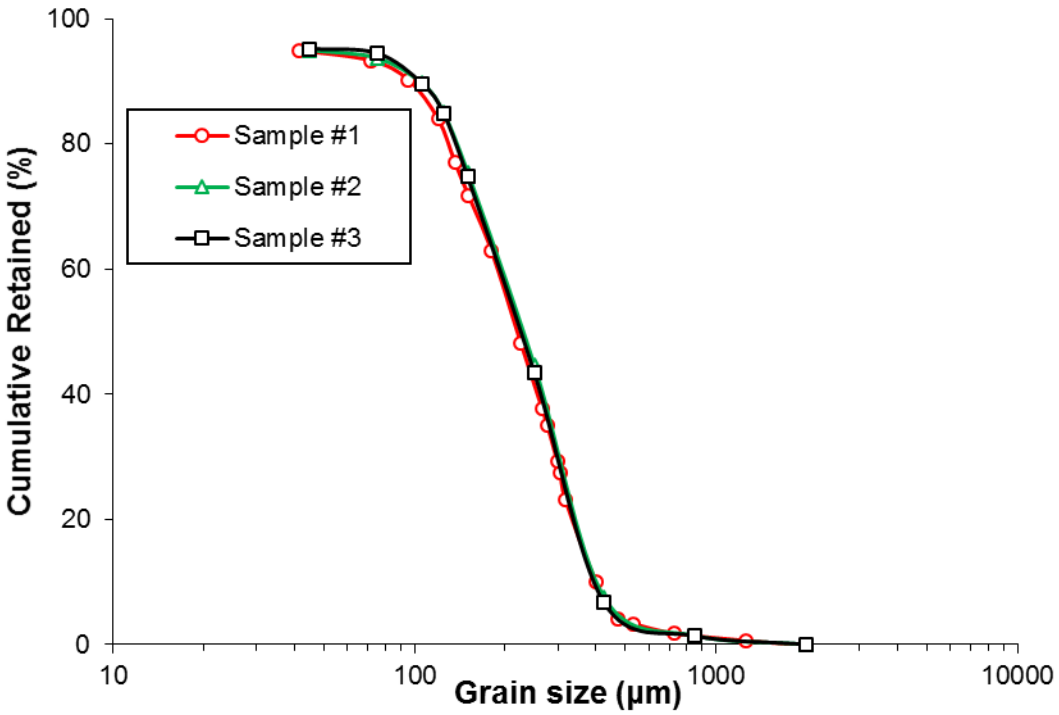

Figure 3-8. PSD verification of three prepared samples (DC-III)

CHAPTER FOUR: SAND RETENTION PERFORMANCE OF WWS IN SAGD OPERATIONS

4.1 Introduction

Wire-wrapped screens (WWS) have been extensively implemented as a filtering screen for oil, gas, mineral, and groundwater production operations. Layne (1918) firstly introduced WWS (U.S Pat. No US6298914B1) and rapidly transferred from water production wells to the oil industry. In SAGD wells, WWS act as stand-alone completion to provide sand control and well support against the naturally-formed "gravel pack." The borehole gradually collapses onto to screen due to bitumen melting and drag forces, creating a high-porosity zone (Fattahpour et al. 2016b).

The preference for the selection of SCD has changed throughout time. Early SAGD pilots, such as the AOSTRA UTF project, employed WWS as the sand control method (Edmunds et al. 1987; Wells et al. 1997; Chakrabarty et al. 1998; Saltukaroglu et al. 1999; Grills et al. 2002). WWSs were selected due to their high deliverability, vast industry experience, and slot manufacturing deficiencies for narrow apertures in SL designs (Xie et al. 2008). However, the operations faced several issues, and sand-cleanout operations were required (Chakrabarty et al. 1998; Edmunds 2000; Hollies et al. 2001). Inadequate running operations and improper aperture and hole sizing resulted in screen damage (Xie et al. 2008). Thereafter, companies relied on SLs owing to their low price and superior mechanical integrity (Spronk et al. 2015). Nonetheless, SLs started exhibiting severe plugging tendencies due to corrosion by-products, fines accumulation and scaling (Romanova and Ma 2013). Therefore, in recent years, high OFA devices such as WWS and PPS gained more attention. For formations with high fines content and reactive clays, SLs are less effective, and WWS is usually preferred (Romanova et al. 2015). Currently, the industry recommends the use of WWS for production wells and SL for injection wells (O' Hara 2015; Spronk et al. 2015).

WWSs ability to retain or control the production of solids relies on the stability of particle bridges and size-exclusion provided by the slot aperture. In conditions were the borehole collapses over the screen such as in SAGD, the primary mechanism of retention is particle bridging over the slots (Mahmoudi et al. 2016a). Since the screen is exposed to several particles sizes, bridges will occur as several particles attempt to flow simultaneously through

a restriction (Vittal and Sharma 1999; Chanpura et al. 2011). If several particles were not available (less than 1% by volume), particle retention by the slot is by size exclusion only (Valdes and Santamarina 2006).

Bridge stability is mainly controlled by the ratio of aperture size over particles diameter (Chanpura et al. 2012a), local fluid velocity (Penberthy 1992; Muecke 1979), grains shape (Santamarina 2002), water cut (Wu and Tan 2001; Vaziri et al. 2002) and flowing phases. Moreover, the shape of the coarser tail of the PSD or the number of particles of that size of the slot will also influence the amount of sanding (Mondal et al. 2010).

The tolerance for sanding varies depending on specific operating conditions. Veeken et al. (1991) presented a limit range of 0.95-95.38 g/bbl for conventional oil producers and 453.6 g/MMscf for a gas producer in vertical wells. For SAGD wells, the acceptable limits depend on sand transportability along the horizontal well, artificial lifting restrictions and requirements of surface facilities. By comparing the screen performance history of several fields with that of experimental studies, Hodge et al. (2002) proposed a limit of 0.12 lb/ft^2 for cumulative sand per screen area. Moreover, the use of Electrical Submersible Pumps (ESP) constrains the production sand to 50 gr/bbl (Devere-Bennett 2015).

Generally, the slot aperture represents the main sand control factor and the design specification most studied. On the other hand, the impact of OFA on sanding seems to be less pronounced (Mahmoudi 2017; Fattahpour et al. 2018), although it changes among SCD. For instance, an increase in the slot density for an SL do not translate into a drastic change in OFA, whereas varying the aperture size for WWS noticeably alter the OFA. Higher OFA signifies more space available for sand to be produced. Furthermore, the proximity of the slots in WWS presents a stronger aperture-aperture interaction.

Existing design criteria usually provide a range of aperture sizes in which the upper bound relates to limit sand production and the lower bound to prevent plugging (Markesad et al. 1996). A conservative approach of SAGD developments is to use apertures in the lower bound to minimize sanding. However, this may increase the risks of slot and porous plugging (Mahmoudi 2017). As per Chapter 2, the limitations of current design criteria (PSD based only) prompt companies to further assess the performance of preferred SAS before field

applications are carried out. In this regard, laboratory testing helps to narrow down the aperture selection of the appropriate SAS.

Bennion et al. (2009) introduced a testing protocol for SAGD applications that have been adopted by authors such as Romanova et al. (2014), Devere-Bennett (2015) and O'Hara (2015). These studies implement pre-packed set-ups with a non-suitable representation of the actual OFA of an SCD. Besides, the limiting criteria for produced sand have not been supported, and the comparison between devices is biased. In this study, a large-scale pre-packed SRT is employed to capture the interaction of screen and sand pack better. Besides, objective criteria are implemented for the analysis of sand production and flow performance. The core objective of this chapter is to understand the role of slot width on the sand control response of WWS. The influence of different production scenarios is incorporated in the analysis and will fund the elaboration of new design criteria.

4.2 Testing program

The pre-packed SRT introduced in Chapter 3 was implemented in this study. Produced particles were collected by a tube receptacle located inside the sand trap. At any stage, the produced solids could be retrieved. Moreover, the flow rates used during the test account for different constraint factors such as blank pipes, reservoir heterogeneity, and slot plugging. Time for pressure stabilization varied depending on the flow rate and flowing phases.

The sand production thresholds were established as 0.12 lb/ft2 for moderate sanding and 0.15 lb/ft2 as the upper limit for cumulative sanding. These numbers correlate well with the limit of 0.12 lb/ft2 proposed by Hodge et al. (2002) and the empirical rule of thumb of constraining sand to less than 1% of the screen/liner volume (Chanpura et al. 2011; Devere-Bennett 2015). Most SAGD wells employ 7-inch or 8 5/8-inch liners with a tubing size ranging from 2 7/8 inches to 4 1/2 inches. The 1% limit for these typical SCD sizes translates into approximately 0.15 lb/ft2 for the cumulative sand produced per unit surface area of the SCD over the entire life cycle SAGD well (Mahmoudi 2017).

4.3 Results and discussion

Figure 4-1, **4-2** and **4-3** show the cumulative sand production for all the stages for DC-III, DC-II, and DC-I, respectively. The production of particles is categorized in a progressive single, dual and multiphase flow stages.

Negligible sand production occurred during the injection of single-phase oil for all sand classes, DC-I, DC-II, and DC-III. Even at high flow rates, minimal sanding is observed, and there is no significant difference between wider slots (0.018 in - 0.022 in) and narrow slots (0.006 in - 0.010in). It is well known in the industry that the wetting-phase should mobilize in order to have strong particles production (Skjaerstein et al. 1997). Therefore, these results confirm the findings of authors such as Bennion et al. 2009, Romanova et al. (2014), O'Hara (2015) and Devere-Bennett (2015).

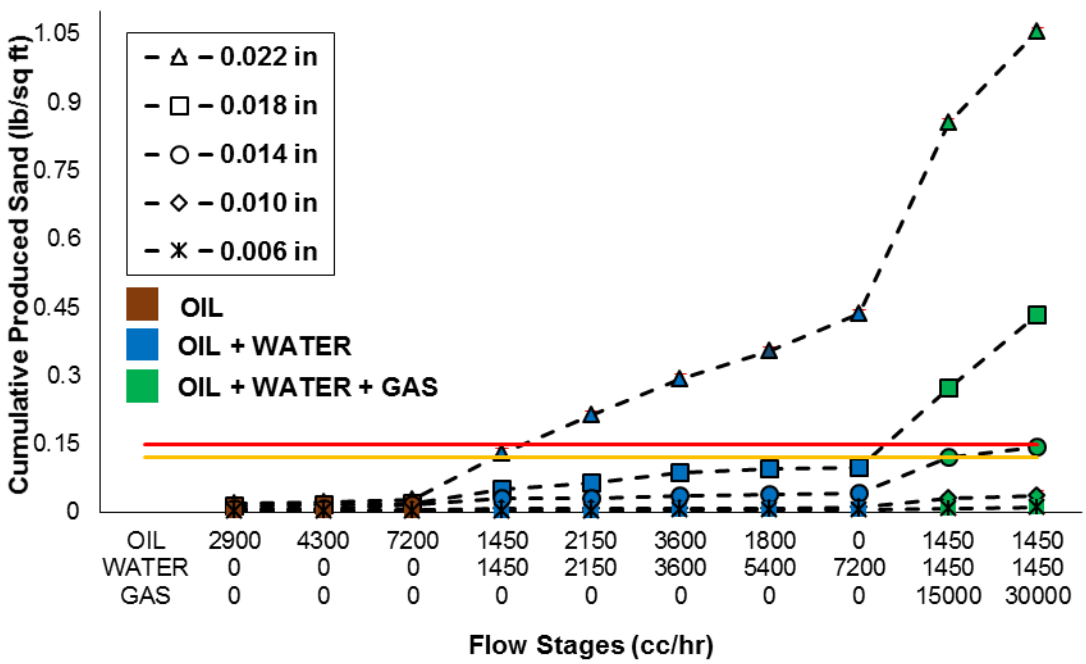

Figure 4-1. Cumulative sand production for different flow rate steps for DC-III. Red and yellow lines represent the sanding limits of 0.15 lb/ft2 and 0.12 lb/ft2, respectively

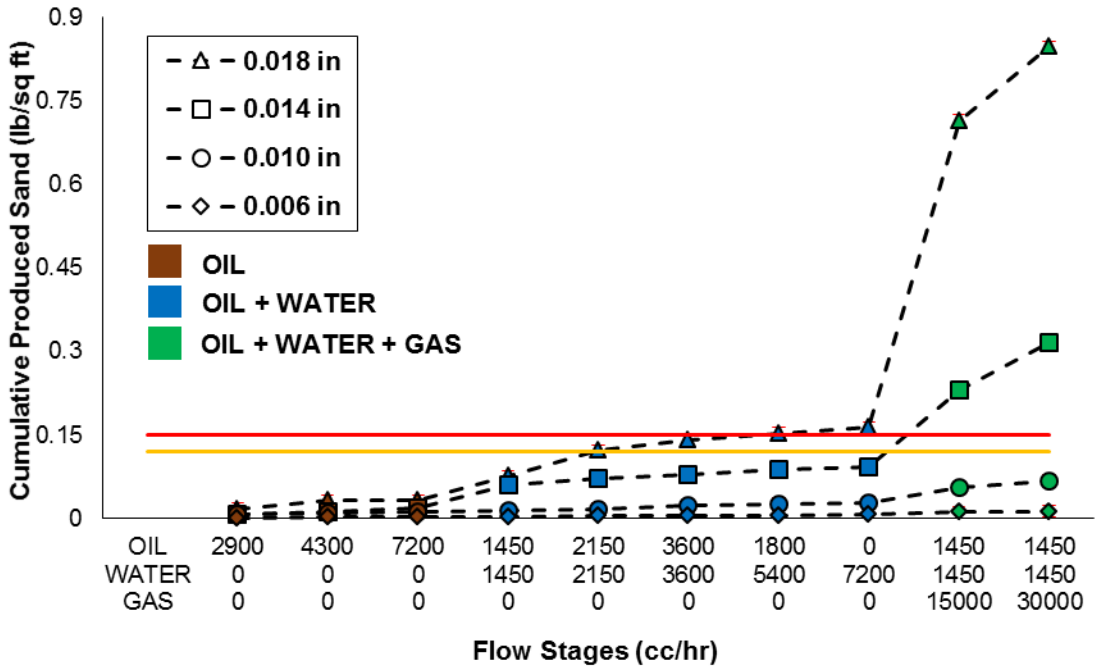

Figure 4-2. Cumulative sand production for different flow rate steps for DC-II. Red and yellow lines represent the sanding limits of 0.15 lb/ft2 and 0.12 lb/ft2, respectively

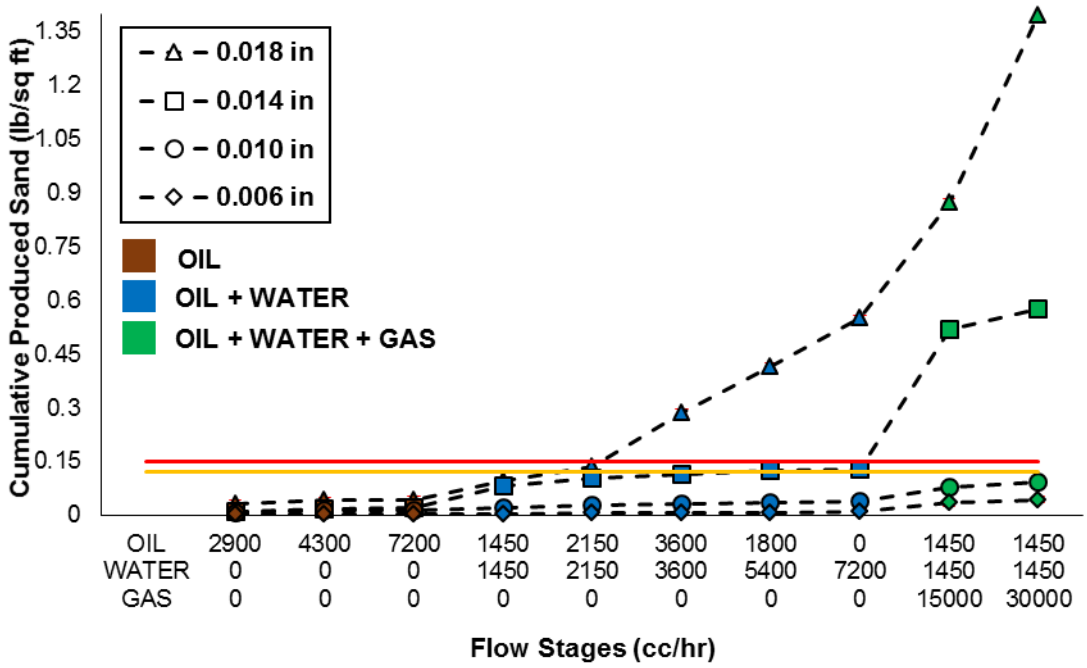

Figure 4-3. Cumulative sand production for different flow rate steps for DC-I. Red and yellow lines represent the sanding limits of 0.15 lb/ft2 and 0.12 lb/ft2, respectively.

Similarly, mode-I is also present for narrower apertures during the flow of oil and water stages. After the breakthrough of water production, there is no further sanding, which means sand bridges achieve sufficient stability for the following liquid flow rates. The onset of water production reduces the capillary pressure of the porous media and the bonding between grains (Vaziri et al. 2002; Han and Dusseault 2002). Mode-I for oil-water stages is detected for 0.006″ for all sand classes and 0.010″ for DC-III.

For remaining slots sizes, the sanding tendency exhibited a transient production behavior. As the flow rate increases, the pressure gradient through the sand bridge rises, and the drag forces exceed the frictional resistance of the bridge. This type of sanding, also named mode-II by Mahmoudi et al. (2016a), denote varying levels of sanding upon the change of flow rate or water cut. In this mode, the rate of sanding declines with time and eventually stops once the sand bridges achieve stability at a constant flow rate or fluid ratio. Moreover, for the flow scheme implemented in this study, it seems that the influence of flow velocity is more significant than the water cut.

As per **Figures 4-1** to **4-3**, the intensity of transient sanding episodes increases with slot size for each sand. The wider the aperture, the higher the OFA exposed to sanding. Additionally, the impact of transient production increases as the grain size decreases. This is due to the higher slot size over grain size ratio, which results in weaker sand bridges. For instance, during liquid stages, DC-I showed a maximum difference in sanding between 0.018″ and 0.014″ of 76% while DC-II and DC-III had a difference of 52% and 44% respectively. It is evident that the percentages of variation are closer between DC-II and DC-III due to their similar PSD shape.

Mode-II sanding also persisted during the co-injection of gas, oil, and water for most apertures, except 0.018″ for DC-I. The flow of gas is able to even disrupt the stability of bridges over narrow apertures such as 0.006″. For the 0.006″ tests, the amount of sand after the gas-liquid stages for both DC-II and DC-III doubled the cumulative sanding during liquid stages, while DC-I increased it by four times. However, the cumulative sanding is below the acceptable limits of production.

On the contrary, wider slots (0.014″ or higher) displayed a much more drastic amount of sanding due to high fluid velocities and strong forces acting on the sand bridges. During gas

flow, the velocities (0.85 m/hr to 1.65 m/hr) are five to ten times higher than the velocities encountered in the first oil-water stage. For example, the gas-liquid steps increased the produced sand to a maximum of ten times the 0.15 lb/ft2 limit for DC-I and six times for DC-II (**Figure 4-5(a)**).

The high velocities, inadequate aperture size to grain size ratio and the close distance between slots results in sand bridges taking a longer time to reach stability. As noted by Coberly (1938), the close spacing between slots reduces the "range of bridging." In cases like the 0.018″ test for DC-I (finest sand), bridge stability is never reached, and particles are continuously produced. This type of sanding is known as mode-III (Mahmoudi et al. 2016a). It is important to note that the data points for such scenarios are subjected to the duration of constant-flow rates steps.

The sanding rates during the second gas influx stages decreased, except for the continuous sanding case. It appears that the abrupt injection of gas at the first gas-liquid stage generates strong liquid displacements that significantly affect the stability of bridges. For the second gas rate, the gas has already been distributed in the core, minimizing the effect of liquid displacement.

In general, the results indicate that production scenarios greatly influences the levels of sanding. **Figure 4-4** shows the relationship between cumulative produced and slot width sand at the end of liquid stages, for the three sands. Likewise, **Figure 4-5** show the cumulative produce sand at the end of the entire test (after liquid-gas stages) as a function of the slot width.

Both figures show an exponential increase of cumulative sanding with the increase of aperture size. From **Figure 4-4(a)** and **4-5(a)**, the curves denote a steeper trend as the grain size decreases from DC-III to DC-I and the bridges loss stability for finer sands over the same slot size.

In this study, the responses of WWS up until the end of liquid stages are considered to emulate the regular SAGD operations. Steam short-circuit to producer wells is an undesired event and operators strive to prevent its occurrence due to the risks of erosion, uneven steam

chamber distribution and low productivity (Bennion et al. 2009). A comparison of the scale **Figure 4-4(a)** and **4-5(a)** signify the impact of the production scenarios.

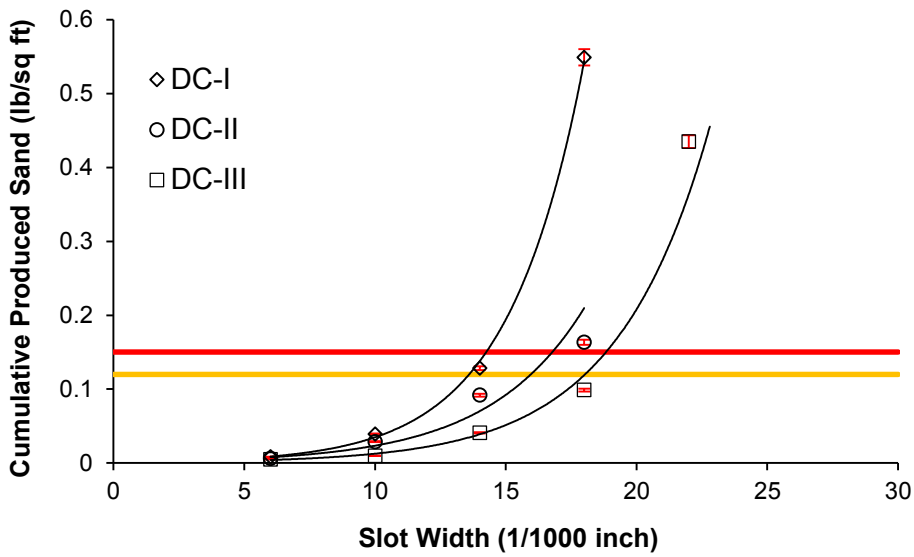

(a)

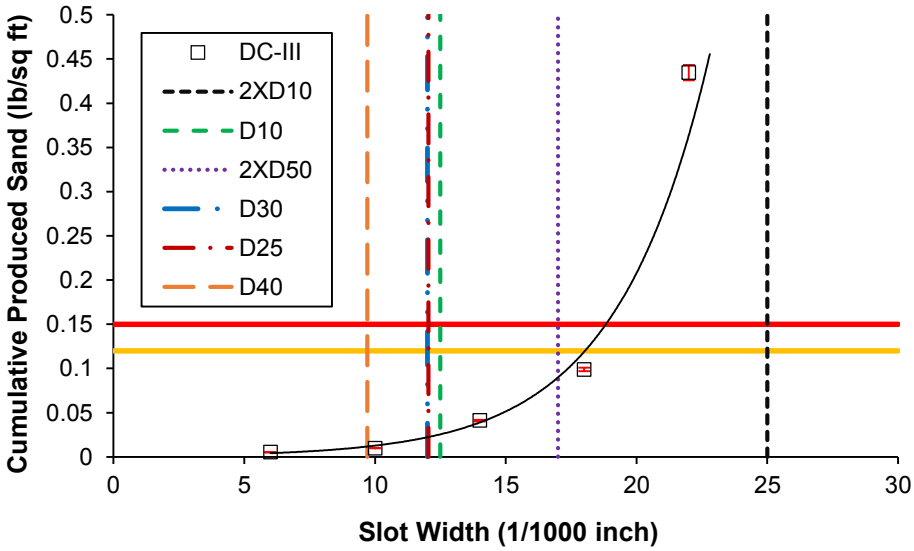

(b)

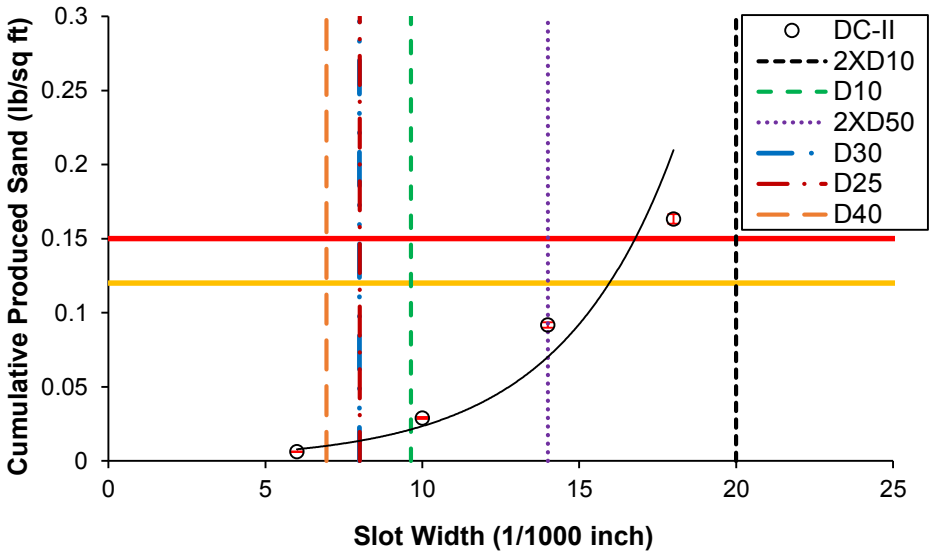

(c)

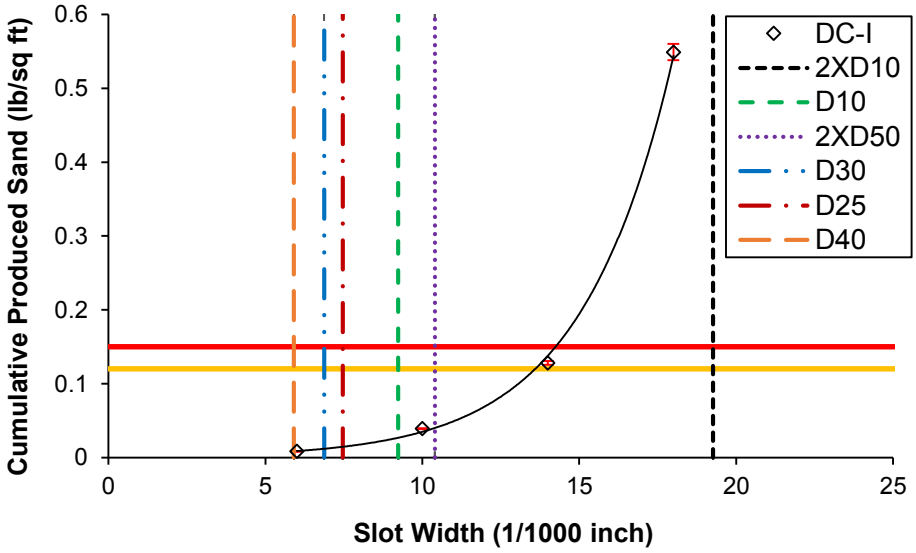

(d)

Figure 4-4. Produced sand at the end of liquid stages for different slot widths, (a) Comparison of three sands, (b) DC-III, (c) DC-II, (d) DC-I

A positive outcome from the experiments is that wide slots displayed reasonable performance throughout liquid stages, especially for coarse sands (**Figure 4-4(b), 4-4(c), 4-4(d)**). Satisfactory performances were observed below 0.018″, 0.016″ and 0.014″ for DC-III, DC-II, and DC-I, respectively.

Figures 4-4(b) to **4-4(d)** also compare the produced sand with existing criteria: 2xD10 (Coberly 1938), D10 (Rogers 1975), 2xD50 (Gillespie et al. 2000) and D30 (Ballard&Beare 2012). The early industrial criterion of 2XD10 proved to fail for the three sand classes, and it does not work as an upper bound. In contrast, the rest of the criteria result in an acceptable level of sanding. However, D10, D30, D25, D40, and 2XD50 provide a conservative aperture size, especially D10 to D40. With the increase of grain size, the upper limit of 2XD50 criterion seems to be closer to experimental results. Additionally, the difference between 2XD50 and the other criteria significantly decrease for DC-I. This is related to the poor grain distribution (PSD shape) of DC-I compared to DC-II and III, which highlights the deficiency of criteria that only rely on one point of the PSD.

Conversely, **Figure 4-5(a)**, **4-5(b)** and **4-5(c)** show that aperture sizes above 0.014″ exhibited moderate to severe sanding. This time, the upper limit of 2XD50 do not provide an adequate aperture size for high-velocity scenarios. While other criteria seem to be appropriate for challenging conditions and matches the experimental results. This show that the typical approach is to design aperture for worst-case scenarios.

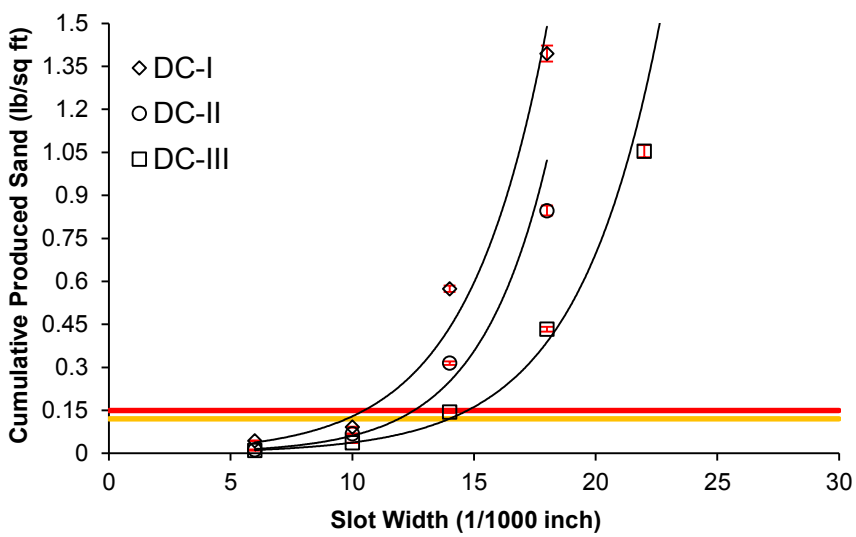

(a)

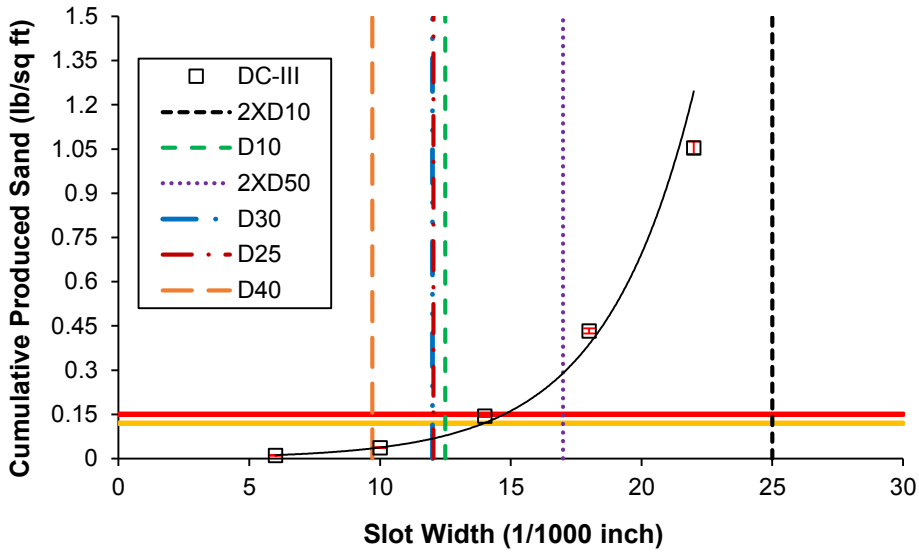
Cumulative Produced Sand (lb/sq ft)
1.5
1.35
1.2
1.05
0.9
0.75
0.6
0.45
0.3
0.15
0
0
5
10
15
20
25
30
Slot Width (1/1000 inch)
DC-III
2XD10
D10
2XD50
D30
D25
D40

(b)

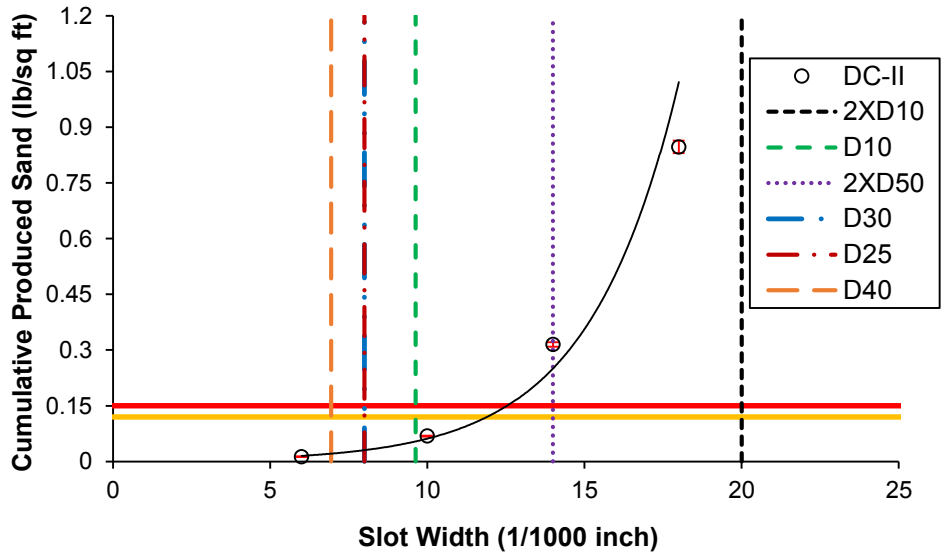
Cumulative Produced Sand (lb/sq ft)
1.2
1.05
0.9
0.75
0.6
0.45
0.3
0.15
0
0
5
10
15
20
25
Slot Width (1/1000 inch)
DC-II
2XD10
D10
2XD50
D30
D25
D40

(c)

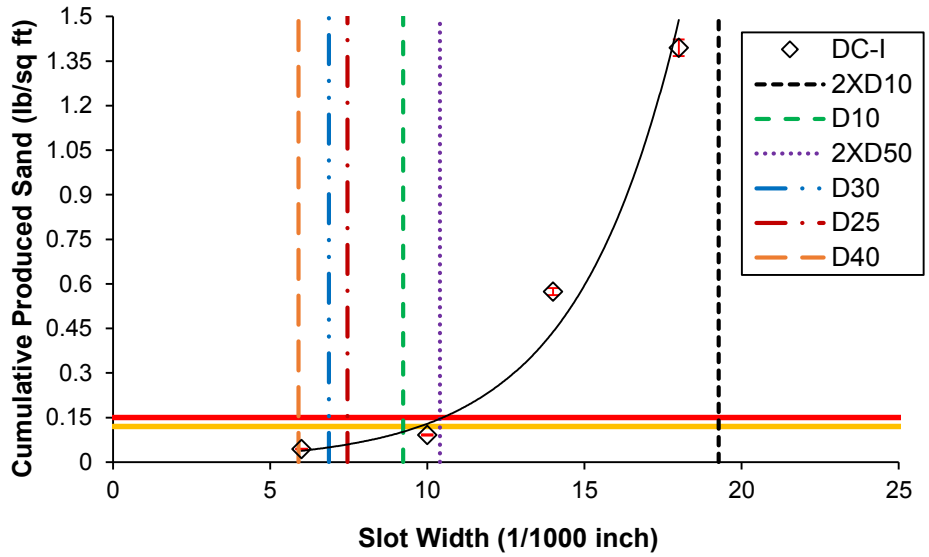

(d)

Figure 4-5. Produced sand at the end of gas-influx stages for different slot widths, (a) Comparison of three sands, (b) DC-III, (c) DC-II, (d) DC-I

4.4 Conclusions

This chapter presents the results of pre-packed SRTs to investigate the role of slot width and production scenarios on produced sand. The laboratory testing aimed at reviewing and validating the current industrial WWS design regarding sand control.

The experimental approach uses high flow rates to simulate various cases, where local plugging of slots, heterogeneity and completion design results in increased fluid velocities in the open slots. Also, the test incorporates single-phase flow to multiphase flow to represent the life of a SAGD well in a progressive fashion.

The most important finding of this chapter is the observed modes of sand production and their dependence on the flowing phases. During oil stages, initial or Mode-I sanding occurred for all apertures. Similarly, narrow apertures (0.006″) show this behavior during oil and water flow. There is an initial sanding occurrence, but the sanding ceases after the onset of water. In transient sanding or Mode-II, the impact of flow rate dependency increase with the slot size over grain size ratio. At constant flow rate or constant water cut the sanding gradually

stops, as observed for slot sizes 0.010″ to 0.018″. Mode-III relates to continuous sanding as the flow velocities during gas flow exceed the resistance of bridges on wider slots.

It is manifest that near-wellbore velocities and production scenarios play a critical role in forming and destructing the sand bridge. Current criteria provide conservative recommendations for the regular conditions of SAGD but appropriate to challenging events such as steam breakthrough. Certainly, for low sub-cool production strategies, the impact of steam influx should be considered for the selection of aperture sizes. It is important to note that the duration and severity of such events are not known entirely and the sanding thresholds are still a focus of investigation. Depending on the features of steam-influx episodes the limits may become more conservative or relaxed, affecting aperture selection.

CHAPTER FIVE: FLOW PERFORMANCE OF WWS AND THE EFFECT OF SLOT WIDTH ON FINES MIGRATION FOR SAGD OPERATIONS

5.1 Introduction

SAGD wells are equipped with sand control devices (SCDs) to support the collapse of the borehole and to restrain the production of sand particles. SCDs design should also allow the inflow of reservoir fluids and the production of fines particles (Bennion et al. 2009).

The introduction of SCDs inside the wellbore generates an additional restriction for the fluid flow near the wellbore. This restriction in terms of pressure drop contributes to the overall "skin" of the well (Furui et al. 2007). A good flow performance will depend on the capacity of the screen slots and the neighboring pores to remain uncluttered (Mahmoudi 2017). In SAGD wells, plugging of screen and porous media can occur due to liner corrosion (Romanova and Ma 2013), fines migration (Williamson et al. 2016), scaling (Goodman et al. 2010), asphaltene precipitation (Kar et al. 2015) and thermal formation-damage (Romanova et al. 2015). Due to the time limitation of the tests, plugging source is only attributed to fines migration and accumulation at the near-screen zone.

Fines migration have been recognized as the primary source of plugging in SAGD wells (Romanova and Ma 2013; Williamson et al. 2016). The degree of fine particles release in a porous media depend on the initial amount present in the formation and the physical and chemical conditions of the moving fluids (Khilar et al. 1984, 1990; De Zwart 2007). For large particles (>10μm), hydraulic drag force is the dominant particle removal mechanism. Whereas, electro-kinetic forces dominate in smaller particles (<1 μm) (De Zwart 2007). Hydrodynamic forces are mostly dependant on the flow velocity and microscopic forces strongly driven by the properties of the fluid and phases.

Extensive studies have been carried out to evaluate the effect of brine properties such as pH and salinity. Khilar et al. (1984) indicated that there is a critical salt concentration (CSC) with values below this level favoring fines mobilization. Additionally, varying pH levels alter the electrical charges of clay materials (Van Olphen 1965). Mahmoudi et al. (2016b) showed how high values of pH and low values of salinity reduce the permeability of the sand.

Moreover, the flow of single-phase brine represents the worst case scenario for fines mobilization (Mahmoudi 2017). During two-phase flow, the severity of fines migration decreases with the increase of fractional oil flow (Gabriel and Inamdar 1983; Sarkar and Sharma 1990). Interestingly, the presence of polar components in the oil can slow the fines-release while mineral non-polar oil would represent greater reductions in permeability. On the other hand, gas wells show high fines migration when water is associated with it. Only unconventional low-permeability gas reservoirs seem to mobilize fines at irreducible water conditions due to high-pressure drops (Zeinijahromi et al. 2012).

Once fine particles flow through the porous media, the severity of plugging will depend on the particles size, the number of particles in motion and pore-throat size distribution. At a macro scale, phenomena such as straining control the entrapment of fine particles (McDowel-Boyer et al. 1986; Sen and Khilar 2006). While Van-der-Waals forces, interception, deposition, and Brownian diffusion dominate at a micro scale (Logan 1995; Valdes 2002; De Zwart 2007). Additionally, SCDs and wellbore trajectories induce changes in the flow geometry, affecting the concentration of fines (De Zwart 2007). Flow convergence accelerates the flow close to the well (Kaiser et al. 2000), and radial flow encourages particle retardation as streamlines change of direction (Valdes and Santamarina 2006).

Previous studies estimated formation impairment through experimental work, and several rules of particles bridging ($1/3^{th}$-$1/7^{th}$ -$1/14^{th}$) were developed based on experimental results (Barkman and Davidson 1972; Abrams 1977; Van Oort et al. 1993). Particles equal or larger than one-third of the average pore throat size ($1/3^{th}$) form a bridge at the entrance of pore throat. Particles between one-seventh and one-third ($1/7^{th}$ - $1/3^{th}$) of the pore throat size will deposit in the pore. Similarly, particles between one-fourteenth and one-seventh ($1/14^{th}$ - $1/7^{th}$) will deposit under low flow rates. Finally, particles smaller than one-fourteenth ($1/14^{th}$) of the pore throat size pass through the pores with minor impairments.

The flow performance of SCDs is analyzed in terms of pressure gradients (Ballard and Beare 2006; Bennion et al. 2009; Romanova et al. 2014) or retained permeability (Markesad et al. 1996; Mahmoudi et al. 2016a). In this study, the effective retained permeability is employed because it normalizes the initial and final conditions for different sands. Additionally, the study includes the evaluation of fines content over the coupon and fines production.

5.2 Testing program

The flow scheme consisted of a progressive single, dual and multiphase flow. The brine has a salinity of 400 ppm, whereas the pH level was 7.9. These values were selected after reviewing the salinity levels of produced water from oil sands projects in Canada (Mahmoudi et al. 2016b). The 400ppm value represents the lowest encountered for NaCl in literature. Low values of salinity and the use of monovalent cations are considered to be the worst-case scenario for fines mobilization (Khilar and Fogler 1984; Mahmoudi et al. 2016b). Likewise, the oil had a viscosity of 10 cp at room temperature in order to match the bitumen condition under SAGD reservoir temperatures (Devere-Bennett 2015). Co-injection of nitrogen of 0.01749 cp with water and oil flow emulates a steam breakthrough event. Moreover, in every test, the flow continued for 30 minutes after pressure readings stabilized.

The retained permeability is defined as the ratio of near-screen permeability to the initial absolute permeability at residual oil conditions. Separate tests were performed to obtain the relative permeability (K_{rel}) of the three sands at residual oil saturation. In these tests, the absolute permeability (K_{abs}) was measured by brine flow. Then, oil was injected at low rates (1000 cc/hr) to avoid pore damage. Once the sample is saturated with oil at irreducible water condition, brine is injected at variable ratios to achieve residual oil saturation. **Table 5-1** show the results for the three sands. The relative permeability at residual oil saturation conditions of the three sand classes was obtained separately to avoid additional damage during an actual test.

Table 5-1. Relative permeability at residual oil conditions

Sand	K_{abs} (md)	K_{rel} (fraction) at S_{or}
DC-I	950	0.48
DC-II	1870	0.50
DC-III	2400	0.55

In this study, the 2-inch interval immediately above the coupon was considered as the near-screen zone (**Figure 5-1**). The final retained permeability for each test is calculated upon the last liquid stage at 100% brine flow. Therefore, retained permeability is the ratio of absolute permeability of the 2-inch sand interval to the sand-pack original absolute permeability, as shown below:

$$k_{abs,bottom} = \frac{q_w \times \mu_w \times L_b}{\Delta P_b \times A} \times \frac{1}{k_{rw,@Sor}} \tag{5.1}$$

$$k_{retained} = \frac{k_{abs,bottom}}{k_{abs,i}} \tag{5.2}$$

Where q_w is the water flow rate; μ_w is the water viscosity; A is the cross-section area of the sand pack. L_b and ΔP_b represent the length and pressure drop of the bottom section of the sand pack, respectively. $k_{rw,@Sor}$ denotes the relative permeability of the sand pack at residual oil saturation as shown in **Table 5-1**. $k_{abs,i}$ represents the initial absolute permeability of the sand pack, while $k_{abs,bottom}$ is the final absolute permeability of the bottom section. $k_{retained}$ is the retained permeability of the near coupon zone (bottom section).

After the gas-liquid stages, brine was injected to displace gas and oil. It was observed that gas bubbles remain inside the core and were trapped in the cell. The presence of gas complicates the assessment of sample permeability after steam-influx events. Therefore, in this study, flow performance is evaluated only for liquid stages, which are representative of the typical conditions of a SAGD well. In addition, the stage at 100% brine flow avoids any discrepancies about the saturation distribution of two phases throughout the long core and gravity segregation effects. Additional tests were performed at increasing water rates to confirm that water injection rates result in no further displacement of oil.

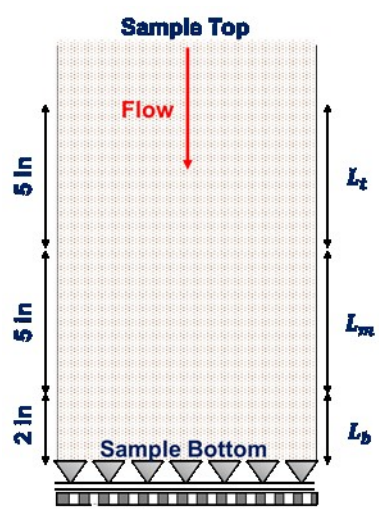

Figure 5-1. Core sample sections

Regarding the limits for flow impairment, Burton and Hodge (1998), suggested that a value of 20% retained screen permeability still delivers good performance due to the high permeability of the screens compared to that of a porous medium. In order to account for additional damage factors near the wellbore, a value of 50% retained permeability was proposed. Similarly, Markestad et al. (1996) recommended a threshold for skin value of 50%, including porous media. In this study, a range between 50% and 70% are considered the marginal and acceptable limits for retained permeability.

5.3 Results and discussion

Figure 5-2 shows the retained permeability at the end of the last liquid stage (100% brine) for the three sand classes as a function of the slot width.

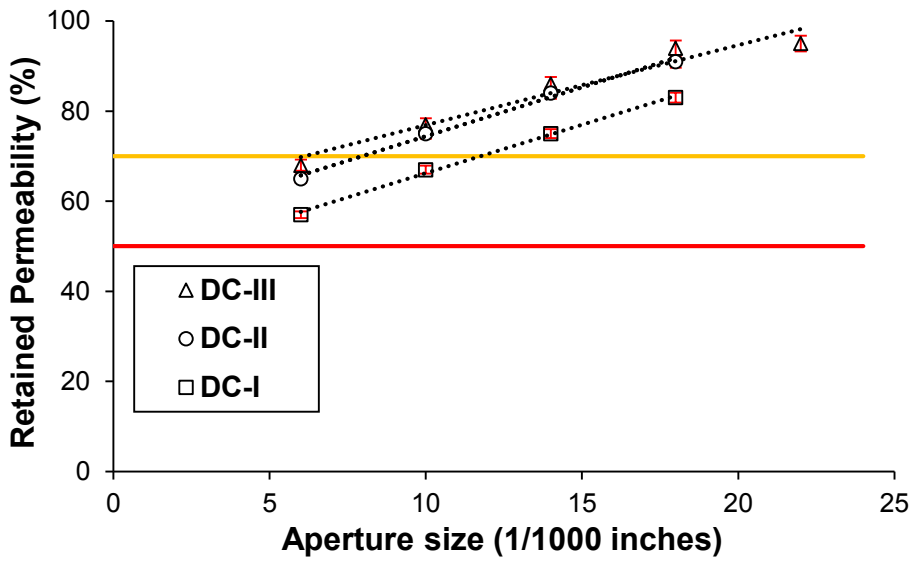

Figure 5-2. Retained permeability at the end of the liquid stages for different aperture sizes. Red and yellow lines represent the retained permeability limits of 50% and 70%, respectively

For the three sands, the retained permeability increased with aperture size. This behavior is the result of more area available to flush fines near the screen, the re-sorting of sand on top of the slots and lower convergence effects. WWSs have constant slot density, and the OFA is dependent on the aperture size only. The narrower the aperture size, the higher the convergence effect and the pressure drops near the coupon.

The drop in retained permeability was more prominent for 0.006″, with the lowest value of 57% for DC-I and 65% and 68% for DC-II and DC-III, respectively. A positive outcome is

that for all sands, the retained permeability stayed above or between the acceptable limits (50%-70%). Remarkably, WWSs provide acceptable flow performance even when narrower apertures are employed in low-quality sands like DC-I (high fines content). The high OFA of WWS grants a plugging-safe characteristic due to the additional area available in case severe plugging occurs.

Due to their similar PSD and fines content, DC-III and DC-II showed a similar trend in permeability reduction, with a maximum difference of 2%. In general, coarser sands with lower fines content show a lesser reduction than finer sand with higher fines content. The higher the amount of fines, the higher the chances of pore clogging.

Interestingly for DC-III, increasing the aperture size beyond 0.018″ does not further improve skin and results in higher levels of sanding. Although it was not observed for DC-II and DC-III, the same behavior is expected. After some aperture size, additional fines are not removed from the near-screen zone.

The notable flow performance of WWS results in all current criteria offering retained permeability values above or between the acceptable limits (**Figure 5-3**). Overall, the suitability of available criteria increases with grain size. All criteria provide retained permeabilities above 70% for DC-III. However, for DC-I, all criteria except 2XD10 produced results between 50% and 70%. Although available criteria yield a reasonable sizing regarding flow performance, it may be deficient for achieving superior performances in finer and poorly sorted sands.

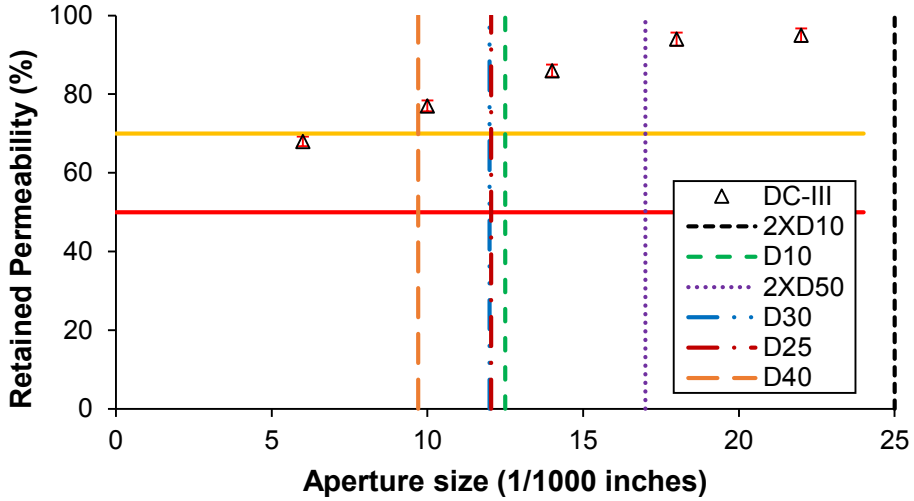

(a)

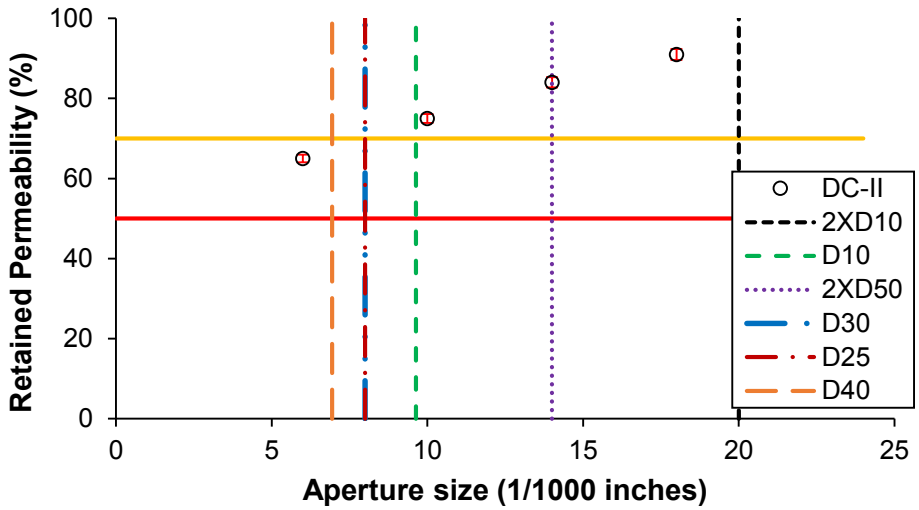

(b)

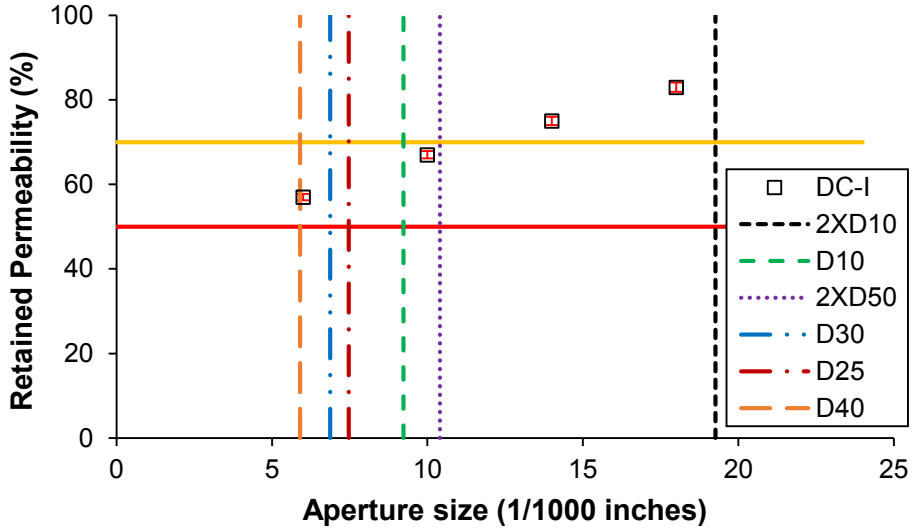

(c)

Figure 5-3. Retained permeability and comparison with design criteria. (a) DC-III, (b) DC-II, (c) DC-I

Post-mortem examinations indicated no plugging or scaling in the screen. Therefore, to evaluate plugging, the focus is given to the changes in the concentration of fines (<44μm) close to the coupons and the concentration of the produced fines. Results indicate that fines

migration and accumulation is strongly correlated to the decay in retained permeability. **Figure 5-4** shows the concentration of fines in the sand pack for the three sand classes.

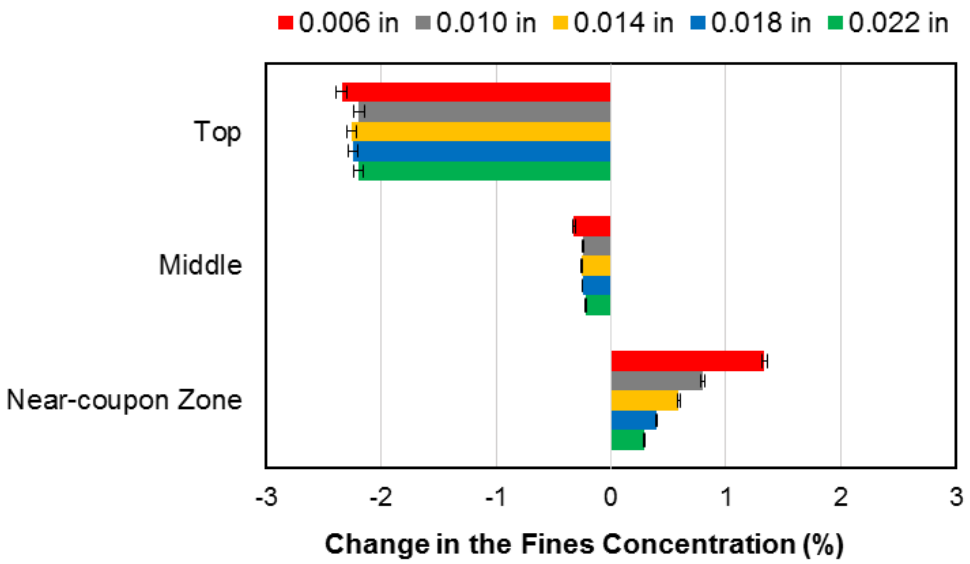

(a)

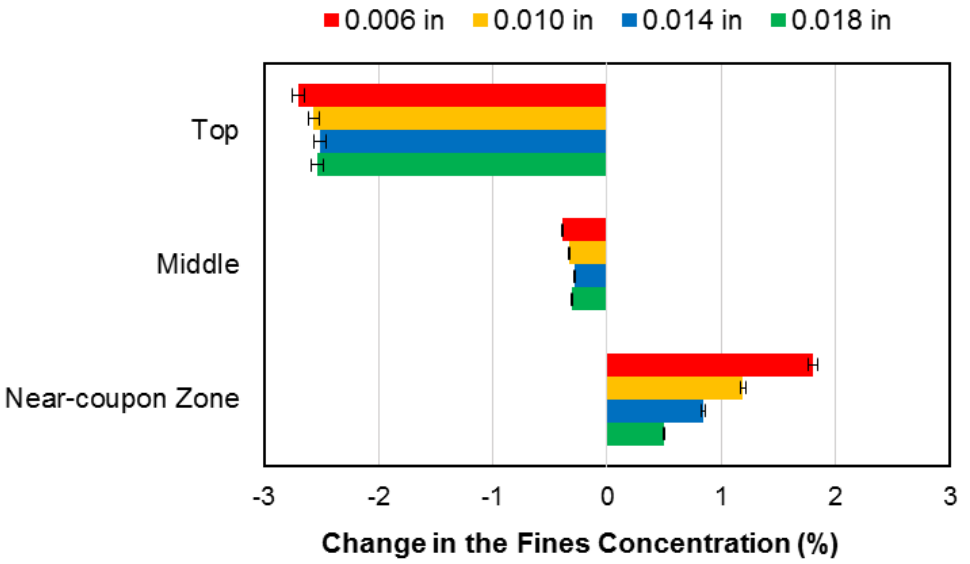

(b)

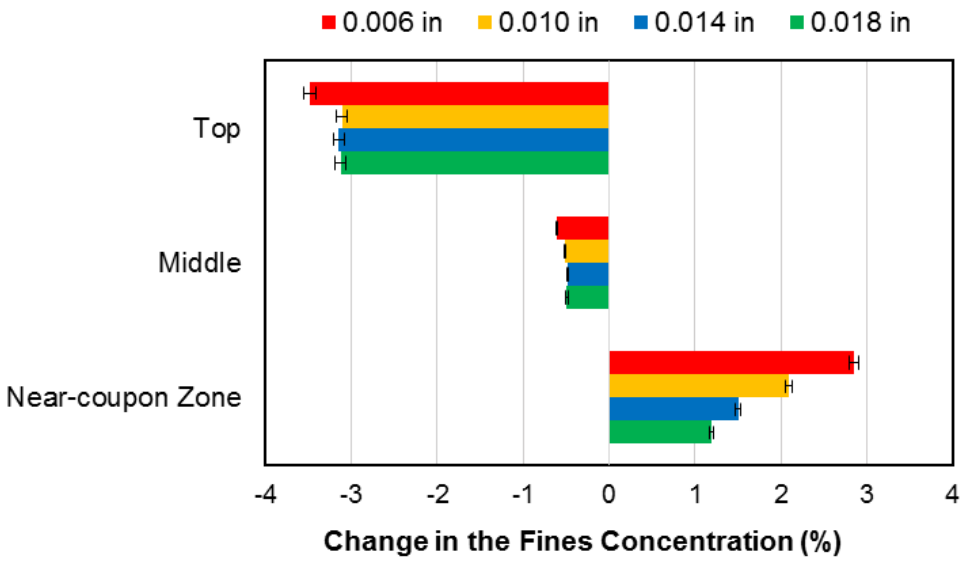

(c)

Figure 5-4. Change in fines concentration along the sand pack for different slot widths, (a) DC-III, (b) DC-II, (c) DC-I

Throughout the test, fines particles are transported from top to bottom (**Figure 5-3**). The top section releases fines that will be transported through the sample. Since there is no feed of fines, the negative change in concentration is higher for the top section. Alternatively, the release of the middle section towards the bottom is countered by the fines being transported from the top. Therefore, it shows the least change in fines concentration. The ability for the bottom section or near-screen zone to discharge fines is dependent on the aperture size.

Higher solid production (fines and sands) is observed as the slot width increases; therefore, there is fewer fines accumulation for wider slots. Besides the smaller area for fines to flow in narrower apertures, there is a local increase in velocity near the screen that results in more accumulation at narrow pore throats.

A comparison of **Figures 5-3(a)**, **5-3(b)** and **5-3(c)** show that the change in fines concentration is greater as the grain size decreases (DC-III to DC-I). Smaller grain size suggests smaller average pore and throat size (lower porosity and permeability); hence, a higher potential to pore plugging by fines for DC-I. For the same fluid flow rate, the pore-scale flow velocities (real velocities) are higher for finer sands. The combination of higher

local velocities and smaller pore throat and slot aperture facilitate the fines migration and accumulation above the screen.

For the narrowest apertures (0.006″), DC-I showed a more significant accumulation of +2.8% while DC-II and DC-III presented a change of 1.8% and 1.4%, respectively. The difference between sands is again attributed to the PSD. It is interesting to note that the fines content for wider slots (≥ 0.014″) approaches the initial concentration of fines, especially for the coarsest sand, DC-III. This advises the benefit of using the widest slot size that can control sanding within acceptable limits while reducing the plugging potential.

Interestingly, the difference in fines concentration for aperture sizes 0.018″ and 0.022″ for DC-III is not significant, only 0.15%, which also correlates to the small difference in retained permeability for 0.018″ and 0.022″.

Figure 5-5 shows the production of fines for different slot sizes as a function of the flow stages with variable water cut and flow rate. The samples were obtained below the coupon and measured using a turbidimeter.

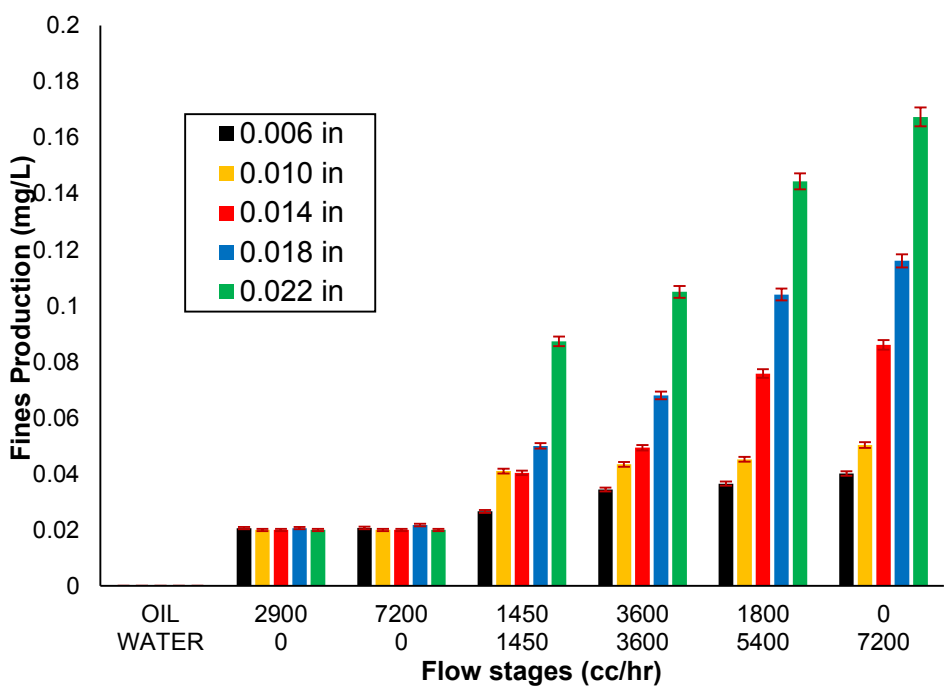

(a)

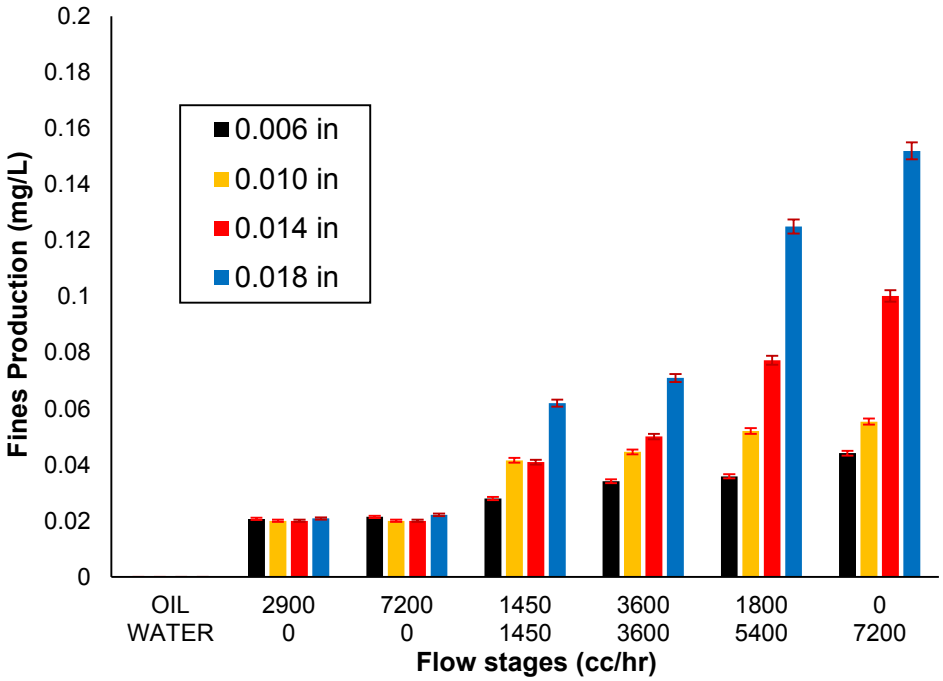

(b)

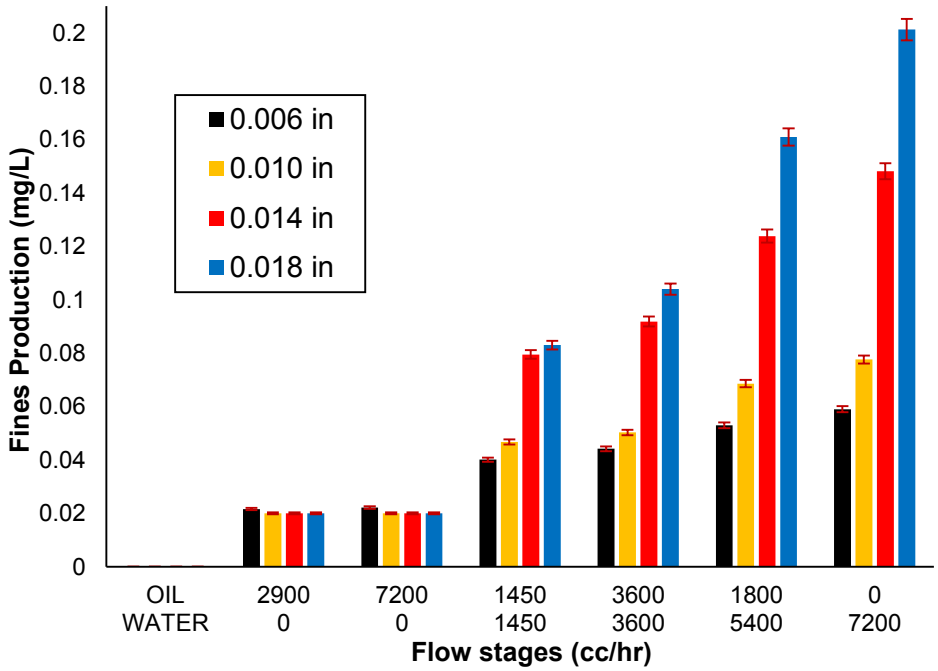

(c)

Figure 5-5. The effect of flow rates and fluid ratio on fines production for different aperture sizes: (a) DC-III, (b) DC-II, (c) DC-I

In general, a significant amount of fines accompanied the production of sand for wider aperture sizes. Narrow slots allow fewer fines production, hence higher accumulation of fines in the near-screen zone, reducing the permeability of the porous media.

Fines production during oil stages is extremely low regardless of the flow rate. Fines and clay particles are typically water-wet, and the wetting phase must mobilize in order to detach fine particles from bigger grains. In the presence of brine flow, fines production increases with flow rate. Also, the difference between fines production for narrow and wider slots grows as the flow rate increases at constant water cut. It seems to be an onset for significant fines production for 0.014″.

During the test, the increase of water cut at the highest flow rate displayed the most significant impact on fines production. Compared to 50% water cut, 100% brine injection showed the highest increment for any aperture size of 100%, 93% and 71% in fines production for DC-I, DC-II, and DC-III, respectively.

Water saturation increases with the water cut allowing the wetting phase to contact more pore spaces and fines particles. It is important to note that the effect of water cut is flow rate dependent and it is expected to be less significant at lower flow rates.

The figures not only re-affirm field observations that indicate extreme plugging when using aggressive flow rates (Williamson et al., 2016) but also highlights the plugging risk when these high flow rates are associated to high water cuts. With the progressive plugging of pore and apertures, the flow towards open well-sections increases, resulting in higher fines concentration and coarser produced fines on clean pores.

Moreover, a comparison of **Figure 5-5(a)**, **5-5(b)** and **5-5(c)** show that the effect of the initial fines content is more evident with the increase of aperture size and higher flow rates. For instance, with 0.018″ DC-I showed the highest difference of 35% with respect DC-II while it almost doubles the production of fines of DC-III.

5.4 Conclusions

This chapter presents the results of pre-packed SRTs to investigate the role of slot width and production scenarios on retained permeability and fines migration. The laboratory testing intended to assess the relation between flow impairment and pore-clogging near the coupon.

Flow impairment was evaluated at the end of liquid stages since it represents the regular and desirable operating conditions of SAGD wells. The pressure drop of two inches above the coupon and through the screen was used to calculate the final effective retained permeability.

Results indicate that WWSs have an excellent ability to limit the formation damage caused by fines migration. The retained permeability for all sands did not fall below the minimum acceptable limit, even at narrow apertures (0.006″). It is evident that wider slot widths allow a substantial amount of fines discharge that results in lower concentrations of fines above the screen. On the other hand, narrow slots presented a drastic increase in fines concentration whose intensity increased with the initial content of fines.

The transportation of fines shows a significant dependency on the fluid flow rates. However, flowing phases and water cut have a stronger impact on the mobilization of fines when required flow velocities are implemented. Fines production during oil flow is negligible, while fines production dramatically increases at high water cuts.

CHAPTER SIX: NEW CRITERIA FOR WIRE-WRAPPED SCREEN DESIGN FOR SAGD PRODUCTION WELLS AND PERFORMANCE FORMULATIONS

This chapter combines the Sand Retention Testing (SRT) results in terms of flow performance and sand production performance to elaborate a set of graphical design criteria for wire-wrapped screens. The proposed criteria specify a slot window that keeps the produced sand within an acceptable limit while minimizing plugging potentials in the zone adjacent to the screen and protecting the wellbore productivity. The formulated criteria differentiate production scenarios to evaluate their influence on the safe-aperture zone.

Current design criteria for WWS solely rely on one or two points of the sand particle size distribution (PSD). Additionally, rules-of-thumb associate the performance of WWS to SL. Sanding and plugging phenomena are related to aspects other than PSD, factors such as fluid properties, PSD shape, fines content and flow ramp-up affect the response of any SCD. Therefore, available criteria do not work for all type of sands. This study aims to apply to typical Alberta oil sands and SAGD operations by evaluating three PSD classes (DC-I, DC-II, and DC-III) out the four initially proposed by Abram and Cain (2014). Although the major categorization of Alberta sands into four major classes (DC-I through DC-IV) miss intermediate sands, it is assumed that include the important variations among Alberta reservoirs.

In proposing the design criteria, this chapter uses the sanding and plugging (regarding retained permeability) data presented in Chapter 4 and 5. The two previous indicators are overlapped to generate the final design criteria.

6.1 Design criteria for Wire-wrapped Screen

The results of several pre-packed SRT experiments fund the elaboration of new design criteria by using three typical PSDs that comprises a broad range of particle sizes and fines content. A range of aperture sizes was implemented for each sand. Experimental results were extrapolated to represent the new design criteria using a Traffic Light System (TLS). The TLS approach was introduced by Mahmoudi (2017) to specify the performance of slotted liners designs as unacceptable, marginal or acceptable.

6.1.1 Traffic Light design approach

Markestad et al. (1996) initially proposed the safe-aperture window approach to find acceptable sanding and flow performance for different sands. The TLS method employs a color based code where red, yellow and green represent unacceptable, marginal, and acceptable performances, respectively. Optimum aperture sizes are those inside the green zone. Moreover, the TLS allows to evaluate the impact of sanding and flow performance on aperture selection and to determine the weaknesses of the device.

6.1.2 Acceptable performance limits

Tolerance to sand production is highly dependent on wellbore trajectory, sand transportability in the produced fluids, artificial lift requirements, surface separator capacity and company policies (Williamson et al. 2016; Mahmoudi 2017).

The long horizontal sections and typical low flow rates associated with SAGD wells increase the chances of sand accumulation along the well that can potentially lead to productivity impairment. Hodge et al. (2002) proposed a maximum acceptable limit of 0.12 lb/ft^2 of screen area based on the correlation of successful field applications to sand retention experiments. This criterion was found to be influenced by high rate gas wells used in the evaluation, and Adams et al. (2006) introduced a more permissible limit of 0.15 lb/ft^2 for oil wells. The previous limits are in close agreement to a general rule of thumb of limiting sand production to less than 1% of the liner volume. For the typical 7-inch to 8 5/8-inch liner completions in SAGD wells, the limit results in approximately 0.15 lb/ft^2 of cumulative sand throughout the well life (Mahmoudi et al. 2016a).

In this study, the TLS use green color (optimum sand retention) for aperture sizes rendering cumulatively produced sand below 0.12 lb/ft^2. The yellow color is defined for sanding levels between 0.12 to 0.15 lb/ft^2, which means that there is a high risk for excessive sanding in the presence of aggressive flow rates. Finally, the red light denotes drastic conditions when levels of sanding surpass 0.15 lb/ft^2 (**Table 6-1**). Excessive amounts of sand in the well can choke the production of fluids by filling up the well and also deteriorate down-hole equipment.

In the past, pressure drop limits and retained permeability have been used to evaluate the flow performance of SCD under laboratory conditions. Rigid pressure differentials neglect

the effect of sand-pack permeability when comparing the response of SCD with different sands. The retained permeability, on the other hand, normalizes initial and final conditions making it more appropriate for appraisal purposes. Markesad et al. (1996) considered 0.5 or 50% as the acceptable limit for retained permeability. Likewise, ConocoPhillips uses 0.5 for its sand control evaluation studies (Chanpura et al. 2010). Analytical models by Burton and Hodge (1998) suggested that retained permeability values above 20% result in low productivity impairment. However, a stricter limit was recommended to account for other possible skin factors.

A range of 50-70% is implemented in this study as the flow performance indicator. For the TLS, values above 70% represent optimum conditions, and the green color is used for this zone. The yellow color encompasses values between 50% and 70%, while red light denotes significant productivity losses when values drop below 50%.

Table 6-1. Performance limits and TLS color code

Sand Retention Performance	
	More than 0.15 lb/ft^2 for cumulative sand production
	Between 0.12-0.15 lb/ft^2 for cumulative sand production
	Less than 0.12 lb/ft^2 for cumulative sand production
Flow performance	
	Retained permeability less than 50%
	Retained permeability between than 50-70%
	Retained permeability less than 50%

6.1.3 SRT testing assumptions and limitations

Laboratory experiments such as SRT are capable of producing relatively fast and repeatable results while incorporating not all, but some of the most relevant physics controlling sand production. A full representation of field conditions at an experimental level would require expensive and laborious efforts. For instance, the time scale of the testing compared to the well life cycle does not allow the observation of phenomena such as corrosion and scaling that significantly contribute to plugging tendencies. The SRT is viewed as a relatively straightforward tool to diagnose and rank the performance of SCD while obtaining an insight into the controlling aspect of the process by using parametric studies.

SRTs serve as a starting point for SCD design and selection. Company policies, cost, and field experience play a major role in the final choice. An excellent approach would be to correlate laboratory experiments to field results to continuously validate the laboratory operating procedures and performance indicator limits. The TLS approach for design criteria offers an optimum aperture range that must be assessed by the factors mentioned above before field application.

Testing conditions incorporate a broad range of operating settings including worst-case scenarios. Low stresses and the single-phase brine stage (low capillary) provide an optimum situation for sand production, whereas low salinity values and high water cuts intensify fines mobilization and plugging. Nonetheless, the procedure does not include all the factors (temperature, fluids composition, emulsion) and SRT methods could change to adjust the conditions for a particular field.

6.2 The new design criteria

The design criteria provide a performance ranking of the three sand classes based on the limits and color code introduced in **Table 6-1**. In order to determine the range of apertures in each performance zone, the criteria use an axial representation of the PSD, as shown in **Figure 6-1**. For each sand, representative D-values are annotated along the axis (red lines), as well as the aperture sizes implemented in the testing (dashed lines).

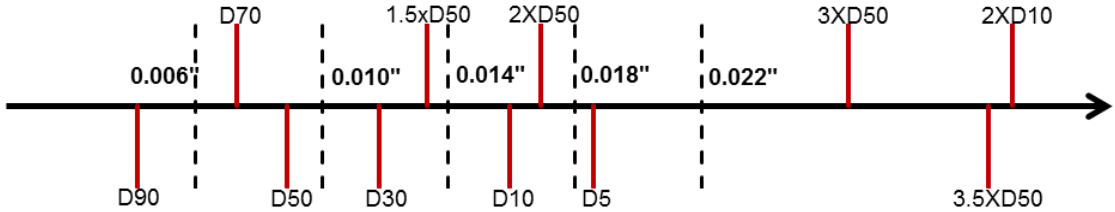

(a)

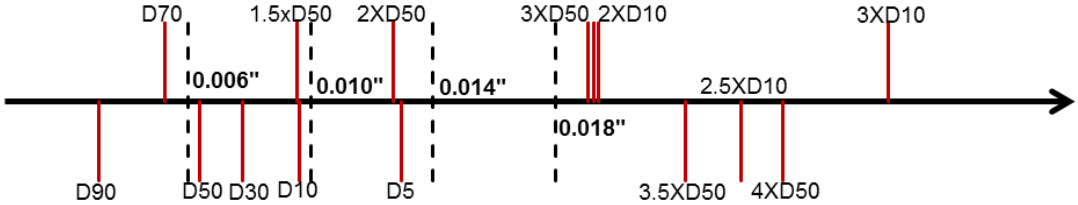

(b)

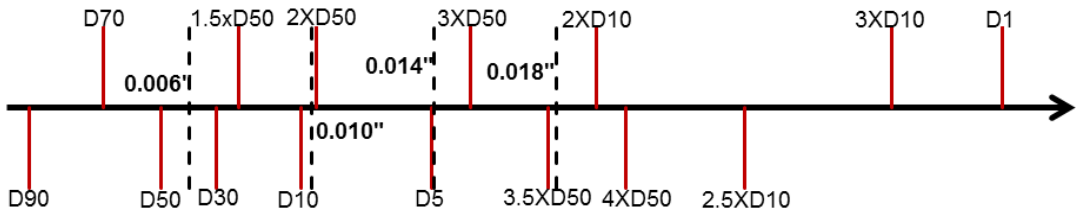

(c)

Figure 6-1. Linear x-axis representation of the PSD and tested slot sizes, (a) DC-III (b) DC-II (c) DC-I

As in Chapter 4, production operations are incorporated into the design criteria. Experimental results up to the last liquid stage represent a regular SAGD case with changing conditions throughout the well life. Since preventing steam short-circuit towards the producer well is a key operational aspect, steam-breakthrough scenarios are deemed as circumstantial and temporary. SAGD operators make efforts in identifying "hot spots" and control these events due to their impact on the steam-chamber growth efficiency and risks of liner damage (Brooks & Tavakol 2012; Irani 2018). Screen performance including the three-phase flow data is considered as aggressive flow conditions.

Three linear axes are generated for each sand class. The first axis accounts for the sand control performance while the second axis illustrates the flow performance in terms of retained permeability. The final axis overlaps both indicators to provide safe aperture windows. **Figures 6-2** through **6-4** present the TLS design criteria for the three sands under regular SAGD conditions. Green lines (+/-) represent aperture windows uncertainties.

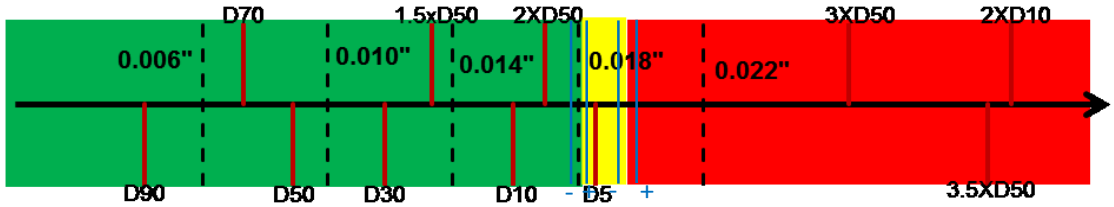

(a)

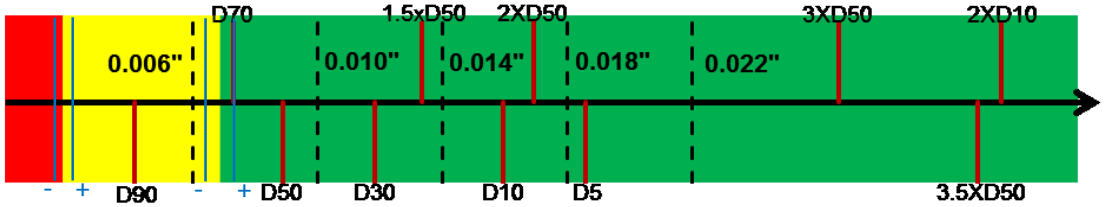

(b)

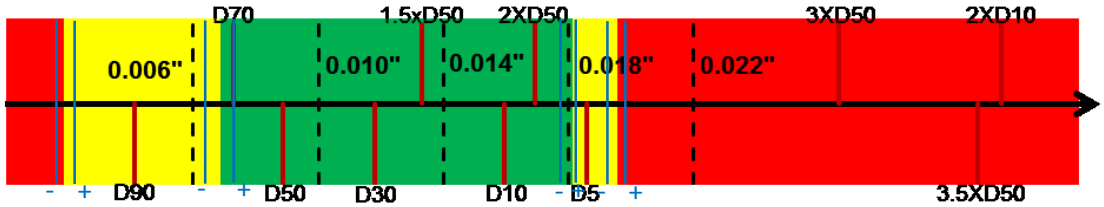

(c)

Figure 6-2. Aperture window for DC-III for regular SAGD conditions, (a) sanding performance, (b) flow performance, (c) overall design window

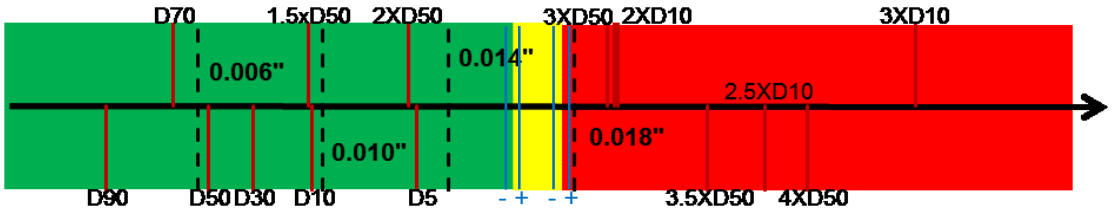

(a)

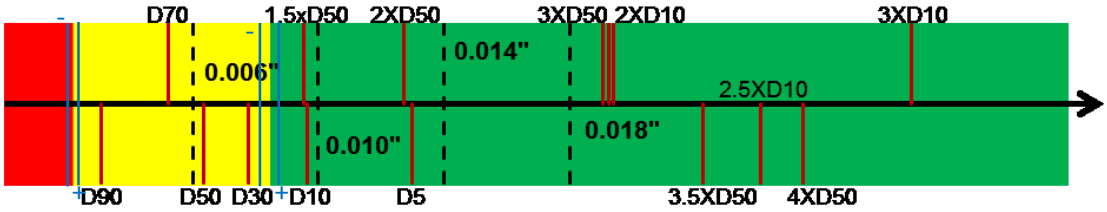

(b)

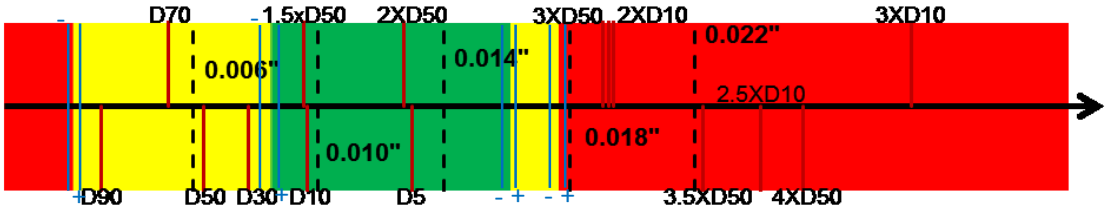

(c)

Figure 6-3. Aperture window for DC-II for regular SAGD conditions, (a) sanding performance, (b) flow performance, (c) overall design window

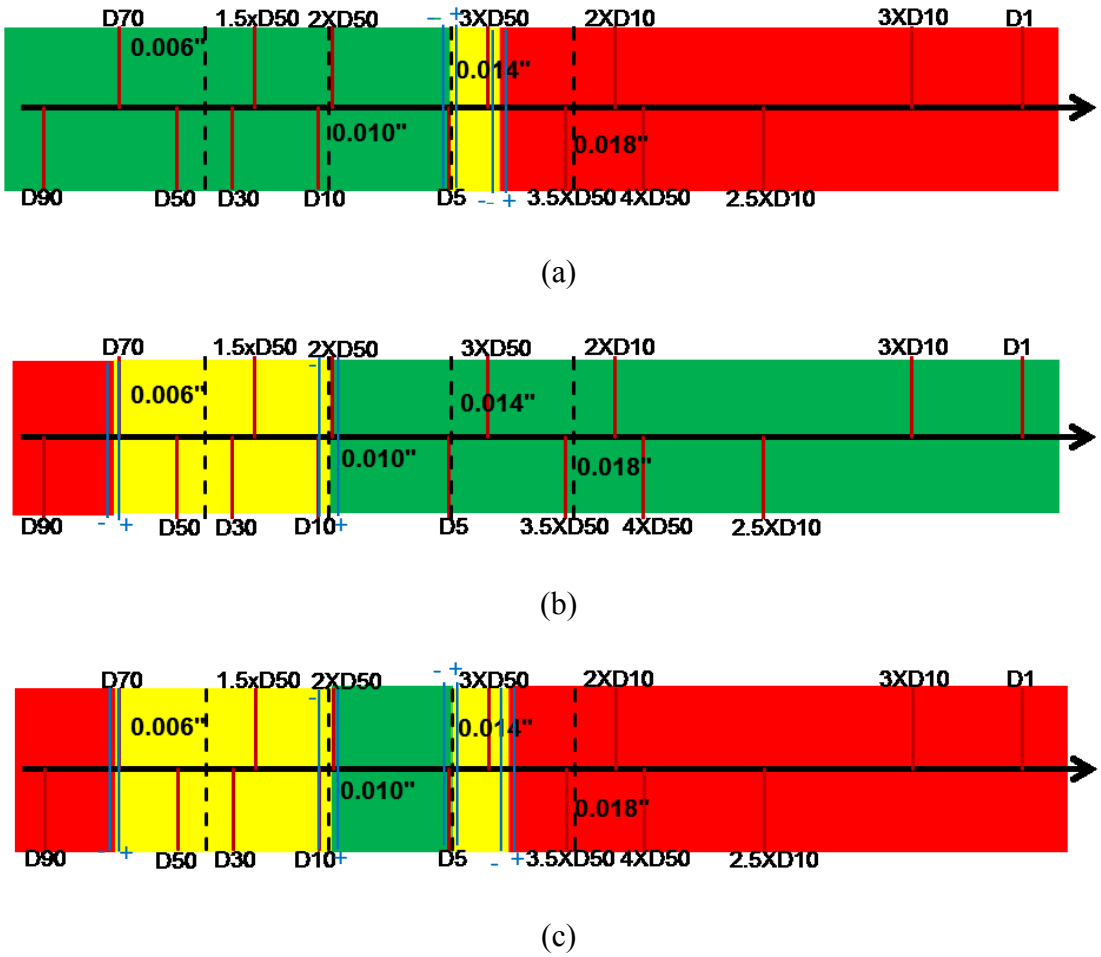

Figure 6-4. Aperture window for DC-I for regular SAGD conditions, (a) sanding performance, (b) flow performance, (c) overall design window

Clearly, from **Figures 6-2** to **6-4**, the aperture window is reduced from DC-III to DC-I. Fine sands produce more particles which advice the implementation of smaller apertures. However, smaller apertures promote pore and slot plugging, reducing the range of optimum sizes. Similarly, **Figures 6-5** through **6-7** present the TLS design criteria for the three sands at aggressive flow SAGD conditions (steam-influx). By comparing the TLS criteria for regular and aggressive flow situations, it is evident that the aperture window shrinks at high flow rates. High levels of sanding due to strong drag-forces during multiphase flow and pore plugging at previous high water cuts shift the upper and lower bound for apertures to the left and right, respectively.

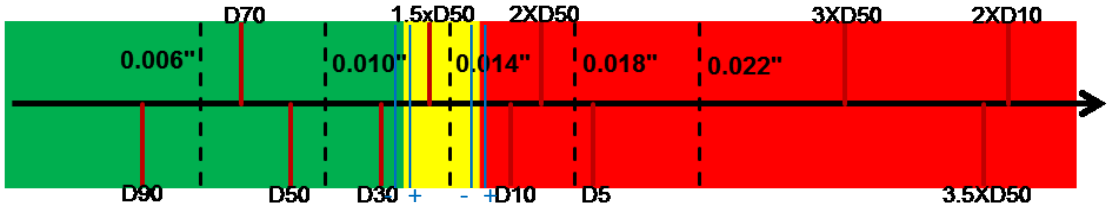

(a)

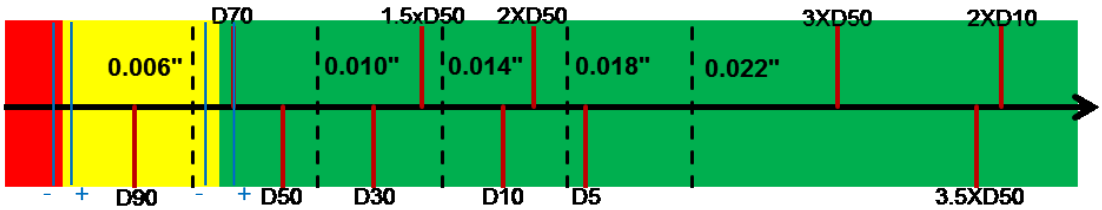

(b)

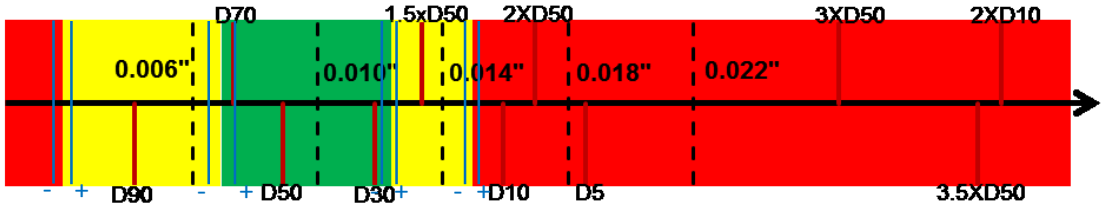

(c)

Figure 6-5. Aperture window for DC-III for aggressive SAGD conditions, (a) sanding performance, (b) flow performance, (c) overall design window

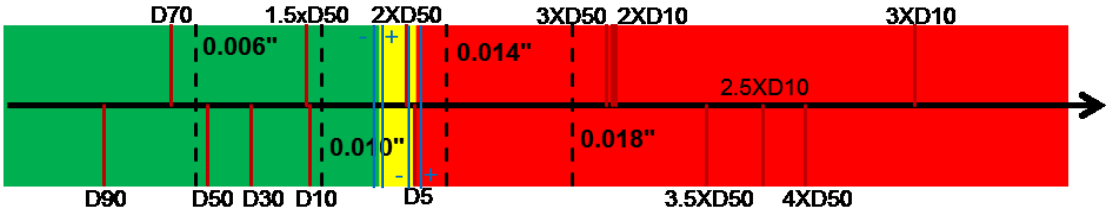

(a)

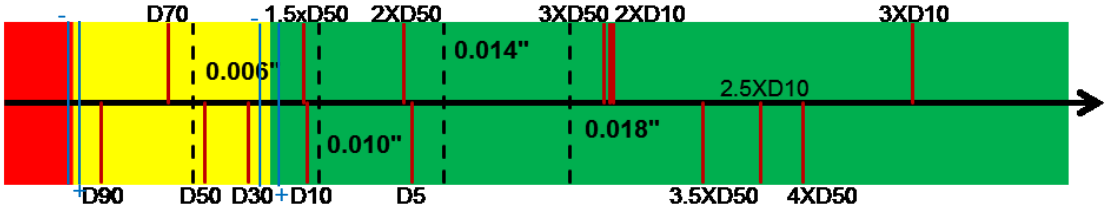

(b)

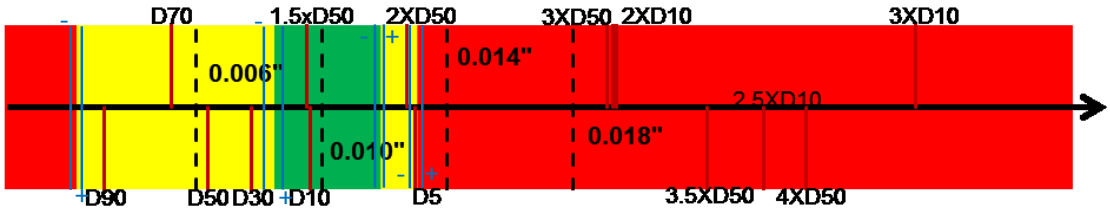

(c)

Figure 6-6. Aperture window for DC-II for aggressive SAGD conditions, (a) sanding performance, (b) flow performance, (c) overall design window

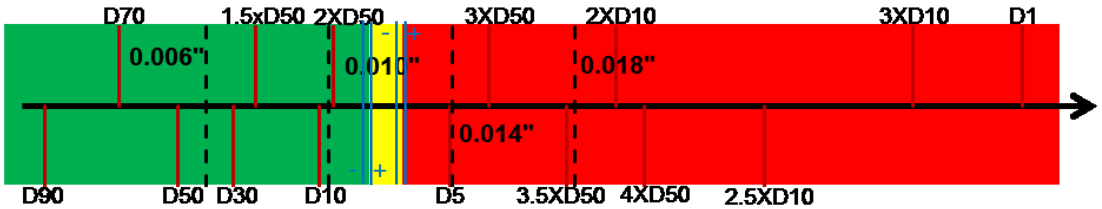

(a)

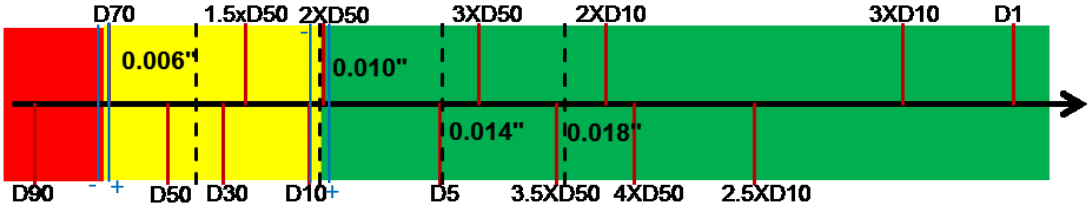

(b)

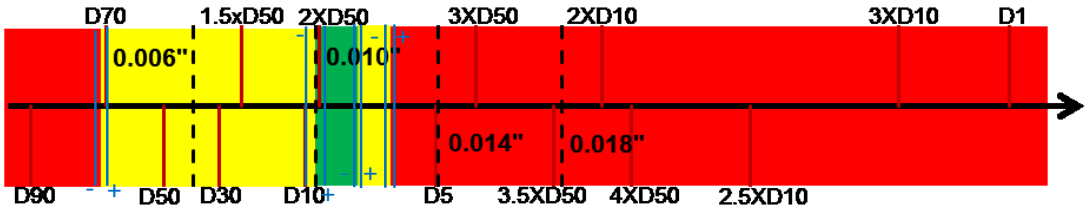

(c)

Figure 6-7. Aperture window for DC-I for aggressive SAGD conditions, (a) sanding performance, (b) flow performance, (c) overall design window

6.3 Performance formulations

Laboratory testing provides a relatively straightforward and low-cost tool to evaluate the performance of SCDs. However, for the experimental approach introduced here, large volumes of mineral oil and commercial sands are implemented which can results in expensive programs if extensive testing is required. This section introduces an initial formulation that predicts the produced sand and retained permeability of a given PSD that undergoes an injection scheme like the one introduced in this research. Moreover, the experimental results and several parametric trends are used to formulate a set of empirical equations that best describes the response of WWS.

6.3.1 An empirical correlation for sand production

As shown in previous chapters sand production and sanding modes are both flow rate and phase dependent. Additionally, the intensity of transient or continuous sanding is greatly influenced by the ratio grain size to aperture size. Therefore, sanding is a function of the ability of particle bridges to withstand the drag forces changes of flow conditions.

Firstly, the relationship between each parameter was identified to obtain an idea of the structure of the equation. For instance, cumulative sand production showed a power function or exponential growth with the progressive change in injection rates. Steeper trends are observed with wider slots and finer sands. Authors such as Constien and Skidmore (2006), Gillespie et al. (2009), Mondal et al. (2010), Ballard and Beare (2012) and Chanpura et al. (2012a) have recognized the prominence of the ratio aperture to particle size on the stability of particles bridging.

After examining the experimental results and the relationship between the different variables a uniform and compact function structure was defined for cumulative sand production. A genetic algorithm was also used to identify various possible forms. Additionally, coefficients were obtained through multiple iterations and regression analysis until obtaining the minimum Mean Absolute Error (MAE). The equation is as follows:

$$P_{sand} = (52.4v_g + 45.6v_w + 1.41v_o)^{\left(\frac{2.7w}{1.34+PSDc}\right)} \tag{6.1}$$

Where each variable is defined as:

v_g = Superficial gas velocity [cm/hr]

v_w = Superficial water velocity [cm/hr]

v_o = Superficial oil velocity [cm/hr]

w = Aperture width or size [mm]

PSD_c = Particle size distribution parameter [mm]

P_{sand} = Cumulative produced sand [mgr/cm^2]

Equation 6.1 shows that cumulative sand production increases with flow velocity and that a coefficient modulates the impact of each flowing phase. As observed in the experimental results, water and gas produced the biggest impact on sand production. Therefore their coefficients are higher than that of oil. Moreover, the produced sand growth is controlled by the aperture size to PSD coefficient ratio.

PSD_c intends to capture the features of the PSD shape that impact the production of sand and the formation of stable bridges. PSD_c was defined as:

$$PSD_c = \frac{D_{10} * C_c}{f_c * 100} \tag{6.2}$$

Where

D_{10} = Sieve size that retains 10% of the sample mass [mm]

C_c = Coefficient of curvature [dimensionless]

f_c = Fines content in the sample [percentage %], fines particles: < 44 μm

PSD_c = Particle size distribution variable [mm]

D_{10} provides an idea of the biggest particles in a sand mixture. C_c is known as the curvature coefficient, and it is used to classify soils regarding their gradation:

$$C_c = \frac{{D_{70}}^2}{D_{40} * D_{90}} \tag{6.3}$$

C_c values between 1 and 3 indicate a well-graded soil. The coefficient of curvature also denotes if there are missing grain sizes in a distribution.

Over the years, authors have recognized the importance of biggest particles (D_5, D_{10}) in the formation of stable bridges (Coberly 1938; Suman 1985; Tiffin et al. 1998; Ballard and Beare 2003; Chanpura et al. 2011). Studies by Chanpura et al. (2012b), show that particles finer than the aperture size have a negligible effect on sand bridges formation and that the shape of the coarse part of the PSD plays an essential role in sand retention. A group of big particles (D_5, D_{10}) lodge onto the aperture and retain smaller particles (McCormack 1988; Meza-Diaz et al. 2003). In other words, big particles provide the scaffold for sand bridges by providing higher frictional forces between the grains and slot edges and improved distribution of bridging stresses (Meza-Diaz et al. 2004).

The coefficient of curvature and fines content was included in the PSD variable to account for the amount of smaller particles produced before stable bridges are developed. Mondal et al. (2010) showed that poorly sorted sands result in higher production of small and fines particles. Similarly, Mondal et al. (2010) performed a dimensionless analysis and proposed a PSD-aperture width parameter that relates a representative particle diameter and the uniformity coefficient to the aperture width:

$$w_D = \frac{D_p * UC}{w} \tag{6.4}$$

Where D_p is a representative particle diameter, usually D_{10} or D_{50}. UC is the uniformity coefficient and, w is the aperture size. w_D is a dimensionless effective formation size.

The goodness of fit between the predicted values and experimental results is shown in **Figure 6-8**. The empirical correlation seems to be in good agreement with experimental data, with an R-squared (R^2) of 0.941. **Figure 6-9** shows a comparison of experimental and predicted results for each sand. Excellent results are obtained during liquid stages while the correlation presents some differences during gas phases for wider slots (>0.014 in).

The correlation introduced in this study is applicable for tests following a sequential injection like the one implemented here. For instance, the impact of a flow rate change is carrying the cumulative effect of previous injection stages. For properly design apertures, bridge stability

is achieved at several levels of flow rate and the state of these bridges may or not be strong enough to support higher fluid velocities.

The separate impact of distinct variables requires extensive parametric testing at different fluid rates, phases, and PSD.

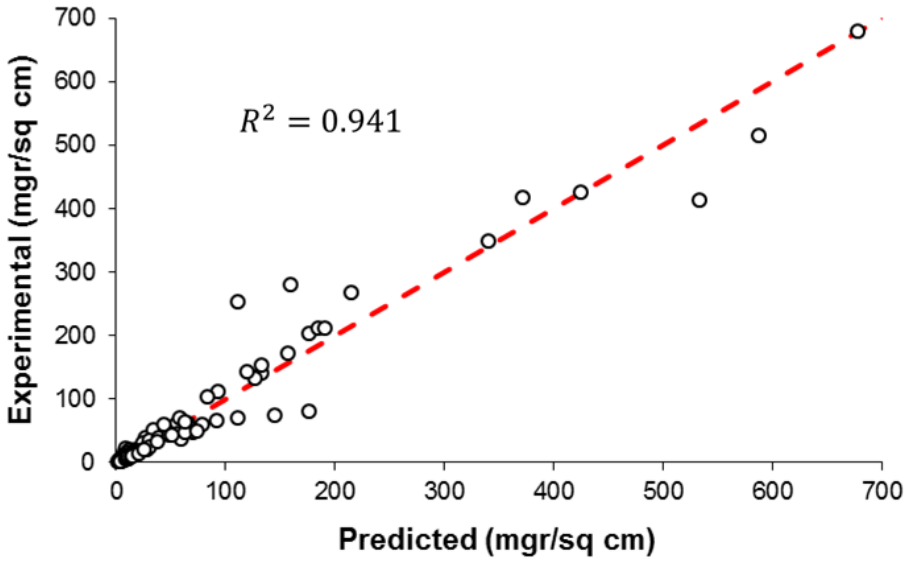

Figure 6-8. Comparison of predicted versus experimental cumulative produce sand

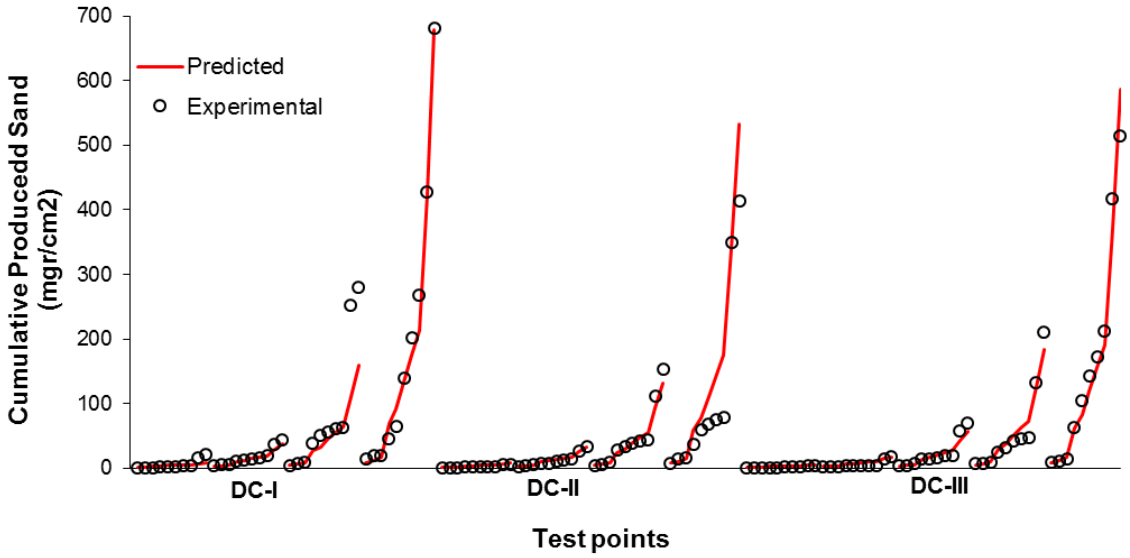

Figure 6-9. Predicted and experimental results of cumulative sand production for different sand classes

The adequacy of the correlation is verified by performing additional tests with different PSD characteristics and aperture sizes and comparing the results with the predicted values. Tests included a poorly sorted sand (New PSD-1) and medium coarse sand (New PSD-2) (**Figure 6-10**). **Table 6-2** presents the distinctive D-values of the new PSDs. The New PSD-1 have large D_{10} grain size with a fine D_{50} while New PSD-2 presents better gradation. Coupons of 0.014 inches and 0.022 inches aperture size were implemented to test New PSD-1 and New PSD-2 respectively.

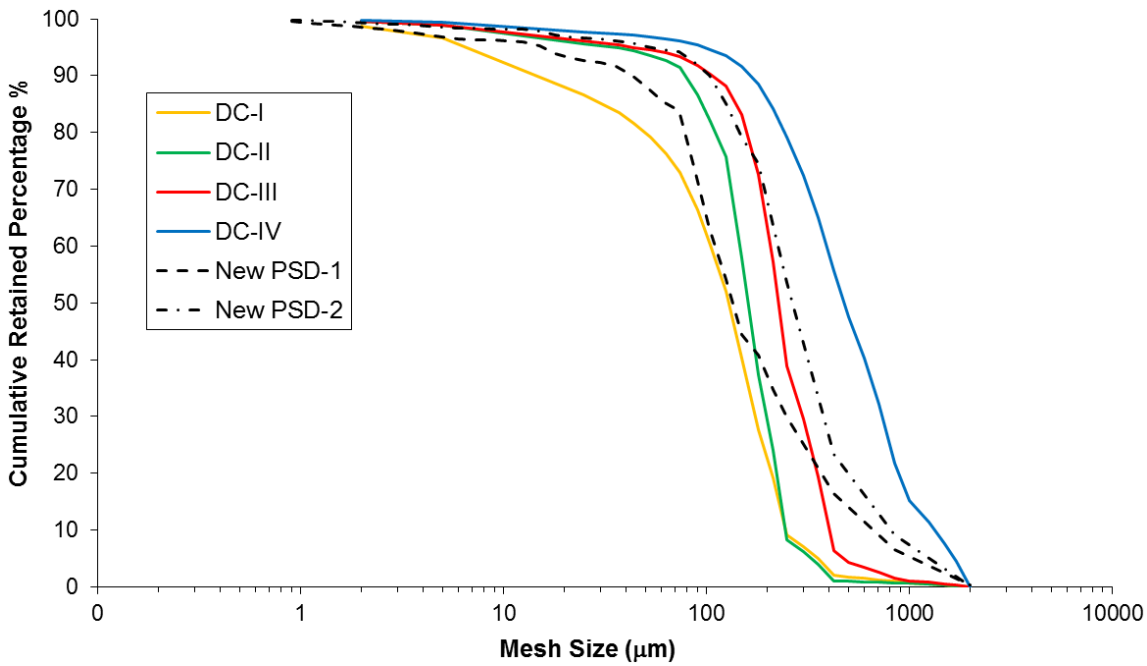

Figure 6-10. New PSDs implemented for verification testing compared to other PSDs

Table 6-2. Sand types characteristics

Type of sand	D90	D70	D50	D10	% fines	Coefficient of Curvature (C_c)
New PSD-1	43	92	135	657	10.7	1.11
New PSD-2	101	190	264	837	4.93	2.7

Experimental results showed good agreement with the predicted values of the correlation (**Figures 6-11** and **6-12**). A deviation of 18% was observed for the tests for New PSD-1 in terms of cumulative production and 5% for New PSD-2. Generally, perceived trends were consistent with the previous testing. Remarkably, verification tests confirm the role of bigger grain sizes in the development of stable bridges. Despite the large amount of fine and small particles of New PSD-1, both experimental and predicted results demonstrate that the coarse size of D_{10} results in low to moderate sanding.

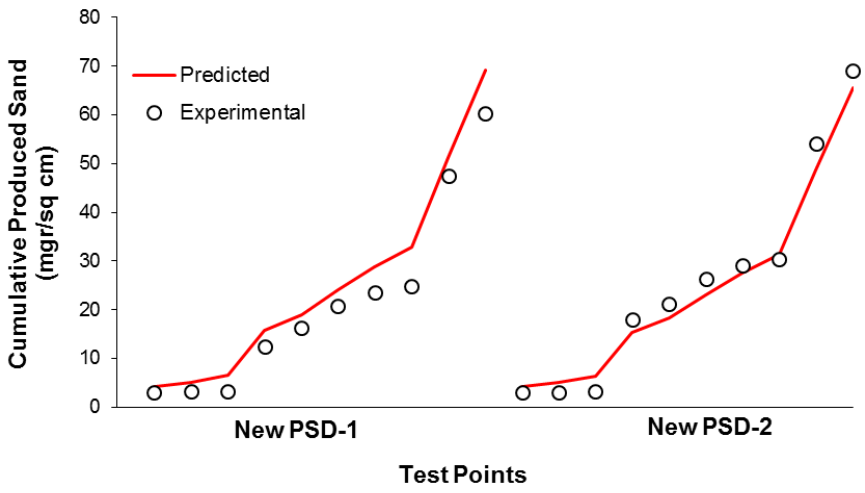

Figure 6-11. Predicted and experimental results for verification tests

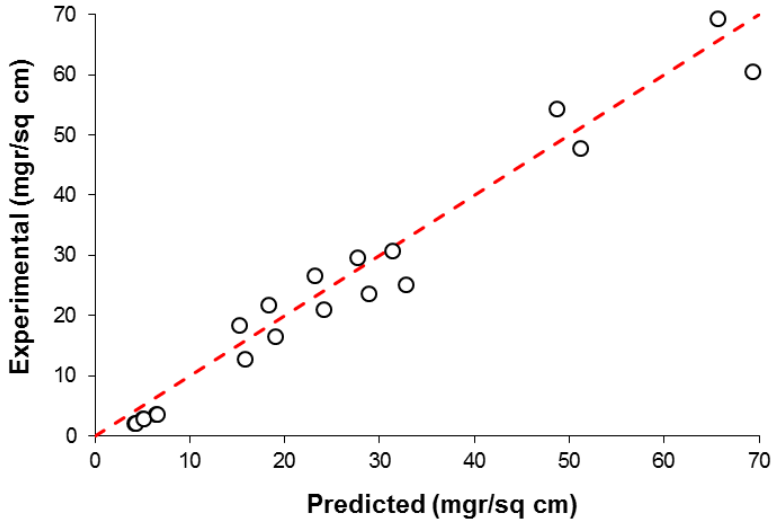

Figure 6-12. Comparison predicted versus experimental cumulative produced sand for verification tests

The correlation introduced in this study is an initial trial to capture the overall response of WWS. Further testing and thorough examination are needed to refine and tune an empirical formulation. The purpose of the correlation build in this study is to identify the major structure and dominant variables in the sanding behavior of WWS.

Accordingly, a formulation for determining the upper bound for aperture sizing in WWS can be obtained from the sanding correlation. The upper bound represents the wider aperture size that can maintain sanding below the acceptable sanding thresholds (0.12 lb/ft^2). **Equation 6.5** provides the upper bound aperture as a function of flow rate and PSD.

$$A_{ub} = (0.37PSD_C + 0.496)\frac{\ln(58.59)}{\ln\left(52.4v_g + 45.6v_w + 1.41v_o\right)} \tag{6.5}$$

Where A_{ub} is the upper bound of the aperture window in millimeters, other variables were defined in the discussion above.

6.3.2 An empirical correlation for retained permeability

As shown in Chapter 5, reduction in retained permeability is associated with the accumulation of fines in the near-screen zone. The aperture size will dictate the ability of the screen to release fines. Since the retained permeability was evaluated at the last liquid stage, the correlation assumes a cumulative impact of flowing phases at flow rate levels similar to those implemented in this study. The correlation will only work if there is water flow through the sand pack.

Trend analysis of experimental results shows a relatively linear increase of retained permeability with aperture size. Additionally, the slope or decay in permeability depends on the grain size; finer sands show a greater reduction in permeability. The higher initial content of fines particles increases the risk of formation impairment (Khilar et al. 1990; Mahmoudi et al. 2017). Therefore, high relevance is given to the fines content of the sand. After several trials and iterations the empirical formulation has the following form:

$$K_{ret} = 62.6 + \frac{155.54w}{1.53 + D_{10}} - 1.31f_c \tag{6.6}$$

Where:

K_{ret} = retained permeability [percentage %]

w = aperture size [mm]

D_{10} = Sieve size that retains 10% of the sample mass [mm]

f_c = fines content [percentage %], fines: particles < 44µm

Figures 6-13 and **6-14** show the agreement between predicted and experimental values. The formulation delivers an R-squared (R^2) of 0.971. The D_{10} grain size is also included in the correlation because produced sand is always accompanied by fines. The higher the aperture to grain size ratio, the higher the amount of fines can be displaced.

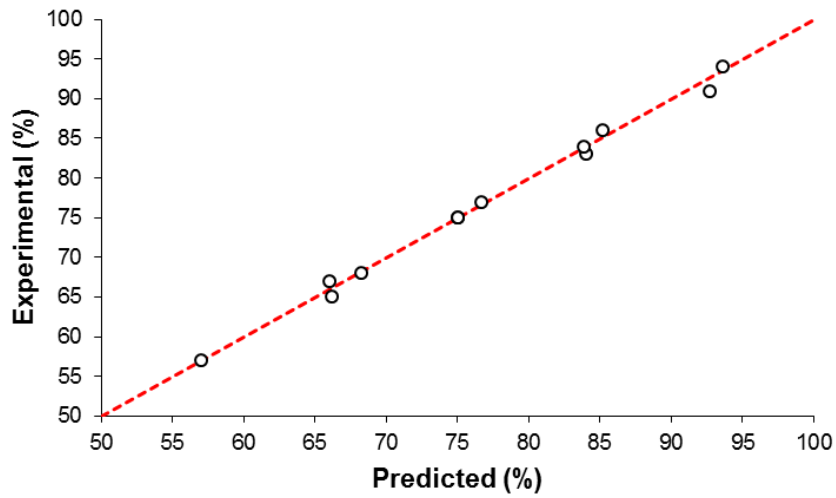

Figure 6-13. Comparison of predicted versus experimental retained permeability

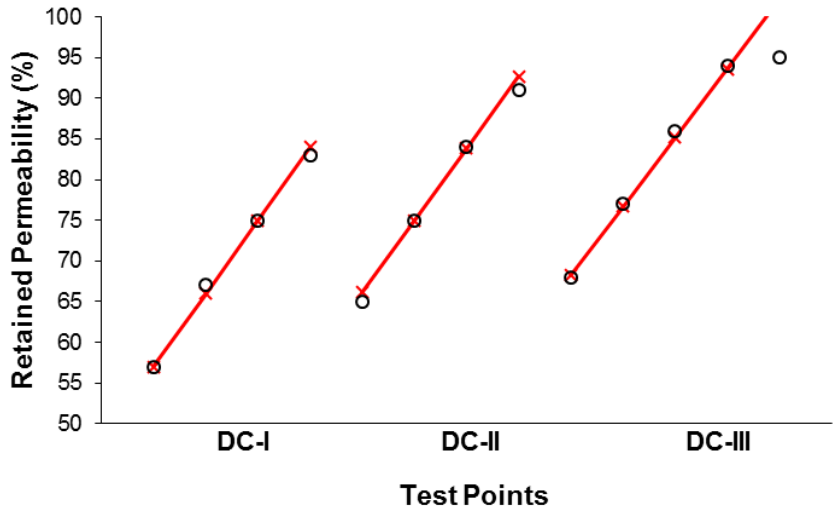

Figure 6-14. Predicted and experimental results of retained permeability for different sand classes

As in the previous section, New PSD-1 and New PSD-2 are used to verify the adequacy of the correlation. Separate tests allowed the calculation of the relative permeability of each sand type. The retained permeability (K_{ret}) was calculated using the same procedure introduced in Chapter 5. **Table 6-3** compares the predicted and experimental values of retained permeability showing a deviation of 5.1% for New PSD-1 and 3.3% for New PSD-2.

Table 6-3. New PSDs and verification tests for retained permeability

Sand type	K_{abs} (md)	Krel (fraction) at Sor	Predicted K_{ret}	Experimental K_{ret}
New PSD-1	1570	0.47	74	78
New PSD-2	4000	0.57	93	90

In general, WWSs produce excellent flow performance. The formulation introduced in this section simplifies the evolution of formation impairment, and it does not capture the complex phenomena that control fines migration or other sources of plugging. The formulation is a simple tool to obtain an idea of the range of retained permeabilities expected depending on the formation sand and aperture widths.

Based on the formulation the lower bound limit for the acceptable aperture window can be defined as:

$$A_{lb} = \left(\frac{D_{10}}{155.4} + \frac{1}{101.56}\right) * (1.31 f_c + 7.4) \tag{6.7}$$

Where A_{lb} is the lower bound of the aperture window in millimeters.

6.4 Conclusions

This chapter presented a set of graphical design criteria for aperture sizing of WWS that incorporated the effect of production scenarios, sand PSD and aperture size. The results of several pre-packed SRTs funded the criteria for three sand types. Optimum aperture windows were obtained by combining the sand retention and flow performances of the screens. The sanding response dominates the upper bound of the criteria while the lower bound is governed by the retained permeability of the near-screen zone.

Experimental results indicated that safe-aperture windows are highly affected by well production scenarios. Aggressive flow conditions like those encountered during steam-breakthrough episodes significantly shrink the aperture window. Steam-influx event is considered a worst-case scenario. In general, finer grain sizes showed slim aperture windows due to the limited space to control both plugging and sanding.

Additionally, empirical performance formulations for sanding and retained permeability were formulated based on the experimental results. The equations aim to provide a quick tool to predict the sanding and flow performance of WWS. However, it is essential to note that further extensive testing is required to tune the correlations. Fundamental research is vital to capture the phenomena involved in sand production and formation impairment.

CHAPTER SEVEN: CONCLUSIONS AND RECOMMENDATIONS FOR FUTURE WORK

7.1 Main results and contribution

This research introduced a sand control testing facility or Sand Retention Test (SRT) to study the role of operational procedures, flow rate, PSD and screen specifications on the performance of Wire-wrapped Screens (WWS). The experimental results are used to create a set of design criteria for WWS in SAGD applications.

Initially, previous works on sand control evaluation were reviewed to identify the strengths and deficiencies of experimental assessments and to analyze their relevance for thermal operations. Findings were implemented to commission a new large-scale and multiphase facility. Moreover, the testing procedure included both single-phase and multiphase flow to evaluate the changing conditions of SAGD wells. Flow scheme included several levels of injection to emulate progressive plugging conditions and also to vary water cut percentages. Steam-breakthrough episodes were emulated by co-injecting nitrogen, brine and mineral oil.

Results showed the dominance of the ratio particle size to aperture size on sand retention and fines production. Production scenarios strongly influence sanding intensity. Wider slots exhibited extreme levels of production during steam-breakthrough replication stages but responded reasonably well during liquid stages. Single-phase oil injection presented only initial sanding or mode-I production while transient sanding (mode-II) was observed upon the change of liquid flow rates and water cut. It was evident that drag forces play a critical factor in disrupting particles bridges and that water flow is necessary to observe sand production. Likewise, fines production is only observed when brine flows through the sand pack. Fines and clay particles detach from bigger grains due to their wettability preference towards the water. Wider apertures allowed greater production of fine particles and hence less accumulation close to the coupon. Additionally, fines production measurements denoted that increasing water cuts augment the production differences due to increasing saturation and interaction between fines and water.

Interestingly, a strong correlation was observed between fines content in the near-screen zone and retained permeability — the risks of pore plugging increase for finer low-quality sands

which displayed lower flow performances. However, a positive outcome from this research is the maintenance of retained permeability values above acceptable limits (50-70%), even for finer sands.

Finally, sanding and flow performance results were combined to determine optimum-aperture windows for three sand classes. The performance of several aperture sizes was categorized as unacceptable, marginal and acceptable and brought into an axial axis with representative D-values annotated on it. The previous approach is known as the Traffic Light System (TLS). Unlike previous criteria, the graphical criteria incorporate not only particle size points but also production scenarios. Remarkably, aggressive conditions shrink the safe-aperture window when compared to regular SAGD conditions (liquid flow). Wider aperture ranges can be utilized for coarser sands due to the superior flow performance of WWS even at narrow apertures. Overall, the results signify the importance of experimental testing to design screens and the impact of operational procedures. Field applications should consider expected flow conditions and customize the design for particular sand prints.

Also, empirical formulations were introduced to predict the response of WWS under laboratory testing conditions. The equations provide both upper and lower bounds for optimum aperture sizing based on PSD and flow conditions of the test.

7.2 Recommendations for future work

The following aspects are suggested to improve the design criteria for any sand control device further. Also, it will allow validating the performance of WWS under additional settings.

7.2.1 Effect of PSD curve and a broader spectrum of sand sizes

PSD of the sand pack profoundly affects the screen performance. It was evident in DC-I testing that sanding is significantly impacted by particle sorting (PSD shape). Additional PSD sorting and size ranges should be included in the testing program for further verification of the controlling phenomena in sanding and flow.

7.2.2 Effect of clay composition

Clays display different swelling behavior and particle bonding depending on the mineralogy and structure. Therefore, it is expected that fines migration tendencies change if a different

mixture of clays is implemented. Clay minerals such as Smectites may be present in low-quality sands.

7.2.3 Effect of oil-brine-fines emulsions

SAGD wells produce oil and brine in the form of emulsions at different ratios. It is believed that bubbles of the dispersive phase in an emulsion can play a critical role in capturing or releasing fines from the porous media. Emulsions are known to stabilize depending on the number of solids present in the reservoir, temperature and flow conditions. Injection of stabilized emulsions and different sand types and clays can provide a more accurate evaluation of the screen flow performance.

7.2.4 Effect of radial flow

Flow streamlines towards SAGD wells follow a radial geometry that can induce particles retardation and collision. Flow convergence towards the well generates additional pressure drops that can increase sand production. The collision of particles also may scale up pore plugging in the proximity of the screen. Tests under radial flow allow validating the performance of WWS.

BIBLIOGRAPHY

Addis, K.A (2014). *A Corrosion Model for Production Tubing*. Doctoral Dissertation, Ohio University.

Abram, M., and Cain, G. (2014). Particle-Size Analysis for the Pike 1 Project, McMurray Formation. *J Can Pet Technol*, **53**(6): 339-354. SPE 173890-PA.

Abrams, A. (1977). Mud Design to Minimize Rock Impairment Due to Particle Invasion. *J Pet Technol*, 29(5): 587-892. SPE 5713-PA.

Anderson, M. (2017). SAGD Sand Control: Large Scale Testing Results. Presented at the SPE Canada Heavy Oil Technical Conference, 15-16 February, Calgary, Alberta, Canada. SPE 185967-MS.

Ballard, T., Kageson-Loe, N., and Mathisen, A. M. (1999). The Development and Application of a Method for the Evaluation of Sand Screens. Presented at the SPE European Formation Damage Conference, 31 May-1 June, The Hague, Netherlands. SPE-54745-MS.

Ballard, T., and Beare, S. (2003). Media sizing for premium sand screens: Dutch twill weaves. Presented at the SPE European Formation Damage Conference, 13-14 May, The Hague, Netherlands. SPE 82244-MS.

Ballard, T., and Beare, S. (2006). Sand Retention Testing: The More You Do, the Worse It Gets. Presented at the International Symposium and Exhibition on Formation Damage Control, 15–17 February, Lafayette, Louisiana, USA. SPE 98308-MS.

Ballard, T. J., and Beare, S. P. (2012). An Investigation of Sand Retention Testing With a View To Developing Better Guidelines for Screen Selection. Presented at the SPE International Symposium and Exhibition on Formation Damage Control, 15-17 February, Lafayette, Louisiana, USA. SPE 151768-MS.

Barkman, H., and Davidson, H. (1972). Measuring Water Quality and Predicting Well Impairment. *J Pet Technol*, 24(7): 865-873. SPE 3543-PA.

Bennion, D. B., Ma, T., Thomas, F. B. et al. (2007). Laboratory Procedures for Optimizing the Recovery from High Temperature Thermal Heavy Oil and Bitumen Recovery Operations.

Presented at the Canadian International Petroleum Conference, 12-14 June, Calgary, Alberta. PETSOC-2007-206.

Bennion, D. B., Gupta, S., Gittins, S. et al. (2009). Protocols for slotted liner design for optimum SAGD operation. *Journal of Canadian Petroleum Technology*, **48**(11): 21-26. SPE 130441-PA.

Beshry, M. A., Krawchuk, P., Brown, G. A. et al. (2006). Predicting the Flow Distribution on Total E&P Canada's Joslyn Project Horizontal SAGD Producing Wells Using Permanently Installed Fiber-Optic Monitoring. Presented at the SPE Annual Technical Conference and Exhibition, 24-27 September, San Antonio, Texas, USA. SPE 102159-MS.

Bratli, R. K., and Risnes, R. (1981). Stability and Failure of Sand Arches. *Soc. Pet. Eng. J*, **21**(02): 236-48. SPE 8427-PA.

Brooks, R. T., & Tavakol, H. H. (2012). Experiences in Eliminating Steam Breakthrough and Providing Zonal Isolation in SAGD Wells. Presented at the SPE Western Regional Meeting, 21-23 March, Bakersfield, California, USA. SPE 153903-MS.

Burton, R. C., and Hodge, R. M. (1998). The Impact of Formation Damage and Completion Impairment on Horizontal Well Productivity. In SPE Annual Technical Conference and Exhibition. Society of Petroleum Engineers. SPE 49097-MS.

Butler, R.M. (1992). Gravity Drainage to Horizontal Wells. *Journal of Canadian Petroleum Technology,* 31(4): 31-37. PETSOC-92-04-02.

CAPP (2016) Canada Oil and Natural Gas. Canada's Energy Resources. Retrieved from: https://www.capp.ca/canadian-oil-and-natural-gas/canadas-petroleum-resources.

Chakrabarty, C., Fossey, J. P., Renard, G. et al. (1998). SAGD process in the East Senlac Field: From reservoir characterization to field application. Presented at the 1998 UNITAR conference, October 27–30, Beijing, China.

Chanpura, R. A., Hodge, R. M., Andrews, J. S. et al. (2011). A review of screen selection for standalone applications and a new methodology. *SPE Drilling & Completion*, **26**(01): 84-95. SPE 127931-PA.

Chanpura, R. A., Fidan, S., Mondal, S. et al. (2012a). New Analytical and Statistical Approach for Estimating and Analyzing Sand Production Through Wire-Wrap Screens During a Sand-Retention Test. *SPE Drilling & Completion*, **27**(03): 417-426. SPE 143731-PA.

Chanpura, R. A., Mondal, S., Sharma, M. M. et al. (2012b). Unraveling the Myths in Selection of Standalone Screens and a New Methodology for Sand Control Applications. Presented at the SPE Annual Technical Conference and Exhibition, 8-10 October, San Antonio, Texas, USA. SPE 158922-MS.

Clearly, M. P., Melvan, J. J., and Kohlhaas, C. A. (1979). The Effect of Confining Stress and Fluid Properties on Arch Stability in Unconsolidated Sands. Presented at the SPE Annual Technical Conference and Exhibition, 23-26 September, Las Vegas, Nevada. SPE 8426-MS.

Coberly, C. J. (1937). Selection of screen openings for unconsolidated sands. In Drilling and Production Practice. *American Petroleum Institute*. *Drilling and Production Practice.* API-37-189.

Colburn, A. P. (1931). Heat transfer and pressure drop in empty, baffled, and packed tubes1. *Industrial & Engineering Chemistry*, **23**(8), 910-913.

Constien, V. G., and Skidmore, V. (2006). Standalone Screen Selection Using Performance Mastercurves. Presented at the SPE International Symposium and Exhibition on Formation Damage Control, 15-17 February, Lafayette, Louisiana, USA. SPE-98363-MS.

Cowie, B.R. (2013). *Stable Isotope and Geochemical Investigation into the Hydrogeology and Biogeochemistry of Oil Sands Reservoir Systems in Northeastern Alberta, Canada*. Doctoral Thesis, University of Calgary (2013 September).

Devere-Bennett, N. (2015). Using Prepack Sand-Retention Tests (SRT's) to Narrow Down Liner/Screen Sizing in SAGD Wells. Presented at the SPE Thermal Well Integrity and Design Symposium, 23-25 November, Banff, Alberta, Canada. Society of Petroleum Engineers. SPE 178443-MS.

Driscoll, F. G. (1986). Groundwater and wells. Second Edition: *St. Paul, Minnesota: Johnson Filtration Systems Inc*.

Edmunds, N. R., Wong, A., McCormack, M. E. et al. (1987). Design of horizontal well completions, AOSTRA Underground Test Facility. Presented at the 4th Annual Heavy Oil and Oil Sands Symposium, February 18. University of Calgary, Calgary, Alberta, Canada.

Edmunds, N. R. (2000). Investigation of SAGD steam trap control in two and three dimensions. *Journal of Canadian Petroleum Technology*, Vol. 39, No. 1; pp. 30–40. PETSOC-00-01-02.

Edmunds, N., & Chhina, H. (2001). Economic Optimum Operating Pressure for SAGD Projects in Alberta. *Journal of Canadian Petroleum Technology*, **40**(12). PETSOC-01-12-DAS.

Ezeuko, C. C., Wang, J., & Gates, I. D. (2013). Investigation of emulsion flow in steam-assisted gravity drainage. *SPE Journal*, **18**(03), 440-447. SPE 157830-PA.

Fattahpour, V., Mahmoudi, M., Nouri, A. et al. (2016a). A Critical Review of Sand Control Design for SAGD Wells. Presented at the World Heavy Oil Congress, 6-9 September, Calgary, Alberta, Canada. WHOC16 – 613.

Fattahpour, V., Azadbakht, S., Mahmoudi, M. et al. (2016b). Effect of Near Wellbore Effective Stress on the Performance of Slotted Liner Completions in SAGD Operations. Presented at the SPE Thermal Well Integrity and Design Symposium, 28 November-1 December, Banff, Alberta, Canada. SPE 182507-MS.

Fattahpour, V., Mahmoudi, M., Wang, C. et al. (2018). Comparative Study on the Performance of Different Stand-Alone Sand Control Screens in Thermal Wells. Presented at the SPE International Conference and Exhibition on Formation Damage Control, 7-9 February, Lafayette, Louisiana, USA. SPE 189539-MS.

Fermaniuk, B. (2013). *Sand Control in Steam Assisted Gravity Drainage (SAGD) Wellbores and Process of Slotted Liner Design and Process*. Master of Engineering thesis, University of Calgary.

Furui, K., Zhu, D., Hill, A. et al. (2007). Optimization of Horizontal Well-Completion Design With Cased/Perforated or Slotted Liner Completions. *SPE Prod & Oper*, **22**(2):248-253. SPE 90579-PA.

Gabriel, G. A., & Inamdar, G. R. (1983). An experimental investigation of fines migration in porous media. Presented at SPE Annual Technical Conference and Exhibition, 5-8 October, San Francisco, California. SPE-12168-MS.

Gates, I. D., Kenny, J., Hernandez, I. L. et al. (2007). Steam Injection Strategy and Energetics of Steam-Assisted Gravity Drainage. *SPE Reservoir Evaluation & Engineering*, **10** (1): 19-34. SPE-97742-PA.

Gillespie, G., Deem, C. K., and Malbrel, C. (2000). Screen selection for sand control based on laboratory tests. Presented at the SPE Asia Pacific Oil and Gas Conference and Exhibition, 16-18 October, Brisbane, Australia. SPE 64398-MS.

Gillespie, G., Beare, S. P., and Jones, C. (2009). Sand Control Screen Erosion- When are you at Risk?. Presented at the 8th European Formation Damage Conference, 27-29 May, Scheveningen, The Netherlands. SPE 122269-MS.

Goodman, W.H, Godfrey, M.R. and Miller, T.M. 2010. Scale and Deposit Formation in Steam Assisted Gravity Drainage (SAGD) Facilities. Presented at the International Water Conference in San Antonio, Texas, 24-28 October.

Grills, T. L., Vandal, B. V., Hallum, F. et al. (2002). Case history: Horizontal well SAGD technology is successfully applied to produce oil at LAK Ranch in Newcastle Wyoming. Presented at SPE ITOHOS/ICHWT, November 4–7, Calgary, Alberta, Canada. SPE 78964-MS.

Guo, Y. (2018). Effect of Stress Build-up around SAGD Wellbores on the Slotted Liner Performance. Master of Science thesis, University of Alberta.

Guo, Y., Roostaei, M., Nouri, A. et al. (2018). Effect of stress build-up around standalone screens on the screen performance in SAGD wells. *Journal of Petroleum Science and Engineering*, 171, 325-339.

Guobin, M., Gordon, S. M., Arshad, A. et al. (2015). Sand Control Screen Cyclic Thermal Testing for Life of SAGD Wells. Presented at the SPE Thermal Well Integrity and Design Symposium, 23-25 November, Banff, Alberta, Canada. SPE 178441-MS.

Hall Jr, C. D., and Harrisberger, W. H. (1970). Stability of sand arches: a key to sand control. *Journal of Petroleum Technology*, **22**(07): 821-829.

Hamid, S., and Ali, S. A. (1997). Causes of Sand Control Screen Failures and Their Remedies. Presented at the SPE European Formation Damage Conference, 2-3 June, The Hague, Netherlands. SPE 38190-MS.

Han, G. and Dusseault, M. (2002). Quantitative Analysis of Mechanisms for Water-Related Sand Production. Presented at SPE International Symposium and Exhibition on Formation Damage Control held in Lafayette, Louisiana, 20-21 February. SPE 73737-MS.

Hodge, R. M., Burton, R. C., Constien, V. G. et al. (2002). An Evaluation Method for Screen-Only and Gravel-Pack Completions. Presented at the International Symposium and Exhibition on Formation Damage Control, Lafayette, Louisiana, USA, 20–21 February. SPE 73772-MS.

Hollies, D., Wadsworth, G. and W. Hariz (2001). Drilling practices for SAGD wells in the Athabasca oil sands. Presented at the 8th One-day conference on Horizontal Well Technology, November 7, Calgary, Alberta, Canada.

Islam, M. R., and A. E. George (1989). Sand Control in Horizontal Wells in Heavy oil Reservoirs. Presented at the SPE California Regional Meeting, 5-7 April, Bakersfield, California. SPE 18789-MS.

Irani, M. (2018). On Subcool Control in the SAGD Producers. Part II: Localized Hot Spots Effects and Optimization of Flow-Control-Devices. Presented at the SPE Thermal Well Integrity and Design Symposium, 27-29 November, Banff, Alberta, Canada. SPE 193369-MS.

Kar, T., Yeoh, J. J., Ovalles, C. et al. (2015). The Impact of Asphaltene Precipitation and Clay Migration on Wettability Alteration for Steam Assisted Gravity Drainage (SAGD) and Expanding Solvent-SAGD (ES-SAGD). Presented at the SPE Canada Heavy Oil Technical Conference, 9-11 June, Calgary, Alberta, Canada. SPE 174439-MS.

Kaiser, T. M. V., Wilson, S., and Venning, L. A. (2002). Inflow Analysis and Optimization of Slotted Liners. *SPE Drilling & Completion*, **17** (4): 200-209. SPE- 80145-PA.

Khilar, K., and Fogler, H. (1984).The Existence of a Critical Salt Concentration for Particle Release. *J Coll Interface Sci*, **101**(1): 214–224.

Khilar, C., Vaidya, N. and Folger, S. (1990). Colloidally-induced Fines Release in Porous Media. *J Pet Sci Eng*, **4**(3): 213-221.

Kisman, K., and Yeung, K. (1995). Numerical Study of the SAGD Process in the Burnt Lake Oil Sands Lease. Presented at the SPE International Heavy Oil Symposium, 19-21 June, Calgary, Alberta, Canada. SPE-30276-MS.

Ladd, R. S. 1978. Preparing Test Specimens Using Undercompaction. Geotechnical Testing Journal, Vol. 1, No. 1, 1978, pp. 16-23.

Layne, L., & Gerwick, F. (1973). *U.S. Patent No. 3,709,293*. Washington, DC: U.S. Patent and Trademark Office. Issued January 9, 1973.

Logan, B. E. J., D.G. Arnold, R.G., Bouwer E.J., O'melia C.R. (1995). "Clarification of clean-bed filtration models." *Journal of Environmental Engineering*, 121(12), 869-873.

McCormack, M.E. (1988). Mechanisms of Sand Retainment by Wire Wrapped Screens. Presented at the 4th UNITAR/UNDP Conference on Heavy Crude and Tar Sands, Edmonton, AB, August 7 – 12, 1988. Paper #56.

McDowell-Boyer, L. M., Hunt, J. R., and Sitar, N. (1986). "Particle transport through porous media." Water Resources Research, 22(13), 1901-1921.

Mahmoudi, M., Fattahpour, V., Nouri, A. et al. (2016a). New Criteria for Slotted Liner Design for Heavy Oil Thermal Production. Presented at the SPE Thermal Well Integrity and Design Symposium, 28 November-1 December, Banff, Alberta, Canada. SPE-182511-MS.

Mahmoudi, M., Fattahpour, V., Nouri, A. et al. (2016b). An Experimental Investigation of the Effect of pH and Salinity on Sand Control Performance for Heavy Oil Thermal Production. Presented at the SPE Canada Heavy Oil Technical Conference, 7-9 June, Calgary, Alberta, Canada. SPE 180756-MS.

Mahmoudi, M., Fattahpour, V., Nouri, A. et al. (2016c). Investigation Into the Use of Commercial Sands and Fines to Replicate Oil Sands for Large-Scale Sand Control Testing. Presented at the SPE Thermal Well Integrity and Design Symposium, 28 November-1 December, Banff, Alberta, Canada. SPE 182517-MS.

Mahmoudi, M., Fattahpour, V., Nouri, A. et al. (2017). An Experimental Evaluation of Pore Plugging and Permeability Reduction Near SAGD Sand Control Liners. Presented at the SPE Canada Heavy Oil Technical Conference, 15-16 February, Calgary, Alberta, Canada. SPE-184999-MS.

Mahmoudi, M. (2017). *New Sand Control Design Criteria and Evaluation Testing for Steam Assisted Gravity Drainage (SAGD) Wellbores*. Doctoral Thesis, University of Alberta.

Mahmoudi, M., Fattahpour, V., Roostaei, M. et al. (2018). An Experimental Investigation into Sand Control Failure Due to Steam Breakthrough in SAGD Wells. Presented at the SPE Canada Heavy Oil Technical Conference, 13-14 March, Calgary, Alberta, Canada. SPE 189769-MS.

Malbrel, C., Procyk, A., and Cameron, J. (1999). Screen sizing rules and running guidelines to maximize horizontal well productivity. In SPE European Formation Damage Conference. Society of Petroleum Engineers.

Markestad, P., Christie, O., Espedal, A. et al. (1996). Selection of screen slot width to prevent plugging and sand production. Presented at the SPE Formation Damage Control Symposium, 14-15 February, Lafayette, Louisiana. SPE 31087-MS.

Matanovic, D., Cikes, M., and Moslavac, B. (2012). *Sand control in well construction and operation*. First Edition: Springer Science & Business Media.

Menon, V. B., Nikolov, A. D., & Wasan, D. T. (1988). Interfacial effects in solids-stabilized emulsions: measurements of film tension and particle interaction energy. *Journal of colloid and interface science*, **124**(1), 317-327.

Meza-Diaz, B., Tremblay, B., and Doan Q. (2003). Mechanisms of Sand Production through Horizontal Well Slots in Primary Production. *J Can Pet Technol*, **42**(10): 36-46. PETSOC-03-10-04.

Meza-Diaz, B., Tremblay, B., and Doan, Q. (2004). Visualization of Sand Structures Surrounding a Horizontal Well Slot During Cold Production. *J Can Pet Technol,* **43**(12): 39-48. PETSOC-04-12-02.

Mohan, K. K., Vaidya, R. N., Reed, M. G. et al. (1993). Water sensitivity of sandstones containing swelling and non-swelling clays. In *Colloids Surf A: Physicochem. Eng. Aspects*, **73**(1993): 237-254.

Mondal, S., Sharma, M. M., Chanpura, R. A. et al. (2010). Numerical Simulations of Screen Performance in Standalone Screen Applications for Sand Control. Presented at the SPE Annual Technical Conference and Exhibition, 19-22 September, Florence, Italy. SPE 134326-MS.

Mondal, S., Sharma, M. M., Hodge, R. M. et al. (2011). A New Method for the Design and Selection of Premium/Woven Sand Screens. Presented at the SPE Annual Technical Conference and Exhibition, 30 October-2 November, Denver, Colorado, USA. SPE 146656-MS.

Montero, J. D., Chissonde, S., Kotb, O. et al. (2018). A Critical Review of Sand Control Evaluation Testing for SAGD Applications. Presented at the SPE Canada Heavy Oil Technical Conference, 13-14 March, Calgary, Alberta, Canada. SPE 189773-MS.

Montero Pallares, J. D., Wang, C., Haftani, M. et al. (2018). Experimental Assessment of Wire-Wrapped Screens Performance in SAGD Production Wells. Presented at the SPE Thermal Well Integrity and Design Symposium, 27-29 November, Banff, Alberta, Canada. SPE 193375-MS.

Muecke, T. W. (1979). Formation fines and factors controlling their movement in porous media. *Journal of Petroleum Technology*, **31**(02), 144-150.

O'Hara, M. (2015). Thermal Operations in the McMurray; an Approach to Sand Control. Presented at the SPE Thermal Well Integrity and Design Symposium, 23-25 November, Banff, Alberta, Canada. SPE 178446-MS.

Ott, W. K., and Woods, J. D. (2003). *Modern sandface completion practices handbook*. Second Edition: World Oil Magazine.

Oyeneyin, B (2015). Sand Control Completion Strategy. In *Integrated Sand Management for Effective Hydrocarbon Flow Assurance*, Chapter 6, 192-194. Developments in Petroleum Science Series.

Penberthy, W. L., and Shaughnessy, C. M. (1992). *Sand control*. Henry L. Doherty Memorial Fund of AIME, Society of Petroleum Engineers.

Peters, E. J. (2012). *Advanced Petrophysics: Dispersion, interfacial phenomena*. Volume 2: Greenleaf Book Group.

Ranjith, P. G., Perera, M. S. A., Perera, W. K. G. et al. (2013). Effective parameters for sand production in unconsolidated formations: An experimental study. *Journal of Petroleum Science and Engineering*, **105**: 34-42.

Rogers, E. (1971). Sand Control in Oil and Gas Wells. *Oil and Gas J,* November: 54-60.

Romanova, U. G., and Ma, T. (2013). An Investigation on the Plugging Mechanisms in a Slotted Liner from the Steam Assisted Gravity Operations. Presented at the SPE European Formation Damage Conference & Exhibition, 5-7 June, Noordwijk, The Netherlands. SPE 165111-MS.

Romanova, U. G., Gillespie, G., Sladic, J. et al. (2014). A Comparative Study of Wire Wrapped Screens vs. Slotted Liners for Steam Assisted Gravity Drainage Operations. Presented at the World Heavy Oil Congress, 5-7 March, New Orleans, USA. WHOC14-113.

Romanova, U. G., Ma, T., Piwowar, M. et al. (2015). Thermal Formation Damage and Relative Permeability of Oil Sands of the Lower Cretaceous Formations in Western Canada. Presented at the SPE Canada Heavy Oil Technical Conference, 9-11 June, Calgary, Alberta, Canada. SPE 174449-MS.

Romanova, U., Michel, D., Strom, R. et al. (2017). Understanding Sand Control for Thermal Heavy Oil and Bitumen Production Operations. Presented at the SPE Thermal Well Integrity and Design Symposium, 28-30 November, Banff, Alberta, Canada. SPE 188155-MS.

Saltukaroglu, M., Wright, G. N., Conrad, P. R. et al. (1999). Mobil's SAGD experience at Celtic, Saskatchewan. Presented at the CSPG Petroleum Societies Joint, June 14–18, Calgary, Alberta, Canada. Paper 99-251999.

Santamarina, C. 2002. Soil Behavior at the Microscale: Particle Forces. Proc., ASCE Soil Behavior and Soft Ground Construction. 119: 25–56.

Sarkar, A. K., & Sharma, M. M. (1990). Fines Migration in Two-Phase Flow. *Journal of petroleum technology*, 42(05), 646-652. SPE 17437-PA.

Sasaki, K., Akibayashi, S., Yazawa, N. et al. (2001). Numerical and Experimental Modelling of the Steam-Assisted Gravity Drainage (SAGD) Process. *J Can Pet Technol,* **40**(01), 44-50. PETSOC-01-01-04.

Schmitt, G., & Rothmann, B. (1977). Studies on the Corrosion Mechanism of Unalloyed Steel in Oxygen-Free Carbon Dioxide Solutions, *Part I. Kinetics of the Liberation of Hydrogen. Werkstoffe und Korrosion*, **28**: 816-822.

Schwartz, D. H. (1969). Successful Sand Control Design for High Rate Oil and Water Wells. *Journal of Petroleum Technology*, **21**(09), 1-193. SPE 2330-PA.

Sen, T. K., and Khilar, K. C. (2006). "Review on subsurface colloids and colloid-associated contaminant transport in saturated porous media." *Advances in Colloid and Interface Science*, 119(2-3), 71-96.

Skjaerstein, A., Tronvoll, J., Santarelli, F. et al. (1997). Effect of water breakthrough on sand production: Experimental and field evidence. Presented at the SPE annual technical conference and exhibition, September 29 – October 2, San Antonio, Texas, Canada. SPE 77683-MS.

Spronk, E. M., Doan, L. T., Matsuno, Y. et al. (2015). SAGD Liner Evaluation and Liner Test Design for JACOS Hangingstone SAGD Development. Presented at the SPE Canada Heavy Oil Technical Conference, 9-11 June, Calgary, Alberta, Canada. SPE 174503-MS

Stahl, R. M., Smith, J. D., Hobbs, S. et al. (2014). Application of Intelligent Well Technology to a SAGD Producer: Firebag Field Trial. Presented at the SPE Heavy Oil Conference-Canada, 10-12 June, Calgary, Alberta, Canada. SPE 170153-MS.

Stone, T. W., and Bailey, W. J. (2014). Optimization of Subcool in SAGD Bitumen Processes. Presented at the World Heavy Oil Congress, 5-7 March, New Orleans, USA. WHOC14-271.

Suman, G., Ellis, R., and Snyder, R. (1985). *Sand Control Handbook*. Houston: Gulf publishing company.

Sztukowski, D. M., & Yarranton, H. W. (2005). Oilfield solids and water-in-oil emulsion stability. *Journal of colloid and interface science*, **285**(2), 821-833.

Tiffin, D. L., King, G. E., Larese, R. E. et al. (1998). New Criteria for Gravel and Screen Selection for Sand Control. Presented at the SPE Formation Damage Control Conference, 18-19 February, Lafayette, Louisiana. SPE 39437-MS.

Tippie, D. B., and Kohlhaas, C. A. (1973). Effect of Flow Rate on Stability of Unconsolidated Producing Sands. Presented at the Fall Meeting of the Society of Petroleum Engineers of AIME, 30 September-3 October, Las Vegas, Nevada. SPE 4533-MS.

Tronvoll, J., Eek, A., Larsen, I. et al. (2004). The effect of oriented perforations as a sand control method: A field case study from the Varg Field, North Sea. Presented at the SPE International Symposium and Exhibition on Formation Damage Control, 18-20 February, Lafayette, Louisiana. SPE 86470-MS.

Valdes, J. 2002. Fines migration and formation damage-microscale studies. Ph.D. dissertation, Georgia Institute of Technology, Atlanta, Ga.

Valdes, J. and Santamarina, C. (2006). Particle clogging in radial flow: microscale mechanisms. SPE J, 11(2): 193–198. SPE 88819-PA.

Van Oort, E., van Velzen, G., and Leerlooijer, K. (1993). Impairment by Suspended Solids Invasion: Testing and Prediction. *SPE Prod & Fac*, 8(3): 178-184. SPE 23822-PA.

Van Vliet, J., and Hughes, M. J. (2015). Comparison of Direct-Wrap and Slip-On Wire Wrap Screens for Thermal Well Applications. Presented at the SPE Thermal Well Integrity and Design Symposium, 23-25 November, Banff, Alberta, Canada. SPE 178462-MS.

Vaziri, H., Barree, B., Xiao Y. et al. 2002. What is the Magic of Water in Producing Sand?. Presented at SPE Annual Technical Conference and Exhibition held in San Antonio, Texas, 29 September. SPE 77683-MS.

Vitthal, S., and Sharma, M. (1992). A Stokesian Dynamics Model for Particle Deposition and Bridging in Granular Media. *J Colloid Interface Sci*, **153**(2): 314-336.

Wells, D. G., Luhning, R. W., Dyck, R. G. et al. (1997). A tale of two wells: SAGD horizontal well wire wrapped sand control screen placement with mud circulation. Presented at SPE/CIM 6th Annual One-Day Conf. on Horizontal Well Technology, November 12. Calgary, Alberta, Canada. CIM 97-193.

Williamson, H., Babaganov, A., and Romanova, U. (2016). Unlocking Potential of the Lower Grand Rapids Formation, Western Canada: The Role of Sand Control and Operational Practices in SAGD Performance. Presented at the SPE Canada Heavy Oil Technical Conference, 7-9 June, Calgary, Alberta, Canada. SPE 180700-MS.

Wu, B., & Tan, C. P. 2001. Effect of water-cut on sandstone strength and implications in sand production prediction. Presented at the DC Rocks 2001, The 38th U.S. Symposium on Rock Mechanics (USRMS), 7-10 July, Washington, D.C. ARMA-01-0027.

Wu, B., Choi, S. K., Feng, Y. et al. (2016). Evaluating Sand Screen Performance Using Improved Sand Retention Test and Numerical Modelling. Presented at the Offshore Technology Conference Asia, 22-25 March, Kuala Lumpur, Malaysia. OTC-26434-MS.

Xie, J., Fan, C., Wagg, B. et al. (2008). Wire wrapped screens in SAGD wells. In *World Oil Sand Control Technology*.

Zeinijahromi, A., Vaz, A., & Bedrikovetsky, P. (2012). Productivity Impairment of Gas Wells Due to Fines Migration. Presented at the SPE International Symposium and Exhibition on Formation Damage Control, 15-17 February, Lafayette, Louisiana, USA. SPE 151774-MS.

Zhang, W., Youn, S., and Doan, Q. T. 2007. Understanding Reservoir Architectures and Steam-Chamber Growth at Christina Lake, Alberta, by Using 4D Seismic and Crosswell Seismic Imaging. *SPE Reservoir Evaluation & Engineering*, **10** (05): 446-452. SPE-97808-PA.

Zhang, K., Chanpura, R. A., Mondal, S. et al. (2015). Particle-Size-Distribution Measurement Techniques and Their Relevance or Irrelevance to Wire-Wrap-Standalone-

Screen Selection for Gradual-Formation-Failure Conditions. *SPE Drilling & Completion*, **30**(02), 164-174.

Zhao, B., Becerra, M., & Shaw, J. M. (2009). On asphaltene and resin association in Athabasca bitumen and Maya crude oil. *Energy & Fuels*, **23**(9), 4431-4437.

Appendix A: Absolute Permeability from all testing

A.1 Absolute Permeability for DC-III Testing

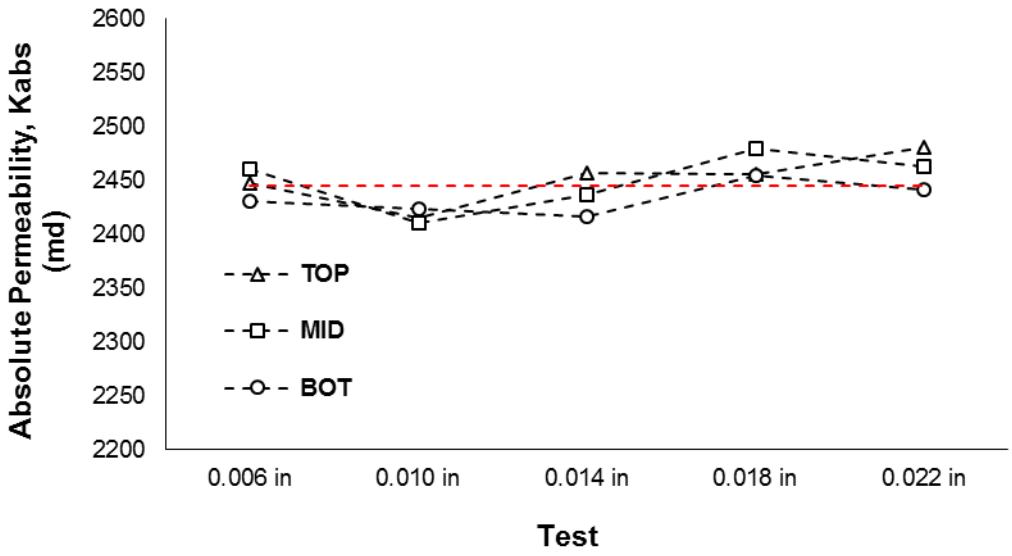

(a)

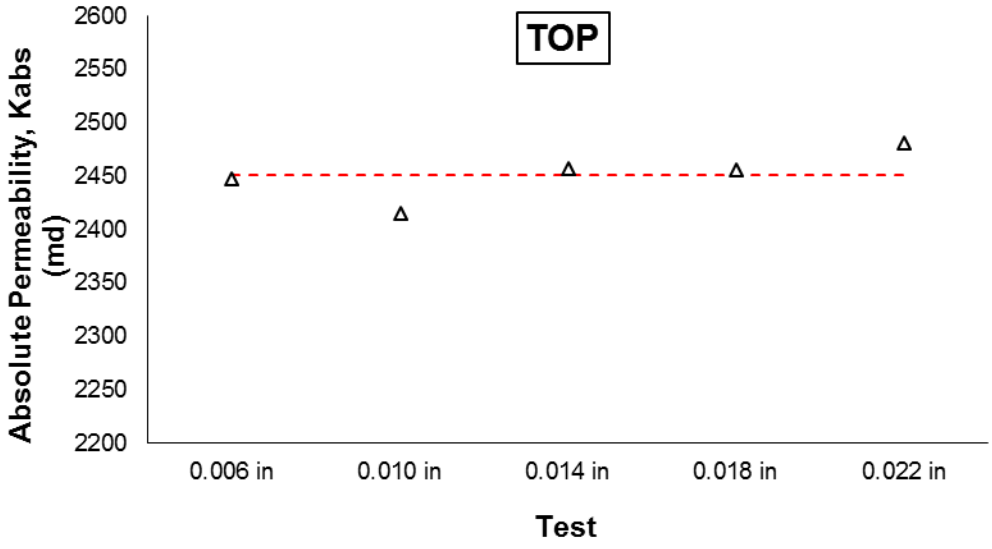

(b)

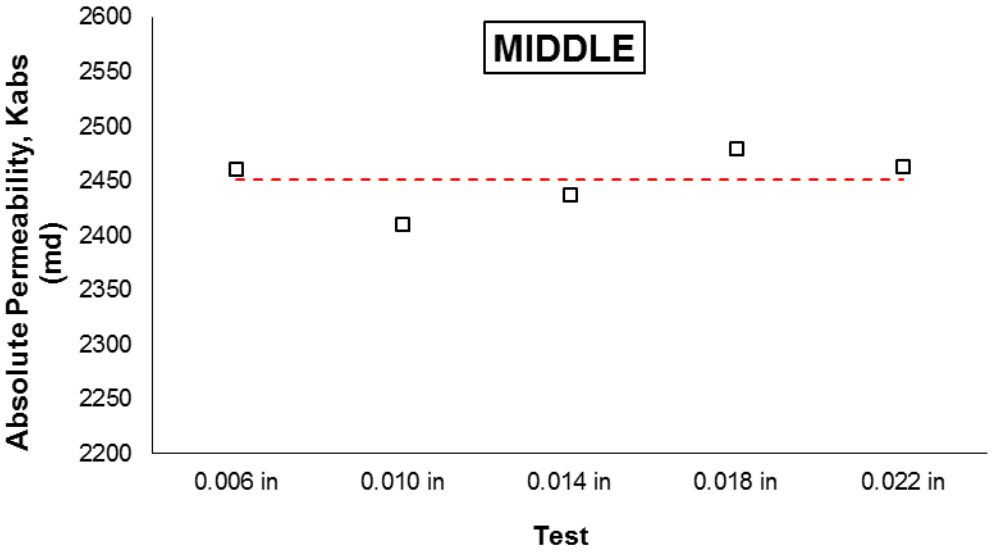

(c)

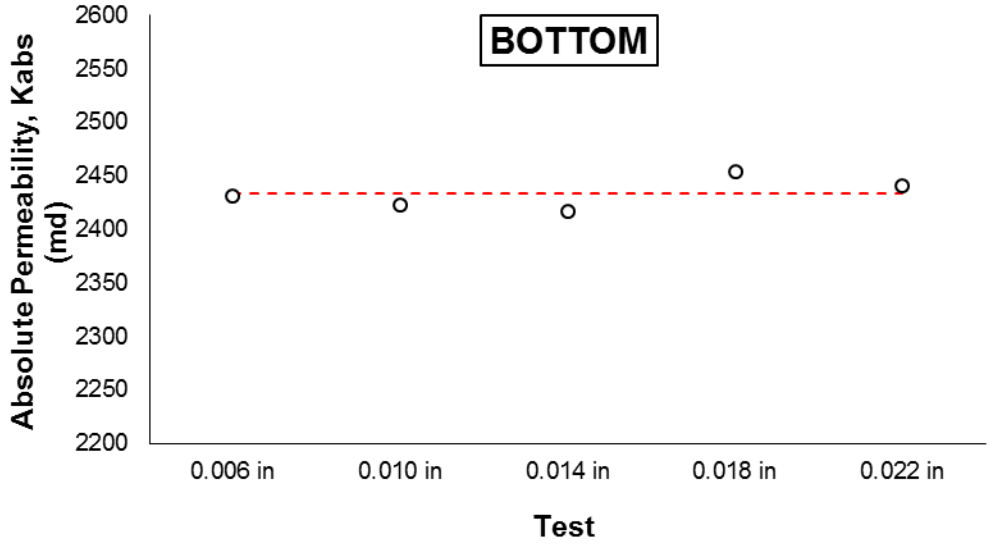

(d)

Figure A-1. Absolute permeability for DC-III tests. (a) All readings, (b) top section, (c) medium section, (d) bottom section. Red dashed line denotes the average permeability.

A.2 Absolute Permeability for DC-II Testing

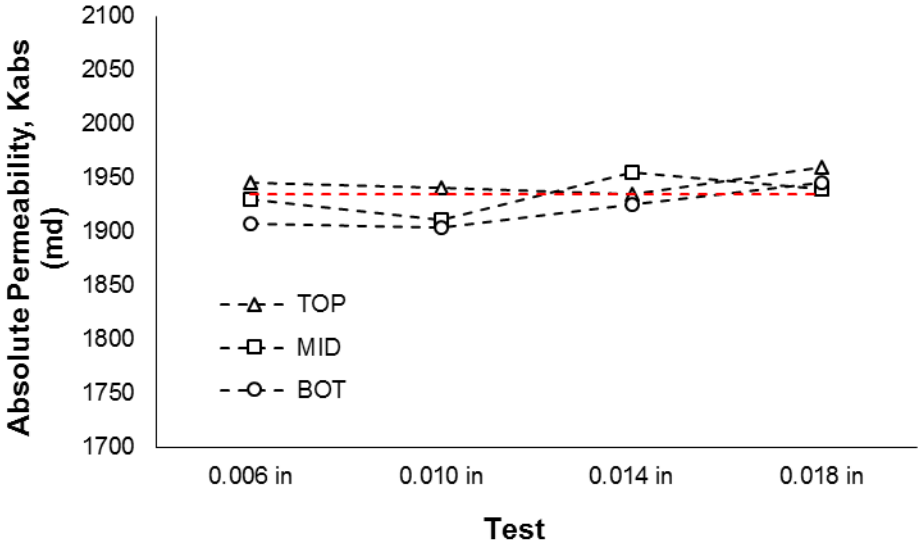

(a)

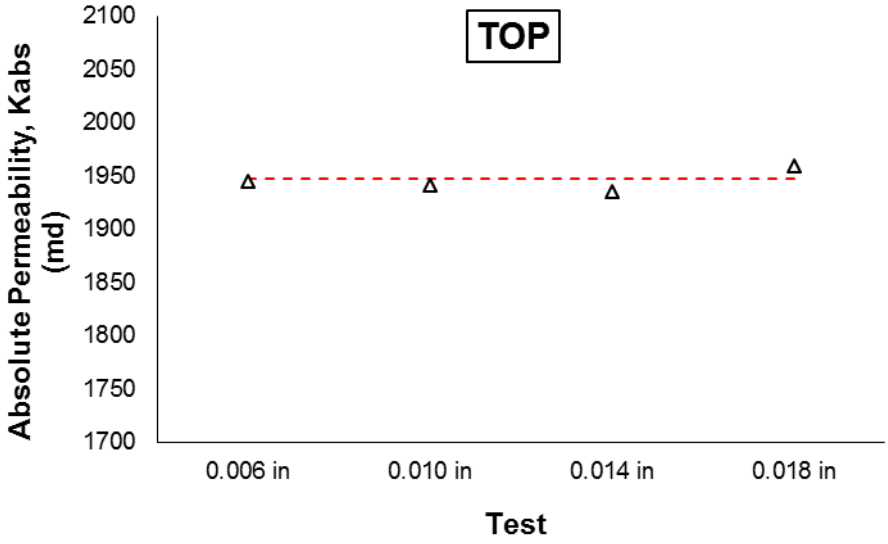

(b)

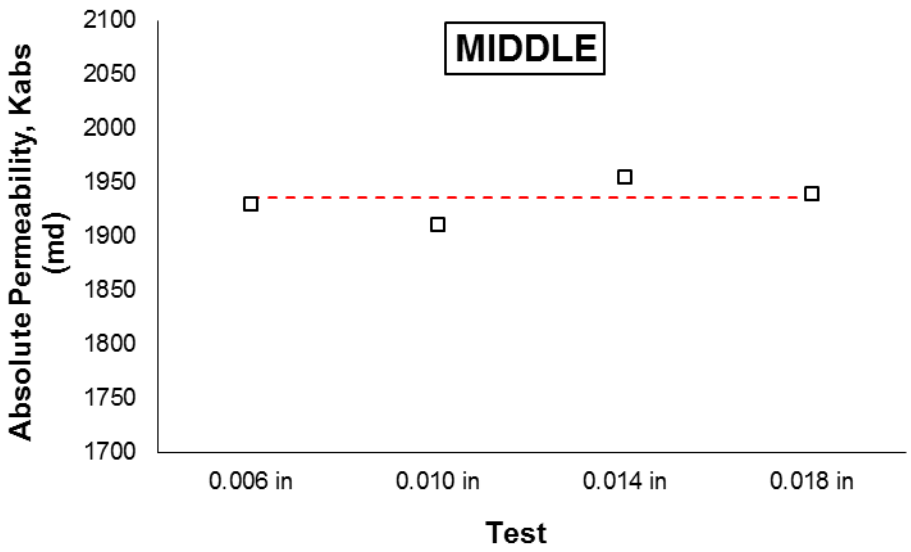

(c)

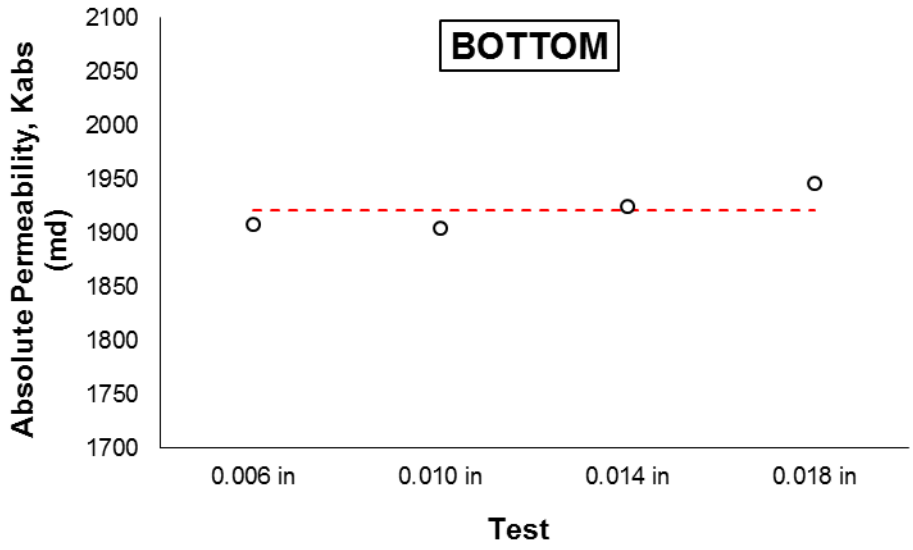

(d)

Figure A-2. Absolute permeability for DC-II tests. (a) All readings, (b) top section, (c) medium section, (d) bottom section. Red dashed line denotes the average permeability.

A.3 Absolute Permeability for DC-I Testing

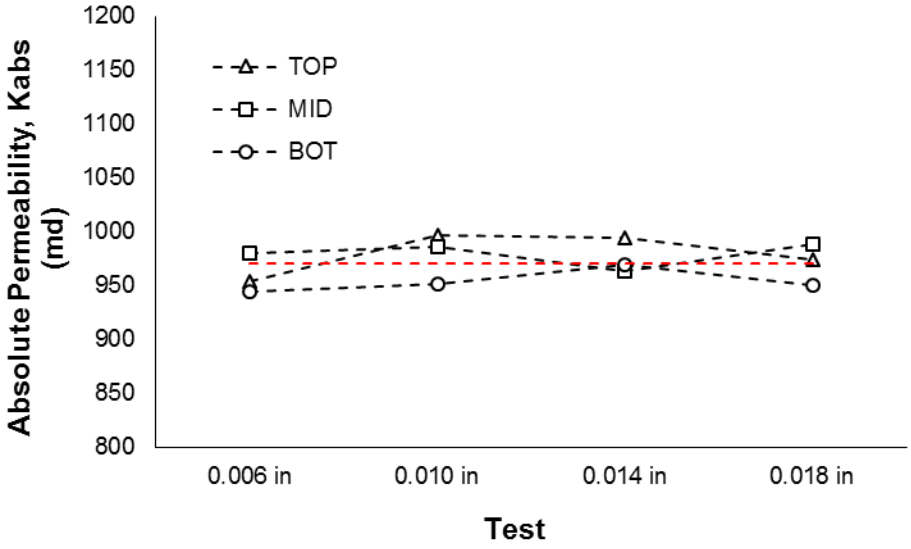

(a)

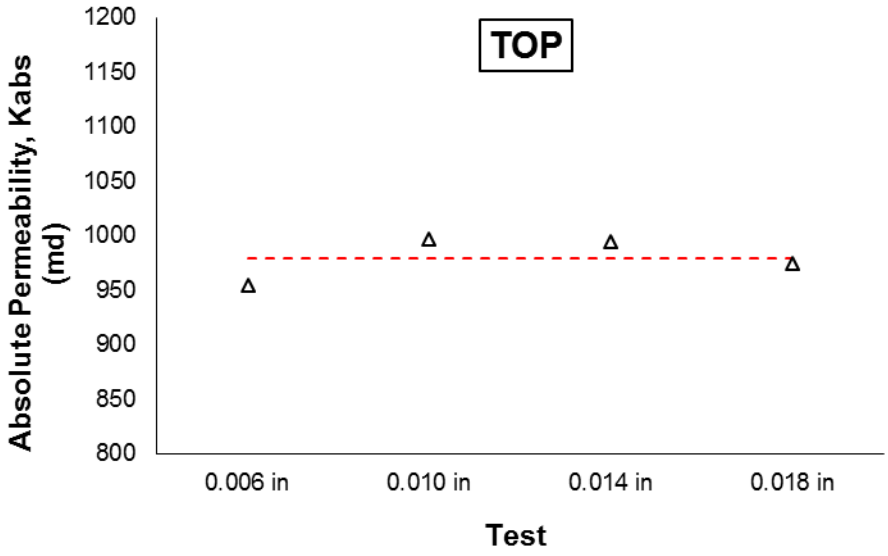

(b)

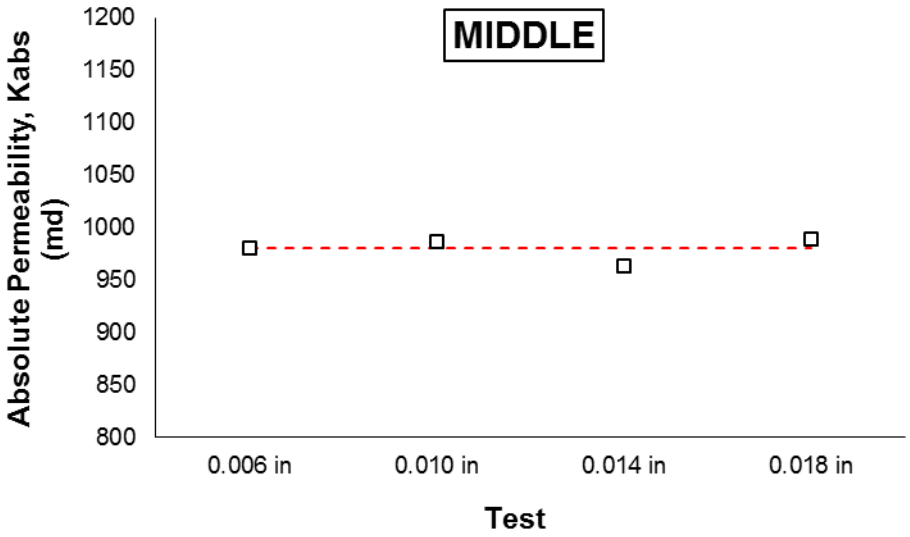

(c)

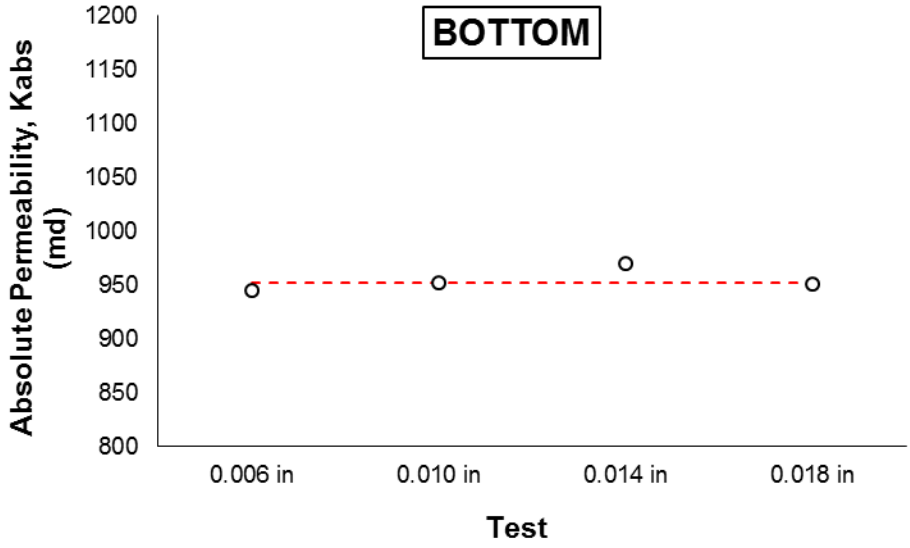

Figure A- 3. Absolute permeability for DC-I tests. (a) All readings, (b) top section, (c) medium section, (d) bottom section. Red dashed line denotes the average permeability.

Appendix B: Pressure drop readings of the near-screen zone

B.1 Pressure drop for DC-III Testing

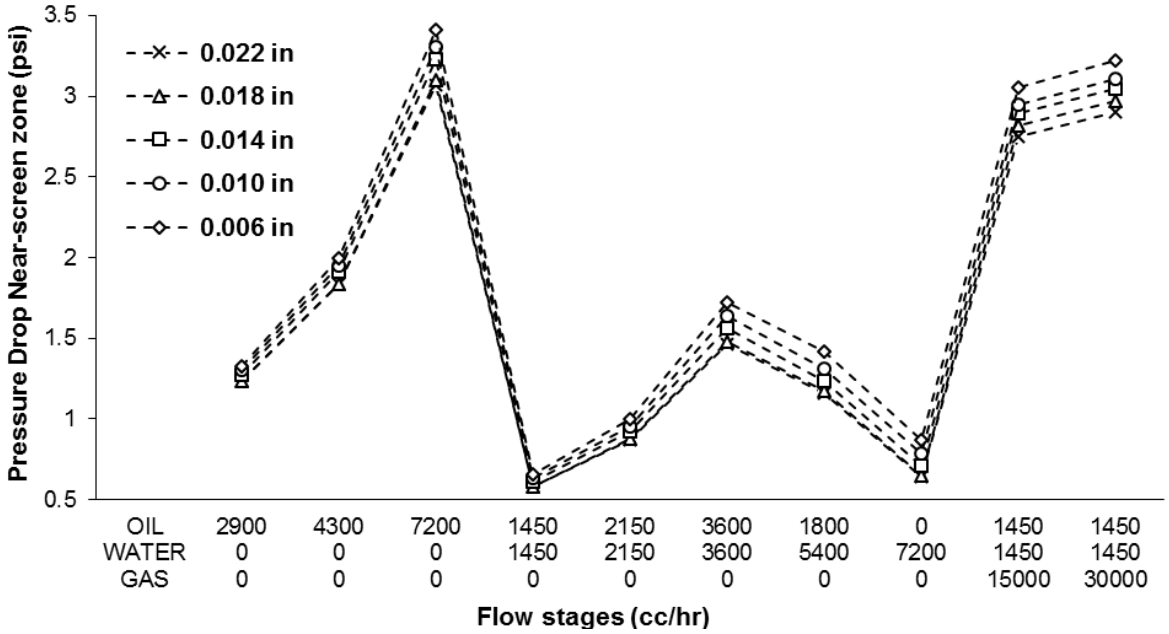

Figure B-1. Near-screen zone pressure drop for DC-III tests

B.2 Pressure drop for DC-II Testing

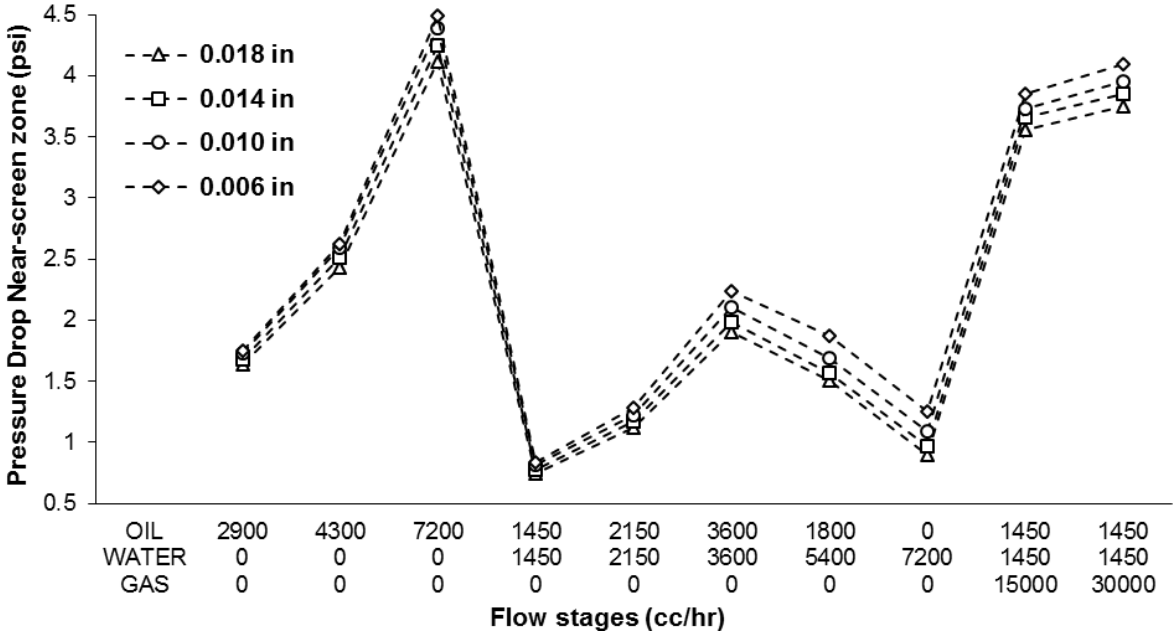

Figure B-2. Near-screen zone pressure drop for DC-II tests

B.3 Pressure drop for DC-I Testing

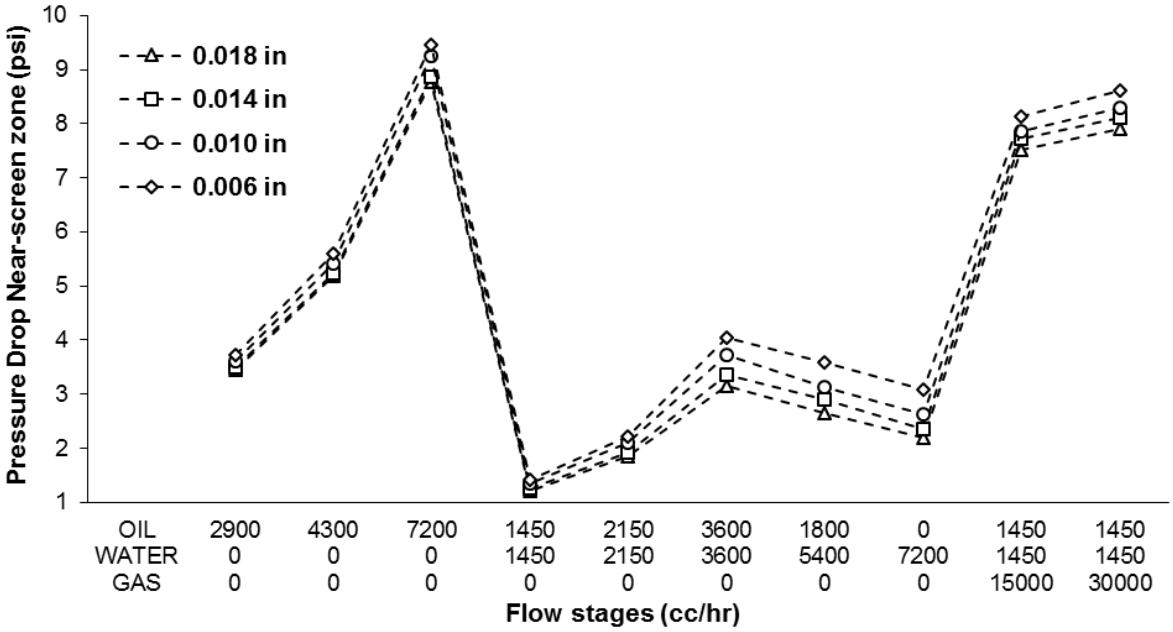

Figure B-3. Near-screen zone pressure drop for DC-I tests